LBNL-52375

BATTERIES FOR ADVANCED TRANSPORTATION TECHNOLOGIES (BATT) PROGRAM FOR ELECTROCHEMICAL ENERGY STORAGE

ANNUAL REPORT

FOR FY 2002

Environmental Energy Technologies Division
Lawrence Berkeley National Laboratory
University of California
Berkeley, California 94720

Edited by Frank McLarnon, Program Manager

February 2003

This work was supported by the Assistant Secretary for Energy Efficiency and Renewable Energy, Office of FreedomCAR and Vehicle Technologies of the U.S. Department of Energy under Contract No. DE-AC03-76SF00098.

CONTENTS

CATHODES

DIAGNOSTICS

MODELING

INTRODUCTION

The Batteries for Advanced Transportation Technologies (BATT) Program is supported by the U.S. Department of Energy Office of Advanced Automotive Technologies (DOE/OAAT) to help develop high-performance rechargeable batteries for use in electric vehicles (EVs) and hybrid-electric vehicles (HEVs). The work is carried out by the Lawrence Berkeley National Laboratory (LBNL) and several other organizations, and is organized into six separate research tasks.

Background and Program Context

The development of an advanced battery for automotive applications is a difficult undertaking. There is a strong need to identify and understand performance and lifetime limitations to help guide battery scale-up and development activities. High cell potentials and demanding cycling requirements lead to chemical and mechanical instabilities, which are important issues that must be addressed. The BATT Program addresses fundamental issues of chemistries and materials that face all lithium battery candidates for DOE EV and HEV applications. The Program emphasizes synthesis of components into battery cells with determination of failure modes, coupled with strong efforts in materials synthesis and evaluation, advanced diagnostics, and improved electrochemical models. The selected battery chemistries are monitored continuously with periodic substitution of more-promising components. This is done with advice from within the BATT Program, from outside experts, and from assessments of world-wide battery R&D. The BATT Program also educates battery and electrochemical scientists who move on to work for battery developers.

Task Descriptions

The six primary BATT Program task areas are: (1) Cell Development, (2) Anodes, (3) Electrolytes, (4) Cathodes, (5) Diagnostics, and (6) Modeling. Task 1 comprises cell fabrication, testing and characterization, Tasks 2-4 are aimed at identifying new materials, and Tasks 5-6 support all BATT Program work. Brief summary descriptions of each task follow.

The Cell Development task has identified three "baseline" rechargeable Li cell chemistries. The polymer-electrolyte cell chemistry includes a Li metal negative electrode (anode), $Li(CF_3SO_2)_2N$ + cross-linked poly(ethylene) oxide (PEO)-based polymer electrolyte, and V_6O_{13} or a tunnel-structure Li_xMnO_2 positive electrode (cathode). The gel-electrolyte cell chemistry includes a natural graphite anode, $LiBF_4$ + cross-linked gel electrolyte, and a $LiFePO_4$ or $Li_{1.02}Al_{0.25}Mn_{1.75}O_{3.92}S_{0.03}$ cathode. The baseline Li-ion chemistry is based on the DOE Advanced Technology Development (ATD) Program "Generation 2" chemistry: a graphite-based anode, a $LiPF_6$ + ethylene carbonate-ethyl methyl carbonate (EC-EMC) electrolyte, and a $LiAl_{0.05}Ni_{0.80}Co_{0.15}O_2$-based cathode. Cell test data are posted on the web page http://isswprod.lbl.gov/battdatasite/.

The Anodes task seeks to overcome the two major problems associated with the carbon-based anodes used in all commercial Li-ion batteries: poor safety characteristics and short lifetimes. It is for these reasons that either improved anode structures or non-carbonaceous anodes must be developed as possible alternatives. Low-cost metal alloys with acceptable capacity, rate, cyclability, and calendar life are under investigation.

Polymer Electrolyte research aims to understand performance characteristics by studies of the transport properties of the electrolyte as a function of polymer and salt structure, polymer structural changes as a function of temperature, and interactions at the electrode/electrolyte interface related to transport and chemical/mechanical stability. A multi-pronged approach involving chemical synthesis, advanced diagnostic tools, and coordinated modeling studies is being used.

The identification and development of novel Cathodes are critical because of the fundamental cost and environmental limitations of cobalt-based and vanadium-based materials used in present-day rechargeable Li

batteries. The focus of this effort is to develop a high-rate and stable MnO_2 cathode. Although manganese is a low-cost constituent, MnO_2 cathodes tend to lose capacity at an unacceptable rate. Research is directed at understanding the reasons for the capacity fade and developing methods to stabilize this material, as well as the evaluation of novel forms of MnO_2 cathodes.

Advanced Diagnostics are essential to investigate life-limiting and performance-limiting processes in batteries. We use post-test analyses and enhanced spectroscopic and microscopic techniques to investigate morphology, structure, and compositional changes of electrode materials. Examples include providing better understanding of electrode surface processes, and a detailed investigation of the Li/polymer interface *via* advanced microscopies and spectroscopies.

Sophisticated Modeling is required to support BATT Program Tasks 1-5. This effort brings physical understanding to complex interactions through the development of comprehensive phenomenological models. Models are being advanced to elucidate the failure mechanisms of Li battery components and to understand the mechanisms for thermal runaway.

This report summarizes the research, financial and management activities of the BATT Program in FY 2002. A website for the BATT Program, which provides Internet links to recent quarterly and annual reports, is found at http://www.berc.lbl.gov/BATT/BATT.html.

CELL DEVELOPMENT

Cell Fabrication and Testing

Kathryn A. Striebel
Lawrence Berkeley National Laboratory, 70R0108B, Berkeley CA 94720-8168
(510) 486-4385, fax: (510) 486-7303; email: kastriebel@lbl.gov

Objective

- Benchmark the performance of new materials for low-cost and high-power Li-ion cells.

Approach

- Prepare uniform electrodes from novel battery materials, assemble them into baseline cells with proven components, and test them with a standard protocol.
- Disassemble the cells, after testing, for analysis by the diagnostic tasks within the BATT Program.

Accomplishments

- Demonstrated 65 Wh/kg, 155 Wh/l (on a cell basis), and a cycle life of 120 cycles for low-cost baseline cells $LiFePO_4$/gel/natural graphite (NG) from Hydro-Québec (HQ) have
- Attributed poor cycle life of the $LiFePO_4$/NG to side-reactions, not structural degradation of the active materials
- Characterized Gen 2 high-power baseline cell performance and fade mechanisms under constant current cycling.
- Received novel components for the baseline cells from Mitsui, Superior Graphite, U. Waterloo, MIT, ANL, SUNY Binghamton and the LBNL materials development tasks.

Future Directions

- Compare performance of $LiFePO_4$ from five sources, improve cyclability and evaluate additives
- Prepare and study low-cost baseline gel cells which need no external compression

Low-Cost Baseline Cell

Li-ion pouch cells containing $LiFePO_4$ and NG with either liquid electrolyte (12 cm^2 LBNL pouch cells) or gel electrolyte (3.8 cm^2 HQ pouch cells) were characterized for cycle performance and capacity fade. The $LiFePO_4$, prepared by U. of Montreal, routinely showed a capacity of 159 mAh/g-active at C/25 and excellent cyclability against a Li-metal anode, with an irreversible capacity loss (ICL) usually <3%. LBNL-$LiFePO_4$ cathodes showed similar high-rate capacity to the HQ-$LiFePO_4$ cathodes when a carbon-coated Al current collector was used.

Figure 1 shows the C/2 cycling performance of $LiFePO_4$/liquid electrolyte/NG pouch cells with three different carbon anodes in $LiPF_6$/EC/DEC electrolyte. The capacity fade rate in all cells is unacceptably high. Post-test electrochemical analysis of anode and cathode samples, in Swagelok half-cells, showed no evidence of capacity fade. Since both anode and cathode cycle efficiently with minimal fade against Li, one electrode must be causing the other to consume the cycleable Li in the cell. We propose that a minor impurity is migrating from the $LiFePO_4$ cathode to the anode causing instability of the solid electrolyte interphase (SEI) layer. Preliminary transmission electron microscopy (TEM) analysis of anodes cycled against $LiFePO_4$ suggest that there is iron on the anode. Confirmation of this mechanism will be obtained through further diagnostics analysis.

Also shown in Fig. 1 is the performance of an HQ gel cell (see pg. 8). The LPK (HQ) cathode has a lower loading than the LFP (LBNL) cathode. A slightly lower capacity is observed with the gel cell, compared to the LBNL-prepared pouch with $LiPF_6$

electrolyte and Celgard, due to the lower conductivity. The similar rate of capacity fade suggests a similar fade mechanism for the gel cell. Calendar life studies of cells at high state-of-charge (SOC) showed a similar fade rate, consistent with a solvent reduction mechanism on the charged anode. The performance of the 3.8cm^2 HQ gel cell was used to prepare the gap chart shown in Table. 1.

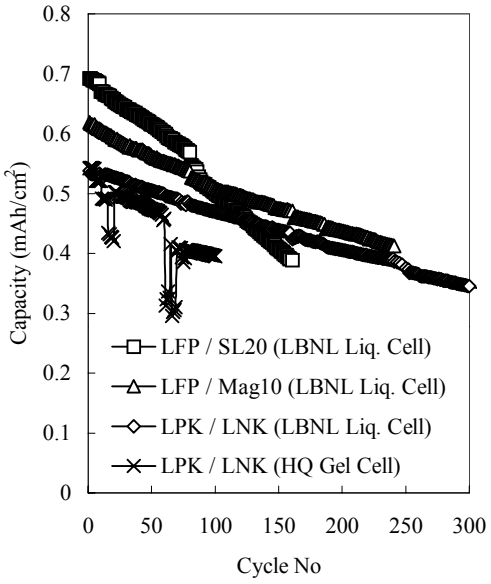

Figure 1. Discharge capacity during C/2 cycling of $LiFePO_4$/NG cells with three different graphites, 25°C.

$LiFePO_4$ samples in the form of powder or electrodes have been received from SUNY Binghamton, MIT, and the U. Waterloo. Full and half-cell studies of these $LiFePO_4$ samples vs. NG are currently in progress. Collaboration with the modeling effort (Newman) is proving very helpful in the comparison of electrode performance at different loadings.

High-Power Baseline Cell

Pouch cells and 100 mAh Quallion cells with the ATD Gen 2 chemistry were cycled at constant-current (C/2) and with the Power-Assist (PA) pulse profile. The capacity loss of the LBNL-pouch cell cycled at 100% depth-of-discharge (DOD) and room temperature for 1000 cycles was ca. 70% (0.07%/cycle). However, a cell cycled at 70% DOD showed no loss after 1000 cycles. Post-test diagnostics of the anodes showed no capacity loss. However, the nature of the SEI was dependent on cycling conditions. The cathode showed different capacity loss behavior due to a loss of conductivity, film formation on its surface and/or dislocation of structure. The 100 mAh Quallion cells cycled with the pulse and constant current profiles showed similar capacity loss rates. However, at an equivalent of 400 full cycles the area specific impedance (ASI) for the cell cycled at constant current increased by a factor of 2.5 while the PA cell impedance was essentially unchanged.

Anode Studies

The effect of anode compression on resistivity, performance and cycle life was studied in collaboration with Sastry (see pg. 55). NG anodes were prepared with SL-20 (Superior Graphite), and two amorphous carbon-coated NG's (Mitsui Mining). Matrix conductivity and current collector contact resistance were found to be strong functions of anode density. The amorphous-carbon coating reduced the electrolyte reduction peak on formation, compared to the SL-20, except for the highly pressed anodes. However, the amorphous carbon coating led to an increased overall ICL. The effect of pressing on the cycling stability of the anodes was less well-defined.

Gel Electrolyte Studies

Thermally crosslinkable gel samples from Daiso (Korea), Dai-ichi gel (Japan), and LBNL (Kerr) were evaluated. Cross-linking conditions for good conductivity and mechanical stability were studied as a function of curing time and temperature for polymer precursors mixed into $LiBF_4$/EC/γBL electrolyte. Gel electrolyte cells were assembled with five types of gel electrolyte with the Daiso gel showing the most promising performance. However, due to poor reproducibility, a decision was made to pursue the poly(vinylidene fluoride) (PVdF) type gel electrolyte cell.

Table 1. Gap Chart for Low-Cost Baseline Cell

		USABC Goals		HQ-gel cell
	Units	**Mid-Term**	**Long-Term**	**$LiFePO_4$/NG**
Power Density	W/l	250	600	618
Specific Power, Dischg (80%DOD/30 s)	W/kg	150	400	262 (18s)
Specific Power, Regen (20% DOD/10s)	W/kg	75	200	597
Energy Density	Wh/l	135	300	155
Specific Energy	Wh/kg	80	200	65
Life	years	5	10	NA
Cycle Life	cycle	600	1000	115 (100%DOD)
Power & Capacity Degradation	% rated	20	20	20
Ultimate Price (10,000 units @ 40 kWh	$/kWh	150	100	NA
Operating Environment	°C	-30 - 65	-40 - 85	25
Normal Recharge Time	hours	6	3 to 6	2
Fast Recharge Time, 40 to 80% SOC	minutes	15	15	NA
Continuous Dischg. in 1 hr	% rated energy	75	75	NA
Cell Weight (electrodes and electrolyte)	mg/cm^2			26
Cell Volume	cm^3/cm^2			0.011

Publications and Presentations

J. Shim, R. Kostecki, T.J. Richardson, X. Song and K.A. Striebel, "Electrochemical Analysis for Cycle Performance and Capacity Fading of a Lithium-Ion Battery Cycled at Elevated Temperature", *J. Power Sources* **112**, 222-230 (2002).

J. Shim and K.A. Striebel, "Effect of Electrode Thickness and Pressure on the Cyclability of Graphite Anodes in Li-ion Cells", *11th International Meeting on Lithium Batteries,* Monterey, CA, June 2002.

J. Shim, and K.A. Striebel, "Cycling Performance of Low-Cost Lithium Ion Batteries with Natural Graphite and $LiFePO_4$," *11th International Meeting on Lithium Batteries*, Monterey, CA, June 2002.

K. Striebel, A. Guerfi, J. Shim, M. Armand, M Gauthier and K. Zaghib, "$LiFePO_4$ Advanced Cathode Material for the BATT Program," *11th International Meeting on Lithium Batteries*, Monterey, CA, June 2002.

Active Materials Characterization Using X-Ray Diffraction and Chemical Analysis

Thomas J. Richardson
Lawrence Berkeley National Laboratory, MS 62R0203, Berkeley, CA 94720-8253
(510) 486-8619, fax: (510) 486-8619, e-mail: tjrichardson@lbl.gov

Objectives

- Support cell development through structural characterization of active electrode components before, during, and after cycling.
- Investigate inexpensive, self-actuating overcharge protection mechanisms.
- Synthesize and evaluate alternative electrode materials.

Approach

- Address primary causes of capacity and power fading by correlating them with the composition and structure of electrode active materials using x-ray diffraction (XRD), vibrational spectroscopy, and voltammetry.
- Develop internal overcharge protection mechanism that becomes active when needed and allows continued, undegraded cycling of unaffected cells.
- Develop improved cathode materials *via* a rational approach to active material synthesis.

Accomplishments

- Evaluated cycled electrodes by XRD and Fourier transform infrared (FTIR) to assist in determining mechanisms for capacity and power degradation.
- Demonstrated self-actuating, internal overcharge protection in Li-TiS_2 cells using separators containing an electroactive polymer with voltage-sensitive electronic properties.
- Prepared and evaluated new manganese and iron phosphates with theoretical capacities similar to $LiFePO_4$ but with better electronic conductivity, intercalant ion mobility, and ease of preparation.

Future Directions

- Extend conducting polymer overcharge protection studies to Li-ion cells.
- Search for polymers with higher switching potentials for use in 3.5 V ($LiFePO_4$) and 4 V cells.
- Examine mixed oxide-phosphate phases for higher capacity while retaining good cycling stability.

Materials Characterization

Active materials for cells built at LBNL were characterized before use. Electrodes taken from cells cycled in Task 1.1 were examined for compositional and structural changes related to decreased performance. XRD and FTIR evaluation of the SOC and the uniformity of charge distribution in cycled cathodes has been useful in determining degradation mechanisms in both ATD-type Gen2 and $LiFePO_4$ cells.

Overcharge Protection

Overcharging of Li batteries can shorten their lifetimes and create hazardous conditions including overheating, toxic releases, and even explosion. A low-cost, internal shunt mechanism is especially desirable for the large multicell stacks required for traction applications where failure of one cell can render the entire stack inoperative and where weight and volume are constrained. We are using a polymer with voltage-sensitive electronic properties to provide self-actuated, internal overcharge protection. The polymer is incorporated within the separator during cell assembly and is inactive during normal charging and discharging. If, at the end of charge, the safe voltage limit is exceeded, a reversible electrochemical reaction converts the polymer to a near-metallic state, temporarily providing an alternative path for the current, and preventing damage to the cell. On subsequent discharging, the polymer returns to its original state and the cell behaves normally. An example is shown in Fig. 2. The potential of an unprotected Li-TiS_2 cell cycled at a 2C rate goes rapidly to the 3.5 V limit at the end of charge (Fig. 2a). If the voltage were allowed to rise further, the cell would be damaged. In a protected cel (Fig. 2b), the polymer shunt becomes conducting at around 3 V, and a 20-fold overcharge can be applied without raising the voltage above 3.2 V.

The relationship between SOC, conductivity, and open-circuit voltage (OCV) of a conducting polymer is important in understanding its characteristics as a charge carrier, and these data are essential inputs for the model of our system being developed by Karen Thomas and John Newman. Measurements reported in the literature have generally not been quantitative due to the inherent difficulty of preparing a uniform sample. An electrode was specially designed to allow us to adjust the oxidation state of the polymer

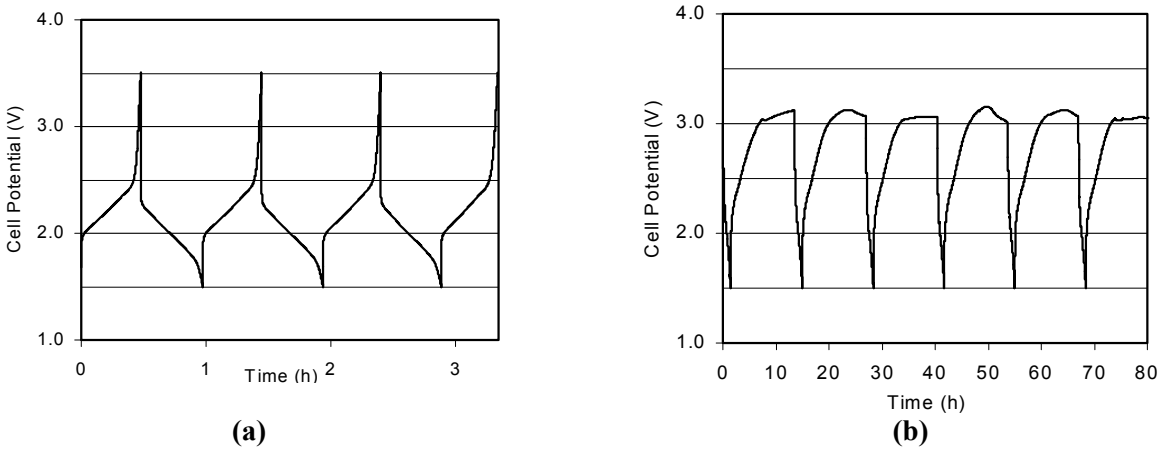

Figure 2. $LiTiS_2$ cells without (a) and with (b) internal polymer shunt.

electrochemically, while sequentially measuring its conductivity. A neutral polymer film was cast on a piece of stainless steel plate. A second stainless steel plate provided contact for the conductivity measurements. The polymer was brought to the desired SOC, the OCV was recorded after relaxation, and its electronic conductivity was determined from AC impedance measurements.

Cathode Development

Discovery of new cathode materials is essential to improving the energy and power performance of lithium batteries. The primary criteria for considering a new material are cost, toxicity, energy density, stability, and ease of preparation. Recent advances in the use of $LiFePO_4$ and related compounds have shown the importance of having a host lattice that is stable toward structural changes caused by exceeding voltage limits and interactions with other cell components. Strongly bonded PO_4 sub-units in the metal phosphates contribute to their excellent stability and cyclability. The low electronic conductivity and two-phase nature of the intercalation reaction in $LiFePO_4$, however, result in poor utilization at high rates. We have prepared novel iron and manganese phosphates with the same metal-to-phosphate stoichiometry but with different crystal structures. These are easily synthesized in air with short reaction times. The metal-oxygen polyhedra share edges, rather than opposite corners as in $LiFePO_4$, giving them higher electronic conductivities. In addition, these structures accommodate mixed metal oxidation states, which should improve rate capability. Other materials under investigation are mixed phosphate-oxides such as $Fe^{III}{}_3O_3PO_4$, which contain some phosphate groups for stability, but have higher theoretical capacities closer to those of simple oxides. While a suitable high-capacity cathode material has not yet been found among the twenty compounds tested thus far, a better understanding of the structural factors that make a useful electrode material is being developed.

Publications and Presentations

M.C. Tucker, M.M. Doeff, T.J. Richardson, R. Fiñones, E.J. Cairns and J.A. Reimer, "Hyperfine Fields at the Li Site in $LiFePO_4$-Type Olivine Materials for Lithium Rechargeable Batteries: A ^{7}Li MAS NMR and SQUID Study," *J. Amer. Chem. Soc.*, **124**, 3832 (2002).

M.C. Tucker, M.M. Doeff, T.J. Richardson, R. Finones, J.A. Reimer and E.J. Cairns, "^{7}Li and ^{31}P Magic Angle Spinning Nuclear Magnetic Resonance of $LiFePO_4$-Type Materials," *Electrochem. Solid State Lett.*, **5**, A95 (2002).

T.J. Richardson, "New Phosphate-Stabilized Cathodes for Lithium Batteries," *11th International Meeting on Lithium Batteries*, Monterey, CA, June 2002.

Research on Lithium-Ion Polymers Batteries Utilizing Low-Cost Materials

Karim Zaghib
Hydro-Québec, IREQ, 1800 Lionel Boulet, Varennes, QC, J3X 1S1
(450) 652 8019, fax: (450) 652 8424, email: karimz@ireq.ca

Objectives

- Fabricate Li-ion polymer cells (4 cm^2 area), graphite/gel polymer/$LiFePO_4$, using cell chemistries proposed by DOE.
- Investigate interfacial phenomena at the anode/electrolyte and cathode/electrolyte in Li-ion polymer cells.
- Determine the cycle life of Li-ion polymer cells at different temperatures (0.0 to 55°C) and self-discharge rates.
- Synthesize $LiFePO_4$ cathode material for Li-ion polymer cells.

Approach

- Synthesize and coat electrodes (anode and cathode) with low-cost materials for evaluation in Li-ion polymer cells containing gel polymer electrolyte.
- Investigate the effect of $LiFePO_4$ particle size, conductive carbon content in electrodes, salt concentration, mixed-salt concentration (from 1 to 2 M) on cell performance.
- Study the effect of pressure and interfacial phenomena on the performance of electrodes.

Accomplishments

- Produced electrodes (graphite and $LiFePO_4$) with optimized porosity that were submitted to LBNL.
- Assembled Li-ion cells with gel polymer and send (50% of the total cells) to LBNL for testing.
- Completed study on the effect of conductive carbon content on the performance of $LiFePO_4$ electrodes, and the influence of Li salt composition and concentration on cell performance.
- Determined that 10-psi cell pressure is necessary to obtain acceptable reversible capacity of anode and cathodes.

Future Directions

- Investigate the effect of $LiFePO_4$ particle size on performance in Li-ion gel polymer cells.
- Develop new gel polymer electrolytes that provide improved performance in cells.

The effect of pressure on the performance of the polymer gel electrolytes at the anode and cathodes interfaces was investigated by impedance spectroscopy and scanning electron microscopy (SEM). The data show that increasing the pressure to 10 psi is necessary to obtain good reversible capacity with both electrodes.

A problem with high irreversible capacity in the anode was observed. Consequently a major effort was undertaken to resolve this problem: (i) a new generation of natural graphite was examined and (ii) the effect of porosity of the anode and cathode was investigated. After optimization of the electrode porosity, the graphite exhibited better performance. In the first cycle, the irreversible capacity was reduced from 50% to less than 25%. The optimized electrodes of $LiFePO_4$ and graphite were evaluated in Li-ion gel cells. The reversible capacity increased by 15% (Fig. 3) compared to the first-generation cells. In the second set of ten cells (March 2002), a new polymer electrolyte based on poly(ethylene oxide) (PEO) that was coated and cross-linked at LTEE (Shawinigan) by electron-beam irradiation was evaluated.

We have studied the effect of solvent mixtures and type of Li salt on Li-ion polymer cell performance. The electrochemical performance of the HQ solvent, tetra-ethyl-sulfamide (TESA), mixed with ethylene carbonate(EC) (3/1) was comparable to EC/γ-butyrolactone (GBL) (3/1). With a mixed salt (1 M LiTFSI + 0.5 M $LiBF_4$ in EC/GBL), a higher capacity fade (>20%) was observed compared to the same molar concentration of the single salt (LiTFSI or $LiBF_4$).

Studies were completed on the effect of different amounts of conductive carbon (1 to 15%) on the performance of $LiFePO_4$ electrodes. The aim of these experiments is to identify the appropriate cathode composition to improve the high-rate performance. Mixtures of carbon black (3 or 6%) and graphite (6% or 6%) were used in electrodes containing a total carbon content of 9% and 12%. The data in Fig. 4 shows that an increase in the carbon content in $LiFePO_4$ improves the performance at high rates. A carbon content of 6% seems to be good compromise for energy and power, while still achieving a reversible capacity of 65% at 2C rate and 62% at 3C rate. Even with only 1% carbon, more that 50% of the reversible capacity was obtained at 3C rate.

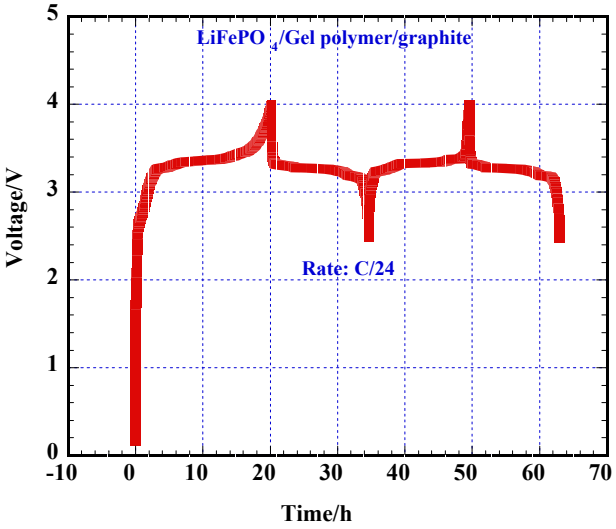

Figure 3. Charge-discharge profiles for graphite/gel polymer/$LiFePO_4$ at charge-discharge rate of C/24.

An investigation on *in situ* SEM of gel polymer cells at 0°C was initiated. We are able to cycle cells under vacuum in an electron microscope using an electrolyte based on GBL, which has a high boiling point. These studies are continuing.

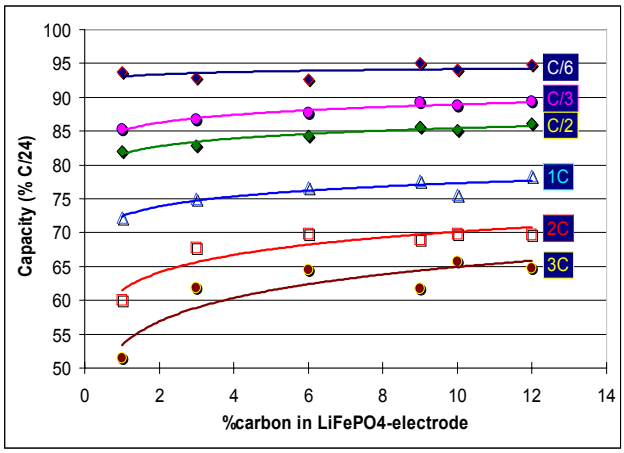

Figure 4. Carbon effect on the reversible capacity of $LiFePO_4$ in Li/gel polymer/$LiFePO_4$ cells.

Presentations

K. Zaghib, X. Song, A. Guerfi, R. Rioux and K. Kinoshita, "Purification of Natural Graphite for Anodes in Li-Ion Batteries: Chemical versus Thermal Processing," *11th International Meeting Lithium Batteries,* Monterey, CA, June 2002.

A. Guerfi, S. Sévigny and K. Zaghib, "Nano-particles $Li_4Ti_5O_{12}$ Spinel Structure Electrode for Electrochemical Generator," *11th International Meeting Lithium Batteries,* Monterey, CA, June 2002.

K. Striebel, A. Guerfi, J. Shim, M. Armand, M. Gauthier and K. Zaghib, "$LiFePO_4$ Advanced Cathode Material for the BATT Program," *11th International Meeting Lithium Batteries*, Monterey, CA, June 2002.

A. Guerfi, S. Sevigny, and K. Zaghib, "High Stable $Li_4Ti_50_{12}$ as Negative Electrode for Electrochemical Generator: Micro vs Nano," *201st Meeting of the Electrochemical Society*, Philadelphia, PA, May 2002.

K. Zaghib, G. Nadeau, A. Guerfi, and K. Kinoshita,"Effect of Particle Size on Lithium Intercalation Rates in Natural Graphite for Li-ion Batteries," *201st Meeting of the Electrochemical Society*, Philadelphia, PA, May 2002.

ANODES

Non-Carbonaceous Anode Materials

Michael M. Thackeray
Chemical Technology Division, Argonne National Laboratory, Argonne IL 60439
(630)-252-9183, fax: (630)-252-4176, email: thackeray@cmt.anl.gov

Objective

- Replace carbon with an alternative anode material that is inexpensive and that will improve the safety of Li-ion cells.

Approach

- Search for, characterize, and develop inexpensive intermetallic electrodes that provide an electrochemical potential a few hundred millivolts above that of metallic Li with capacities >400 mAh/g and 1000 mAh/ml.
- Focus on nickel-arsenide and zinc-blende-type structures, and study their structural and electrochemical behavior during discharge and charge in Li cells.

Accomplishments

- Performed studies to understand the root causes for the capacity loss of intermetallic electrodes in Li cells
- Achieved capacity target of 300 mAh/g for 2002 with Fe-doped Cu_6Sn_5 and MnSb electrodes. Performance was limited by an irreversible capacity loss of 20% or more on the initial cycle, and a slow but steady decrease in capacity on cycling.

Future Directions

- Improve the processing of intermetallic electrodes, particularly those containing copper and/or tin to reduce the irreversible capacity loss on the first cycle.
- Continue to explore intermetallic compounds in which there is a strong crystallographic relationship between parent and lithiated structures and to find improved systems.
- Initiate studies on substituted, electronically conducting $Li_4Ti_5O_{12}$ spinel electrodes with the view to coupling them with high-voltage (4.5-4.8 V) metal oxide electrodes to provide safe, high-rate 3.0 -3.5 V Li-ion cells.

During 2002, efforts were placed on attempts to improve the performance of intermetallic electrodes that operate by Li insertion/metal extrusion reactions and to find new or modified systems. Attention was focused predominantly on $Cu_{6-x}M_xSn_5$ (M=Fe, Ni, Zn), Cu_2Sb and MnSb. Studies were performed to investigate the underlying reasons for the large irreversible capacity loss which is associated with intermetallic electrodes in Li cells and to find ways to combat them . Parameters that were investigated included (i) oxide passivation coatings, (ii) particle size effects, (iii) electrode porosity, and (iv) the addition of additional metal, *e.g.,* Cu to a Cu_6Sn_5 electrode. None of these factors was found to make a major contribution to the capacity loss. It was determined that two of the dominant factors that limited the performance of ANL's intermetallic electrodes were 1) the loss of extruded metal that is displaced from the intermetallic structure and 2) electronic isolation of the electrode particles that occurs because of relatively large volume changes and the consequent pulverization of intermetallic particles during their initial reaction with Li.

Although good reversibility was achieved when the voltage limits of the Li cells were strictly controlled, and although capacities slightly in excess of the targeted 300 mAh/g were achieved from both Fe-substituted Cu_6Sn_5 and MnSb electrodes, the studies showed that these electrodes always suffered from an unacceptably large irreversible capacity loss on the first charge/discharge cycle. For example, Fig. 5 shows that although steady cycling behavior

above the targeted goal of 300 mAh/g could be achieved, the capacity loss on the first cycle of the Li/MnSb cells was >20%. These cells deliver most of their capacity between 1.0 and 0.5 V *vs.* Li during discharge. Cu_6Sn_5 and MnSb electrodes have a hexagonally close-packed NiAs-type structure and they both exhibit hysteresis effects during charge and discharge. This phenomenon can be attributed to the diffusion of the Sb and Sn atoms during phase transitions from the NiAs-type structure to an intermediate cubic-close packed LiMnSb or Li_2CuSn-type structure, respectively. The final discharge products consist of Li_3Sb and the extruded transition metal.

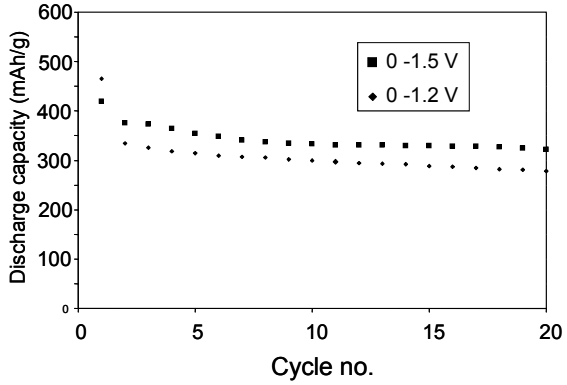

Figure 5. Capacity *vs.* cycle no. for a Li/MnSb cell.

Our findings are consistent with the reported behavior of other intermetallic electrodes, such as SnSb and Mg_2Si. Our attempts to reduce the initial capacity loss associated with intermetallic electrodes will continue to be a major thrust of the research effort in 2003. In addition, in 2003, we plan to initiate studies on substituted, electronically-conducting $Li_4Ti_5O_{12}$ spinel electrodes to investigate their electrochemical properties against high-voltage (4.5-4.8 V) metal oxide electrodes in an attempt to provide safe, high-rate 3.0-3.5 V Li-ion cells.

Publications and Presentations

L.M. L. Fransson, E. Nordström, L. Haggström, J.T. Vaughey and M.M. Thackeray, "Structural Transformations in Lithiated η'-Cu_6Sn_5 Probed by *In situ* Mössbauer Spectroscopy and X-ray Diffraction," *J. Electrochem. Soc*. **149**, A736 (2002).

H. Tostmann, A.J. Kropf, C.S. Johnson, J.T. Vaughey and M.M. Thackeray, "In-Situ X-ray Absorption Studies of Electrochemically Induced Phase Changes in Lithiated InSb," *Phys. Rev. B*. **66**, 014106 (2002).

M.M. Thackeray, J.T. Vaughey and L.M.L. Fransson, "Recent Developments in Anode Materials for Lithium Batteries," *JOM* (a publication of The Minerals, Metals and Materials Society), p. 20 (March, 2002).

M.M. Thackeray, J.T. Vaughey, C.S. Johnson, R. Benedek, L.M.L. Fransson and K. Edstrom, "Structural Considerations of Intermetallic Electrodes for Lithium Batteries," *11th International Meeting on Lithium Batteries, Monterey, CA,* June 2002.

J.T. Vaughey, H. Swinger, C.S. Johnson, M.M. Thackeray, L.M.L. Fransson and K. Edström, "Alternative Anode Materials for Lithium Batteries," *11th International Meeting on Lithium Batteries*, Monterey, CA, June 2002.

L.M.F. Fransson, K. Edstrom, J.T. Vaughey and M.M. Thackeray, "Phase Transformations in MnSb and Mn_2Sb, *11th International Meeting on Lithium Batteries*, Monterey, CA, June 2002.

L.M.L. Fransson, K. Edström, J.T. Vaughey and M.M. Thackeray, "Phase Transitions in Lithiated Intermetallic Anodes for Lithium Batteries – In Situ XRD Studies," *202nd Meeting of the Electrochemical Society, Salt Lake City*, UT, October 2002.

Novel Anode Materials

M. Stanley Whittingham
Chemistry and Materials Research Center, State University of New York at Binghamton, Binghamton, NY 13902-6000
(607) 777-4623, fax: (607) 777-4623, e-mail: stanwhit@binghamton.edu

Objective

- Replace the presently used carbon anodes with safer materials that will be compatible with manganese oxide cathodes and the associated electrolyte. In particular we will investigate manganese-tolerant anode materials.

Approach

- Explore, synthesize, characterize and develop inexpensive materials that have a potential around 500 mV above that of pure Li (to minimize risk of Li plating and thus enhance safety) and have higher volumetric energy densities than carbon.
- Place emphasis on simple metal alloys/composites, and specifically on understanding and mitigating capacity fade. All materials will be evaluated electrochemically in a variety of cell configurations, and for thermal and kinetic stability.

Accomplishments

- Developed a program to understand the cycling of pure metal and alloy anodes that will lead to the mitigation of capacity fading and thus to the possible use of metals in place of carbonaceous materials.
- Determined that pure tin in the foil form can be charged and discharged for at least 10 cycles with no loss of capacity.

Future Directions

- Improve the electrochemical performance of the materials identified.
- Identify the cause of capacity fade in simple metal and metal alloy anodes.
- Investigate the impact of starting with materials in different morphological forms, such as Exmet *vs.* bulk foil.

The goal of this project is to identify low-cost, low-weight anode materials that are safer than the presently used carbonaceous materials and are compatible with next-generation cathode materials. Although carbonaceous materials are being successfully used in the Sony Li-ion cells, there are safety issues as the capacity increases. Aluminum is the ideal anode material, being low cost, readily available and forming a simple alloy with lithium, LiAl. However, it does not cycle well in carbonate electrolytes, in contrast to ether electrolytes where it was successfully coupled with TiS_2 (Exxon-1978).

As agreed in the Annual Plan we are now generating a plan to build a better understanding of the capacity loss in simple binary metal systems, particularly for carbonate-based electrolyte systems. For example $MnSn_2$ cycles well for a few cycles then decays rapidly. There is a complete reaction (turnover) of the Sn of around five before degradation sets in, indicating that the compound is inherently reversible. We will compare this system with the SnBi eutectic, wherein Sn and Bi are present as separate species and no compound formation occurs on Li removal.

This year's major emphasis was on understanding the behavior of pure Sn as an anode material, as it can be used without the addition of any conductive diluent like carbon or a binder. This will then be a reference for all other Sn-containing anode compositions.

Commercial Sn foil was rolled and used as-is as the electrode in a carbonate based electrolyte cell with a pure Li counter-electrode. The cycling capacity is shown in Fig. 6, and as can be seen, the capacity is essentially maintained for more than ten cycles before a marked fall-off is observed. The maximum capacity observed is about 3.6 Li/Sn rather than the expected $Li_{4.4}Sn$.

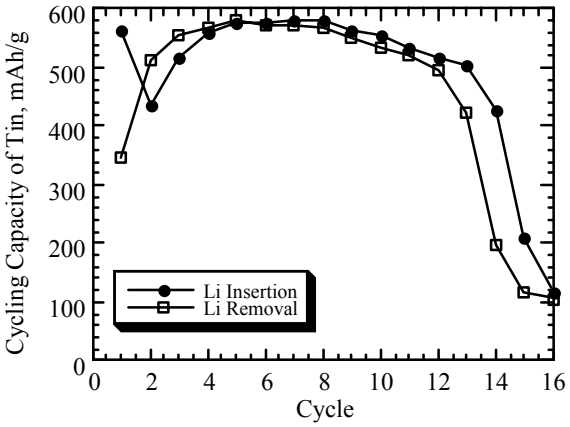

Figure 6. Cycling of Sn foil at 3 mA/cm^2.

In an attempt to determine what might be causing the capacity fall-off, an impedance study was carried out on almost completely discharged Sn electrodes as a function of the number of cycles completed. The preliminary results are shown in Fig. 7. It can be seen that the cell impedance increases at the same time as the cell capacity decreases. There is clearly a correlation here, and we are now determining the source of this impedance increase and why it should suddenly increase at about ten cycles.

The pure Sn foil cycles much better than electrodeposited Sn, and is comparable to Cu_6Sn_5 formed by heating Sn deposited on Cu (Tamura et al, *J. Power Source,s* **107,** 48-55 (2002) , and Sn_2Mn as shown in Fig. 8.

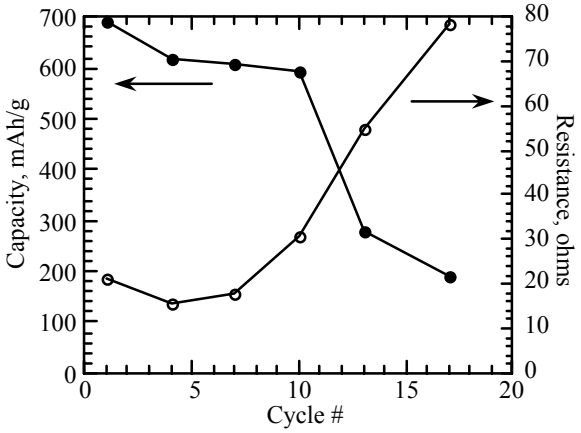

Figure 7. Capacity of Sn foil and cell resistance as function of cycling.

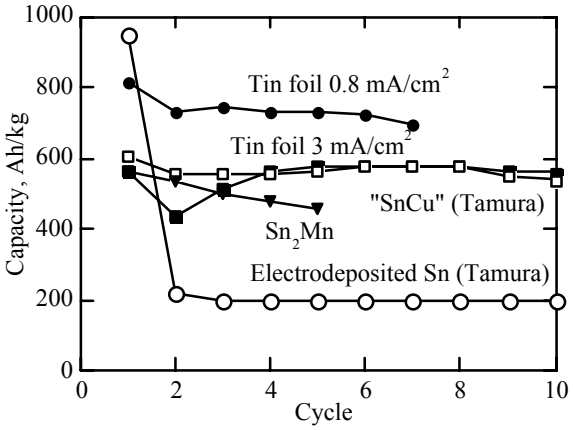

Figure 8. Cycling of tin materials in Li cells.

Presentation

S. Yang, P.Y. Zavalij and M.S. Whittingham, "Sn and SnBi Foil as Anode Materials for Secondary Lithium Battery," *MRS Meeting*, Boston, MA December 2002.

Optimization of Anodes for Li-Ion Batteries

*M. David Curtis, Gholam-Abbas Nazri and Tad Malinski**
*University of Michigan, Department of Chemistry, Ann Arbor MI 48109-1055; *(Ohio University)*
(734) 763-2132, fax: (734) 763-2307; e-mail: mdcurtis@umich.edu

Objective

- Improve the overall safety, cycle life, shelf life, and overall energy density of the Li-ion battery through the development of a novel composite anode with no irreversible capacity loss during initial cycles, and with high-power rate capability.

Approach

- Develop composite anodes through prelithiation of oxides, nitrides, and phosphides (of metals capable of alloying with Li) to remove the irreversible capacity loss and provide high-performance anodes with thermal and chemical stability for application in large Li batteries.
- Engineer the composite anode to be compatible with the existing Li-ion chemistry.
- Use composite anode to provide a new opportunity to construct Li cells using lower-cost and available electrolytes.

Accomplishments

- Prepared a novel composite anode with almost zero irreversible capacity loss during initial charge-discharge cycles.
- Developed a mechanomilling process to eliminate the irreversible capacity loss of oxide, nitrides, and phosphide anodes.
- Investigated the energy density of the composite anode, and monitored the charge-discharge cycling performances of the composite anodes.

Future Directions

- Continue development and scale-up of process to make stable and safe anodes for large Li batteries.
- Test performance of the composite anode in the presence of low-cost propylene carbonate (PC) based electrolytes.
- Test the prelithiated composite anode against high-capacity and high-rate cathodes for EV and HEV applications.

The safety and stability of the anode/electrolyte interface are major concerns for further development of large Li batteries for EV and HEV applications. Alternative anodes such as oxides, nitrides, and phosphides with energy densities much higher than the current carbonaceous anodes have been proposed. These alternatives have large ICLs during initial charge-discharge cycles and are impractical for application in large battery modules and packs. This work has been focused on the development of a safe composite anode with no ICL during initial cycles and with much higher energy density and rate capability than the current carbonaceous and graphitic anodes. The preparation of the new composite anodes involves the mechanomilling process of oxides, nitrides, or phosphides with Li-containing precursors according to the reaction pathways shown in Fig. 9.

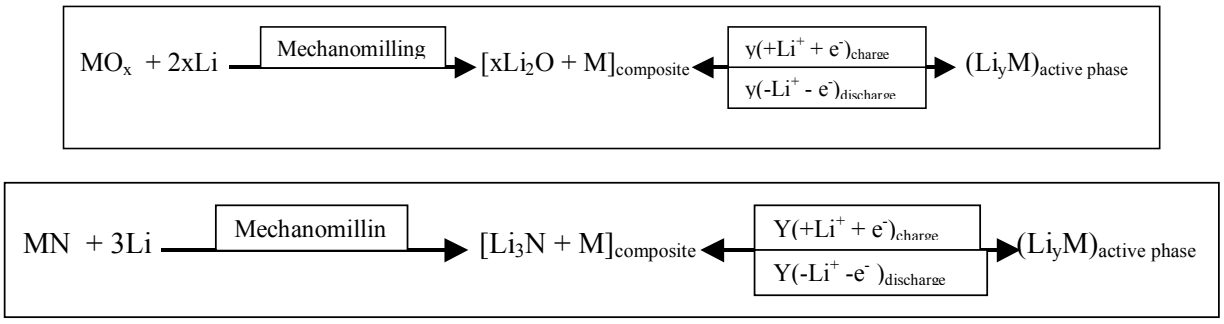

Figure 9. Mechanomilling Process.

The large ICL of oxides, nitrides, and phosphides are removed by mechanomilling of the alternative anodes with Li-containing precursors. During this process a nano-scaled metal phase is formed and protected by the ionic coating (Li_2O, Li_3N, or Li_3P). The metal cluster inner-core serves as an active anode, and the ionic coating serves as a Li^+-conducting membrane to protect the inner core and prevent electrolyte decomposition during Li alloying and dealloying processes (charge and discharge). We have studied several oxides and nitrides using the mechanomilling process. Anode plates were made and tested in conventional multi-blend carbonate-based electrolyte, (EC-DMC-PC, 50:30:20, containing 0.8M $LiPF_6$). Results of electrochemical charge-discharge cycles are shown in Fig. 10. The best result in terms of charge-discharge cycles were observed for oxides with higher oxygen content; $SnO_2 > Sb_2O_3 > Sn_3N_4 > SnO$. The results indicate that the lithium oxide coating provides a more protective film than the lithium nitride films. In order to completely eliminate the first ICL of the anode, we have investigated the PbO as a model compound, where we added a small amount of electrolyte (10 ml to a 20 gram batch) to the ball-milled sample and milled again for a short period (1-2 hrs). The performance of the new composite was studied and compared with PbO milled with Li, without addition of electrolyte. Figure 11 shows less initial capacity for the new composite (black dots), however, the capacity of the new composite was improved by cycling and a higher capacity was obtained after many charge-discharge cycles.

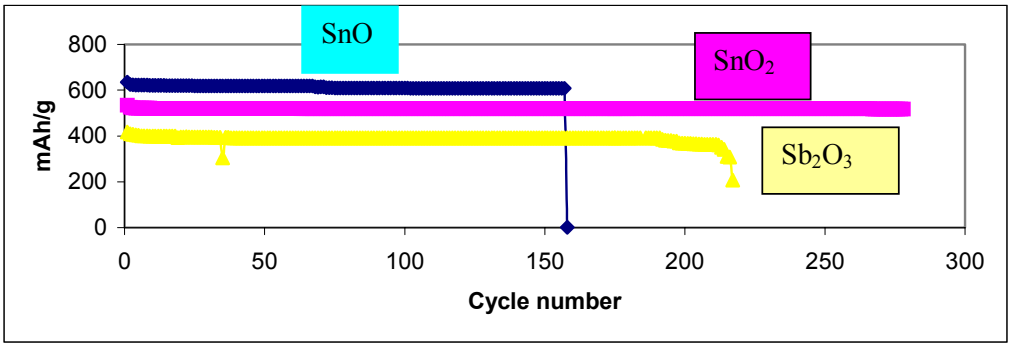

Figure 10. Cell capacity *vs.* cycle number.

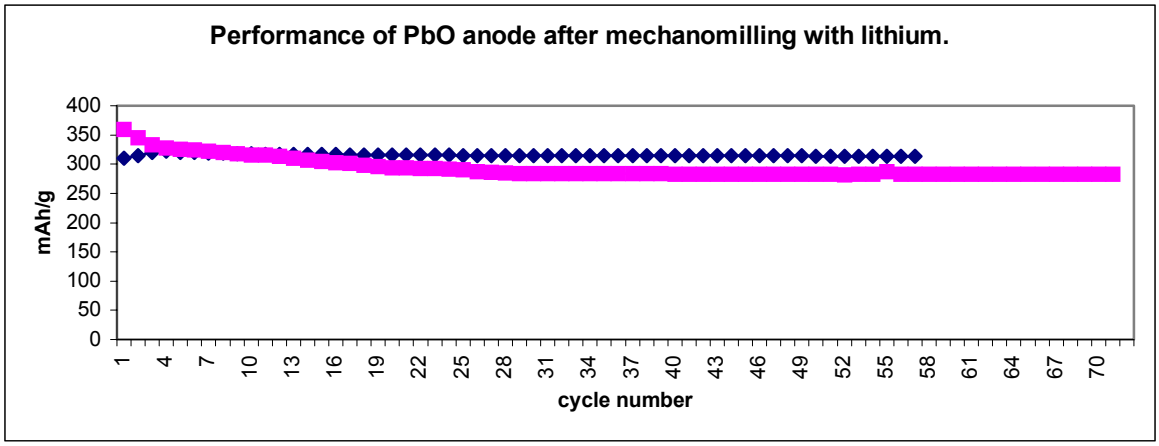

Figure 11. Cell capacity *vs.* cycle number.

ELECTROLYTES

R&D for Advanced Lithium Batteries

Nitash Balsara and John B. Kerr
University of California, Lawrence Berkeley National Laboratory, MS 62R0203, Berkeley, CA 94720-8253
(510)-486-6279, fax (510)-486-4995; email: jbkerr@lbl.gov

Objectives

- Determine the feasibility of the Li metal electrode with organic electrolytes and provide operating conditions that prevent dendrite growth.
- Determine the limitations on Li-ion transport in polymer electrolytes and composite electrodes and develop materials capable of ambient temperature operation with Li metal.
- Determine the limits of stability of organic electrolytes at high-voltage cathode materials (4V) and develop materials and methods to increase stability.

Approach

- Combine synthesis, analysis, modeling, and testing in an approach to electrolyte design, thereby ensuring that not only are the sources of poor performance and failure pinpointed but the problems can be corrected through as-developed materials design and synthesis capabilities.

Accomplishments

- Made quantitative estimates of the properties of polymer electrolytes needed to inhibit dendrite growth sufficiently to meet USABC requirements.
- Showed that polymer electrolytes containing trimethylene oxide solvating units provide significant increases in conductivity and salt diffusion coefficients, which can be clearly related to depression of the glass transition temperature (T_g).
- Performed experiments with addition of nano-particulate filler materials to polymer electrolytes and showed that the widely reported improvements in ion transport properties are due to entrainment of water or other impurities.
- Used polarization experiments on Li half cells combined with impedance measurements to demonstrate that a component of the interfacial impedance is due to salt concentration profiles that lead to phase changes close to the electrode surfaces.

Future Directions

- Carry out detailed quantitative measurements of the transport and mechanical properties of polymer electrolytes to optimize transport *vs.* interfacial behaviors to minimize dendrite growth.
- Prepare and optimize polymers with new ion-solvating groups and appropriate architectures to achieve ambient-temperature operation with polymer electrolytes.
- Develop polymer electrolyte systems capable of operation with 4-volt cathodes and Li metal electrodes.

Links between Dendrite Growth and Mechanical and Transport Properties

Polymer electrolyte properties that affect the growth of dendrites on Li metal electrodes have been identified and measured. Minimum values have been estimated that are required to inhibit dendrite formation These values change as the cell geometry changes, but important properties at the temperature of operation include shear modulus (>6 MPa), conductivity (>5 x 10^{-4} S/cm), salt diffusion coefficient (>4 x 10^{-8}cm^2/s), transference number (t^0_+ >0.3), T_g of polymer (< -70^{o}C), T_g of polymer electrolyte (*e.g.,* 3 molar Li salt T_g< -60^{o}C), a single T_g in dynamic mechanical analysis to indicate uniformity of cross-linking, and morphology profile variations in Atomic Force Microscopy (AFM) after cross-linking <10 nm. Some impurities such as

fumed silica (10%) and BHT (1000 ppm) appear to be tolerable.

Polymers with Improved Ion Transport Properties in the Bulk and at Interfaces

New polymer structures have been prepared with conductivity that is superior to what has been achieved to date with PEO-based polymers. In collaboration with modeling groups (G. Smith, O. Borodin, L. Curtis and J. Halley), who provided theoretical guidance, the polymer structures have evolved from linear PEO-like materials to comb-branch polymers with side chains that contain trimethylene oxide (TMO) solvating groups. Although the TMO groups appear to have little influence on the activation energy involved in Li-ion transport, they greatly reduce the dependence of T_g upon salt concentration. Preliminary experiments show a reduced interfacial impedance compared with PEO, indicating that the surface layers of polymer remain more mobile than PEO.

Composite Polymer Electrolytes

Careful preparation of composite polymer electrolytes with added fumed silica nano-particles (8 nm diameter) such that water is completely excluded shows that the presence of the particles reduces the conductivity and the salt diffusion coefficient. Rheology experiments show that the modulus increases with added filler. Literature reports of increased ion transport appear to be due to adventitious water trapped by the particles.

Property Changes at (Electrode) Surfaces

Impedance measurements of cycled Li half-cells show a time dependence for the interfacial impedance following polarization. These observations are consistent with relaxation of the concentration gradients at the electrodes. The dependence of T_g with salt concentration and the inhibition of segmental motion by the surfaces (as described with fillers) indicate that quite different transport properties and even ion transport mechanisms exist in the interfacial layers that extend out into the bulk. These effects should have a considerable impact upon the operation of composite electrodes and may be mitigated by use of single-ion conductors containing low-T_g groups (*e.g.,* TMO).

Publication

J.B. Kerr, S.E. Sloop, G. Liu, Y.B. Han, J. Hou and S. Wang, "From Molecular Models to System Analysis for Lithium Battery Electrolytes," *J. Power Sources*, **110(2)**, 389-400 (2002).

Composite Polymer Electrolytes for Use in Lithium and Lithium-Ion Batteries

Saad A. Khan, Peter S. Fedkiw and Gregory L. Baker*[+]
Department of Chemical Engineering, North Carolina State University, P.O. Box 7905, Raleigh NC 27695-7905;
[+]*Department of Chemistry, Michigan State University, East Lansing, MI 48824-1322*
**(919) 515-4519; Fax: (919) 515-3465; e-mail: khan@eos.ncsu.edu*

Objective

- Develop composite polymer electrolytes (CPEs) that are low cost, have high conductivities, impart electrode-electrolyte interfacial stability, and yield long cycle life.

Approach

- Use surface-functionalized fumed silica fillers in BATT baseline systems to determine the effects of filler type and concentration on interfacial stability and cell cycling.
- Utilize a combination of electrochemical characterization, rheological techniques, and chemical syntheses to correlate electrochemical characteristics with mechanical properties and materials chemistry (*e.g.,* silica-type or PEO-type).

Accomplishments

- Determined that the presence of fumed silica in CPEs increases rate capabilities and electrochemical efficiency of Li/V_6O_{13}.
- Investigated the effect of the addition of fumed silica into high-molecular-weight (MW) PEO on transport properties (conductivity) and rheological properties.
- Studied the interfacial stability of Li/Li and full-cell cycling of Li/V_6O_{13} using high-MW PEO.

Future Directions

- Determine how fumed silicas (hydrophobic R805 and hydrophilic A200) affect transport and rheological properties of mixed-MW (low + high MW) polymer electrolytes.
- Investigate the interfacial stability and full-cell cycle studies of mixed-MW polymer + fumed silica system.

The objective of this research is to develop a new range of CPEs for use in rechargeable Li and Li- ion batteries. In particular, our goal is to develop highly conductive electrolytes that exhibit good mechanical properties, and at the same time show good compatibility with typical electrode materials. The unique feature of our approach is the use of surface-functionalized fumed silica fillers to control the mechanical properties of the electrolytes and enhance electrode-electrolyte interfacial stability.

Rate capabilities of Li/V_6O_{13} using low-MW PEO

We have previously demonstrated that fumed silica stabilizes the Li/electrolyte interface, and effectively suppresses Li dendrite growth using low-MW PEOs. We have also demonstrated that adding fumed silica significantly improves the capacity fading during cycling using full cells of Li/$LiCoO_2$, Li/$LiMn_2O_4$, and Li/V_6O_{13} cells. In this fiscal year, we investigated the rate capabilities of Li/V_6O_{13} cells using fumed silica-based CPEs. Specific discharge capacity and electrochemical efficiency are improved at middle to high C-rates (C/10 to C/2). Figure 12 shows the average coulombic efficiency over the first 20 cycles as a function of C rate for the different electrolytes studied. For liquid electrolytes, a near unity coulombic efficiency appears at C/15, but with increasing C rate the coulombic efficiency drops rapidly to 71% at C/5. Compared with liquid electrolyte, the coulombic efficiency for the composite gel electrolytes is stable at about 99%, even at C/2 (1.19 mA/cm^2).

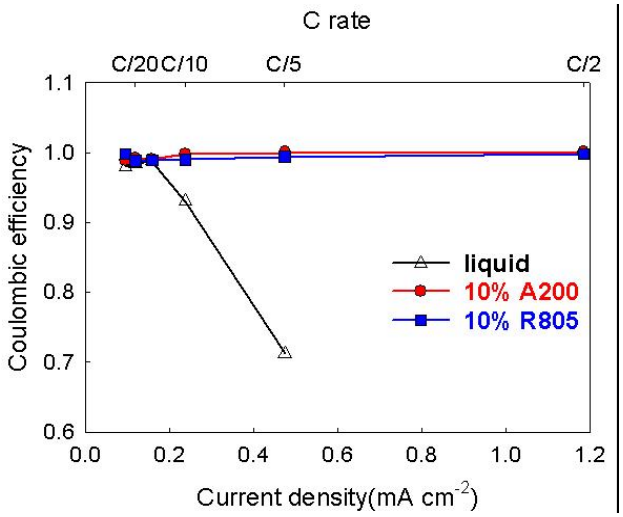

Figure 12. Average coulombic efficiency during first 20 cycles *vs.* current density for Li/V_6O_{13} cells using three different electrolytes: (1) LiTFSI + PEG-dM (250) (Li:O=1:20); (2) LiTFSI + PEG-dM (250) (Li:O=1:20) + 10% A200; (3) LiTFSI + PEG-dM (250) (Li:O=1:20) + 10% R805. Current density from 0.095 (C/25) to 1.185 (C/2) mA/cm^2; voltage range 1.8 to 3.0 V; room temperature; cathode material V_6O_{13} at a loading of 5.8 mg/cm^2; liquid electrolyte could not be cycled at C/2.

Effects of fumed silica on conductivity using high-MW PEO

We have investigated the effect of adding fumed silica into baseline high-MW polymer. Composite polymer electrolytes are obtained by dispersing fumed silica particulates into PEO (MW=200K or 600K) + LiTFSI. We have found that addition of 10% fumed silica causes high-MW PEO to exhibit solid-like behavior (*i.e.,* flat G′ at low frequency) at 80°C, above the melting point of PEO. This ability of fumed silica to produce a mechanically strong

network structure might be exploited to extend the useful temperature range of PEO-based electrolytes. Adding nanoparticles of fumed silica improves the rheological properties of polymer electrolytes, whereas the addition of fillers can be either beneficial or detrimental to ion-transport behavior. In crystalline polymer electrolytes, adding nanofillers increases the conductivity as the crystallinity decreases. In amorphous polymer electrolytes, adding fillers decreases conductivity according to a volume-dilution effect. X-ray diffraction (XRD) and differential scanning calorimetry (DSC) results taken together indicate that fumed silica addition increases the conductivity through a decrease in crystallinity.

Interfacial stability and full-cell cycling using high-MW PEO

We have found that adding fumed silica improves the stability of the Li/composite polymer electrolyte interface: the voltage of a Li/CPE/Li cell oscillates at high frequency without fumed silica present in the electrolyte but the cell voltage is more stable with fumed silica present, which is similar to behavior observed in the low-MW PEO system. We have also demonstrated that fumed silica improves cycle performance of Li/CPE/V_6O_{13} full cells.

Publications and Presentations

Y. Li, P.S. Fedkiw and S.A. Khan, "Lithium/V_6O_{13} Cells Using Silica Nanoparticle-Based Composite Electrolytes," *Electrochim. Acta,* **47**, 3853 (2002).

J. Zhou, P.S. Fedkiw and S.A. Khan, "Interfacial Stability between Lithium and Fumed-Silica Based Composite Polymer Electrolytes," *J. Electrochem. Soc.*, **149**,1121 (2002).

H.J. Walls, M.W. Riley, R.J. Spontak, P.S. Fedkiw and S.A. Khan, "Nanocomposite Electrolytes from Fumed Silica and Clay," *International Polymer Electrolytes Conference*, Santa Fe, NM, August 2002.

H.J. Walls, P.S. Fedkiw and S.A. Khan, "Electrophoritic NMR Measurement of Lithium Transference Numbers in Composite Electrolytes," *International Polymer Electrolytes Conference,* Santa Fe, NM, August 2002.

P.S. Fedkiw, "Electrolytes Based on Fumed Oxides for Rechargeable Lithium Batteries," *invited talk*, University of Iowa, December 2002.

Y. Li, P.S. Fedkiw and S.A. Khan, "Electrochemical Performance of Nanocomposite Gel Electrolyte," *National Academy of Engineering Regional Meeting*, Raleigh, NC, May 2002.

Y Li, P.S. Fedkiw and S.A. Khan, "Self-Discharge of V_6O_{13}/Li Cells Using a Fumed Silica-Based Composite Electrolyte," *11th International Meeting on Lithium Batteries*, Monterey, CA, June 2002.

H.J. Walls, P.S. Fedkiw and S.A. Khan, "Yield Stress and Wall Slip Phenomena in Colloidal Silica Gels," *Society of Rheology Conference*, Minneapolis, MN, October 2002.

Y. Li, J.A. Yerian, P.S. Fedkiw and S.A. Khan, "Effect of Silica Nanoparticles on PEO-LiTFSI Polymer Electrolytes," *202nd Meeting of the Electrochemical Society*, Salt Lake City, UT, October 2002.

J.A. Yerian, P.S. Fedkiw and S.A. Khan, "Role of Monomer in the Reactions of Cross-linkable Fumed-Silica Based Electrolytes," *202nd Meeting of the Electrochemical Society*, Salt Lake City, UT, October 2002.

New Battery Electrolytes based on Oligomeric Lithium bis((perfluoroalkyl)sulfonyl)imide Salts

Darryl D. DesMarteau[1] and Stephen E. Creager[2]
Department of Chemistry, Clemson University, Clemson, SC 29634-0973.
[1](864) 656-4705, fax: (864) 656-6613, email fluorin@clemson.edu
[2](864) 656-4995; email screage@clemson.edu

Objectives

- Develop methods for synthesizing oligomeric ionene d Li salts based on the bis((perfluoroalkyl)-sulfonyl)imide anions.
- Develop methods for preparing solid polymer electrolytes (SPEs) from the target salts.
- Acquire data on the ionic conductivity and Li transference of the target SPEs at variable temperature and composition.

Approach

- Synthesize salts using methodologies developed at Clemson over the last 15 years (D. DesMarteau, *J. Fluorine Chem.* 1995, 72, 203-208). SPEs will be prepared from crosslinked low-MW polyethylene glycol (PEG) and also non-crosslinked PEG for comparison. Conductivities will be measured using electrochemical impedance spectroscopy (EIS).

Accomplishments

- Synthesized small quantities (<10 g) for testing purposes of a new series of Li salts of general structure $F_3CSO_2N(Li)[SO_2N(CF_2)_xSO_2N(Li)]_nSO_2CF_3$, for the following values of x and n: n=1, x=2,4,6,8; n=3, x=4,6,8; n=5, x=4,6; n=17, x=4,6
- Prepared SPEs from the above-cited salts using non-crosslinked and also crosslinked PEO/PEG as host matrix
- Characterized the resulting SPEs using impedance spectroscopy to study ion transport, and DSC and wide-angle x-ray diffraction (WAXD) to study thermal and structural properties.

Future Directions

- Synthesize oligomeric salts with average n values near 4 , 8, 16, 30 and 100, for $R_f = (CF_2)_{4,6}$, and with other R_f linkers between imide groups, containing ether links and longer $–CF_2-$ segments. The effort will result in sufficient samples for electrochemical testing using EIS, and also using DSC and WAXD.
- Use nuclear magnetic resonance (NMR) and electrochemical (galvanostatic polarization) methods to evaluate anion and cation transport, and Li transference, in SPEs prepared using the target salts.
- Pursue exploratory studies of gel electrolytes prepared from the target salts.
- Synthesize several new allyl ether Li salts for use by other BATT program workers in preparing single-ion conductors for Li.

Research under BATT support between Oct 2001 and Sept 2002 was focused on the preparation and characterization of a series of new oligomeric Li salts, and SPEs from those salts, in which the anion has an oligomeric structure illustrated in Scheme 1. It is expected that SPEs containing these salts will possess both very high conductivity due to the low lattice energy of salts containing imide anions, and also high Li transference due to the expected low mobility of the anions due to entanglement with the matrix.

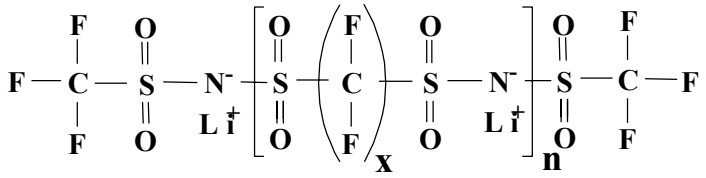

Scheme 1 . Ionene lithium salts with a perfluorohexyl chain linking imide anions.

Synthesis of new salts

A general method was developed for synthesizing oligomeric imide-based Li salts of fixed anion size and oligomer length. The method involves a series of stoichiometric sequential coupling reactions between difunctional reactants, always with one reactant in large excess. A sample reaction scheme is presented in Scheme 2 for synthesis of a dianion. This method was used to prepare a broad range of salts with the general structure in Scheme 1. Specifically, salts were prepared with n and x values as follows: n=1, x=2,4,6,8; n=3, x=4,6,8; n=5, x=4,6; n=17, x=4,6.

Preparation and characterization of SPEs containing the new salts in crosslinked PEG

SPEs were prepared by dissolving salts and PEO host in DMF and removing solvent by evaporation. The crosslinking agent was 4,4',4"-methylidyne-tris(4-phenylisocyanate), which was also added to the formulation to prepare SPEs with crosslinked PEG as host. Figure 13 presents some representative variable-temperature conductivity data, presented in an Arrhenius format, for a SPE with an EO/Li ratio of 10:1. Conductivities of SPEs prepared using crosslinked PEG are consistently less than those for SPEs prepared using non-crosslinked, hi-MW PEO, which probably reflects a greater overall retardation of ion motion in the crosslinked SPEs. The ordering of the different salts with respect to their conductivity is different in crosslinked and non-crosslinked hosts, which again suggests that the anions interact quite strongly with the host. A consequence of this finding is that the optimal anion size/structure for achieving high Li transference and high conductivity may not be the same in crosslinked and non-crosslinked hosts.

Publications

O.E. Geiculescu, J. Yang, R. Bailey-Walsh, G. Shafer, S.E. Creager, W.T. Pennington and D.D. DesMarteau, "Solid Polymer Electrolytes from Dilithium Salts Based on New bis[(perfluoroalkyul)sulfonyl]imide Dianions. Preparation and Electrical Characterization," *Solid State Ionics* **148**, 173-183 (2002).

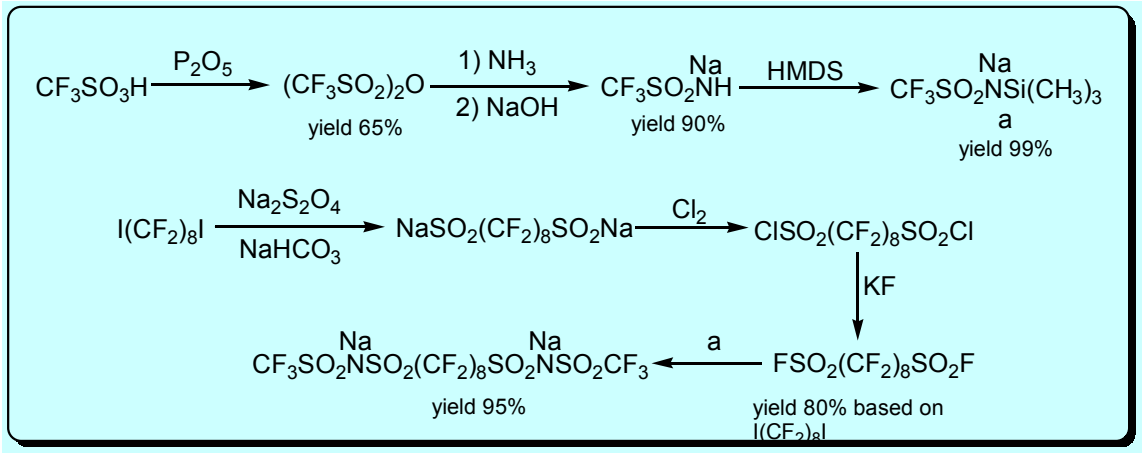

Scheme 2. Preparation scheme for a di-imide Li dimer salt.

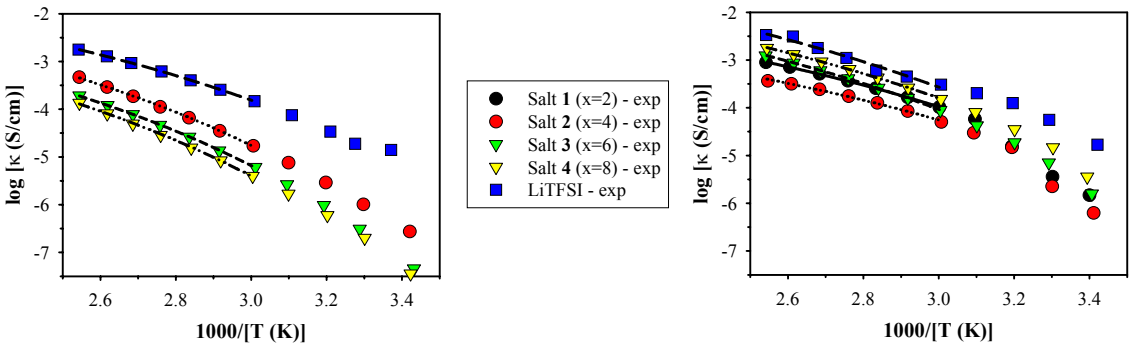

Figure 13. Arrhenius plots for SPEs prepared from dimeric di-imide Li salts using crosslinked (left) and non-crosslinked (right) PEG hosts. The EO/Li ratio for these SPEs was 10:1.

A Molecular Dynamics Simulation Study of the Influence of Polymer Structure on Complexation Thermodynamics, Kinetics and Transport of Lithium Cations in Polyether-based Solid Polymer Electrolytes

Oleg Borodin and Grant D. Smith
Department of Material Sciences and Engineering, University of Utah, 122 S. Central Campus Dr., Rm 304, Salt Lake City, UT 84112-0560
(801)585-3381, fax (801) 5814816, e-mail: gsmith2@gibbon.mse.utah.edu

Objectives

- Understand influence of polymer structure and polymer-ions interaction on ion aggregation and transport in polymer electrolytes.
- Provide guidance to rational design of novel polymer electrolytes.

Approach

- Employ *ab initio* quantum-chemistry calculations to obtain energetics of polyether complexes with Li-salts and use these data to develop classical force fields for polyether/$LiBF_4$.
- Use atomistic molecular dynamics (MD) simulations of polyether-based Li/polymer electrolytes to examine the influence of polyether structure, strength of the polyether-lithium and Li-anion interactions and barrier of conformational isomerization reaction on ion transport.

Accomplishments

- Developed quantum-chemistry based force fields for poly(ethylene oxide) (PEO), poly(methylene oxide) (PMO), poly(trimethylene oxide) (PTMO), poly(propylene oxide) (PPO), and a copolymer of poly(ethylene oxide-trimethylene oxide) (PEO-TMO) and their interactions with $LiBF_4$.
- Performed molecular dynamics simulations on PEO, PMO, PTMO, PPO, PEO-TMO melts. The initial simulations of these polyethers doped with $LiBF_4$ salts are currently being performed.
- Examined the influence of the strength of the polyether-Li and Li-anion interactions, and barrier of conformational isomerization reaction on ion aggregation and transport.

Future Directions

- Develop *ab initio* quantum chemistry based classical force fields and perform molecular dynamics simulations of polyether-based comb-branch copolymers, single-ion conductors and gel electrolytes in order to provide guidance to the experimental efforts aimed at development of novel single-ion conductors and gel electrolytes through synergetic experimental-MD simulations studies.

Influence of polymer-salt interactions on ion aggregation and transport

Optimization of transport properties of polymer electrolytes is a complicated task involving many variables such as polymer-cation and cation-anion interactions, polymer conformational dynamics. Experimental examination of the above parameters on ion aggregation and transport is expensive and cumbersome, hindering progress toward fundamental understanding of polymer electrolytes, whereas atomistic molecular dynamics simulations can be readily used to investigate influence of the polymer-salt interactions on ion aggregation, self-diffusion coefficients, and conductivity in high-temperature polymer electrolytes. PEO doped with $LiBF_4$ at (ether oxygen):Li ratio of 15:1 at 393 K has been selected as a reference point for the parametric investigation. A two-body force field with an approximate mean-field like treatment of polarization interactions has been used. Polarization interactions accounting for approximately 30% of the PEO-Li^+ complexation energy have been varied from 50 to 200% of the original force field covering the range of systems from polymer electrolytes with less than 1% of free Li^+ cations (*e.g.,* only 1% of cations not having any anions in its first coordination shell) to those with almost all (92 %) of Li^+ cations being free from anions in their first coordination shell as shown in Fig. 14. An increase in polarization interaction between polymer and Li^+ resulted in a monotonic increase in the fraction of free cations and a decrease in cation self-diffusion coefficient for the free ion fraction higher than 22 % as shown in Fig. 14. These two factors have an opposite effect on conductivity of polymer electrolytes: an increase in the fraction of free charge carriers (Li^+) increases conductivity, whereas a decrease in ion self-diffusion decreases conductivity. Our simulations demonstrate that over wide range of parameters (22-92 % of free ions) the polymer electrolyte conductivity changes less than 2 times as the benefits of an increase in the fraction of charge carriers on conductivity with increasing polymer-Li^+ interactions are lost due to diminished ion mobility. Indeed, an effect of a 4-times increase in the fraction of free ions from 24 to 92% on conductivity is offset by a roughly 2- times drop of the ion self-diffusion coefficient resulting in only a modest increase in conductivity, *e.g.*, slightly less than 2 times. An effect of the initial increase in the fraction of free ions (from less than 1 to 22%) on conductivity is more dramatic (e.g. an order of magnitude) than the one observed for the range of free ion fraction from 24 % to 92 % due to significantly higher fraction of free ions (22% *vs.*<1%) and comparable ion self-diffusion coefficients between two systems.

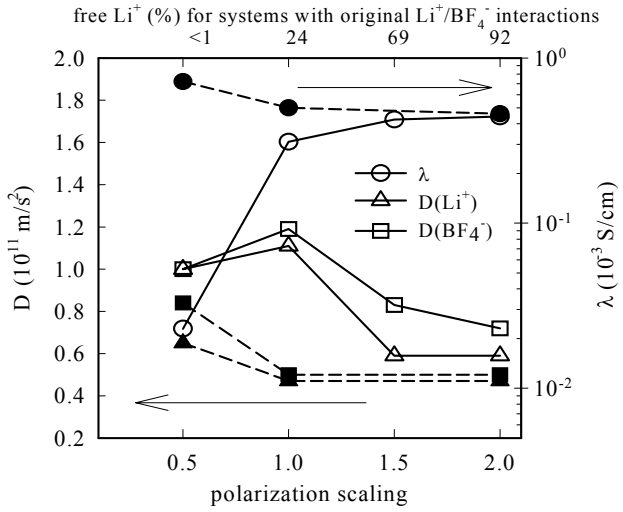

Figure 14. Conductivity (λ) and ion self-diffusion coefficient (D) as a function polarization for PEO/$LiBF_4$ with original Li^+/BF_4^- interactions (open symbols) and Li^+/BF_4^- repulsion increased by a factor of three (closed symbols).

At the next stage we investigated the effect of polymer-Li^+ complexation energetics on ion transport for polymer electrolytes in which nearly all ions are dissociated and thus no ion pairs or aggregates exists. Ion dissociation was facilitated by increasing repulsion between cation and anion by a factor of three resulting in the PEO/$LiBF_4$ systems with no ion pairs or aggregates. MD simulations revealed that the fully dissociated PEO/$LiBF_4$ systems exhibited qualitatively different behavior of conductivity as a function of polymer-Li^+ interaction shown in Fig. 14 from the previously described systems with the partial ion aggregation. In fully dissociated systems a decrease of the polymer-Li^+ interaction was found to enhance conductivity, whereas in the system with partial aggregation the effect was the opposite suggesting that different strategies should be applied for enhancing conductivity in partially aggregated and fully dissociated polymer electrolytes.

A separate set of MD simulations of PEO/$LiBF_4$ employing potentials with various PEO conformational barriers revealed that ion transport is intimately connected to polymer conformational

dynamics, allowing improvement of ion conduction by lowering conformational barriers.

MD simulations of polyethers doped with $LiBF_4$

Quantum chemistry based force fields have been developed for poly(ethylene oxide) (PEO), poly(methylene oxide) (PMO), poly(trimethylene oxide) (PTMO), poly(propylene oxide) (PPO), and a copolymer of poly(ethylene oxide-trimethylene oxide) (PEO-TMO) and their interactions with $LiBF_4$. Molecular dynamics simulations have been performed on PEO, PMO, PTMO, PPO, PEO-TMO melts with a similar number of backbone atoms (≈160). Good agreement with dielectric spectroscopy experiments and NMR data were observed where data were available. Local dynamics of the melts were measured through backbone atom mean-square displacements and dynamic structure factor and was found to follow the order PMO<PPO<PEO≈PEO-TMO≈TMO. Initial simulations at 393 K of these polyethers doped with $LiBF_4$ salts are currently been performed indicating that their conductivity of polyethers will also follow the same order as the polymer dynamics, e.g. PMO<PPO<PEO≈PEO-TMO≈TMO in agreement with the experimental observations.

Highly Conductive Rigid Polymers

Duward F. Shriver and Semyon Vaynman***
**Chemistry Department, Northwestern University, Evanston, IL 60208*
***Department of Materials Science and Engineering, Northwestern University, Evanston, IL 60208*
(847) 491-5655; fax: (847) 491-7713; e-mail: shriver@chem.northwestern.edu, svaynman@northwestern.edu

Objectives

- Synthesize a new class of rigid polymer electrolytes.
- Test rigid polymer electrolytes in rechargeable Li batteries.

Approach

- Synthesize new types of polymer electrolytes that contain a rigid polymer rather than the flexible low-T_g polymers used in conventional polymer electrolytes.
- Fabricate electrochemical cells with these electrolytes and evaluate their performance.
- Correlate the performance of electrolytes in the cells with their chemical structure and their reactivity toward components of the electrochemical cell.

Accomplishments

- Synthesized highly conductive rigid polymer electrolytes that contain functional groups such as carboxy and sulfone and tested them in cells. Polymer-salt complexes that contain carboxy groups have higher ionic conductivity than similar polymer-salt complex that contains sulfone (appr. 10^{-4} S/cm *vs.* $5x10^{-6}$ S/cm at room temperature). However, the polymer-salt complexes that contain carboxy groups are unstable toward Li; they form very resistive interface with Li. Much less-resistive layers are formed between Li metal and sulfone-containing rigid polymer electrolytes.
- Incorporated rigid polymer electrolytes into Li cells. The capacity of the cells with carboxy-containing rigid polymer electrolyte was not satisfactory. The capacity of the cell with sulfone-containing rigid polymer electrolytes was >100 mAh per gram of active cathode material at current density of 15 μA/cm^2. The capacity of the cell was reduced significantly with an increase in current density due to high resistance of that electrolyte.

Future Directions

- This project was completed on May 31, 2002.

During the 2002 FY we continued the synthesis and investigation of the properties of polysulfones (a) - (c) (Fig. 15). The conductivity of the polysulfone (a)-lithium triflate complex is approximately $5x10^{-6}$ S/cm at room temperature. This complex is much more stable toward the Li anode than the complex containing carboxy groups. Due to low ionic conductivity of electrolyte, the capacity of the cells containing the polysulfone (a) - lithium triflate polymer electrolyte was low.

The conductivity of the polysulfone (b)-lithium triflate (2:1 molecular ratio) complex isextremely low; it could not be measured at room temperature. At 60°C the conductivity was ~$3x10^{-9}$ S/cm and this may be due to the low density of cation-coordinating sites in this polysulfone.

The sulfone-containing polymer (c), which has a much higher density of cation-coordinating sites than polysulfone (a or b) was also synthesized. As expected, when doped with lithium triflate in 2:1 molecular ratio, polymer (c) displayed much higher ionic conductivity (~10^{-4} S/cm at room temperature) than polymers (a and b). (Fig. 16). This polymer-salt electrolyte was retested after 2 weeks storage in the glove box and the ionic conductivity was a few orders of magnitude lower. We suspected the decomposition or contamination caused the dramatic conductivity change. The synthesis of polysulfone (c) was repeated several times with fresh starting materials but the high conductivity was not reproduced.

During this project a number of rigid polymers were synthesized. The polymer that contained carboxy group when mixed with lithium triflate exhibited high ionic conductivity. However, the reactivity of this polymer toward Li metal prevents its use in Li batteries. Polymers that contain sulfone groups were found to be much more resistant toward Li metal, but their conductivity was lower than that of carboxy-containing polymer.

This work demonstrates that highly conductive polymer electrolytes (with an ionic conductivity of an order of 10^{-4} S/cm) can be synthesized. Further work is needed to develop new polymer electrolytes that combine good ionic conductivity with redox stability in the battery.

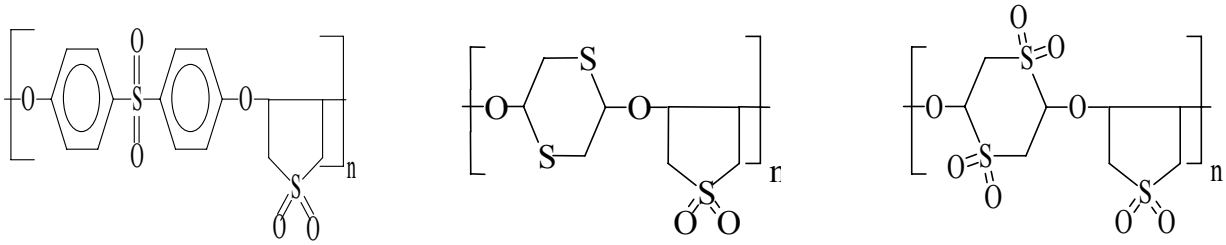

(a) **(b)** **(c)**

Figure 15. Structure of synthesized polysulfones.

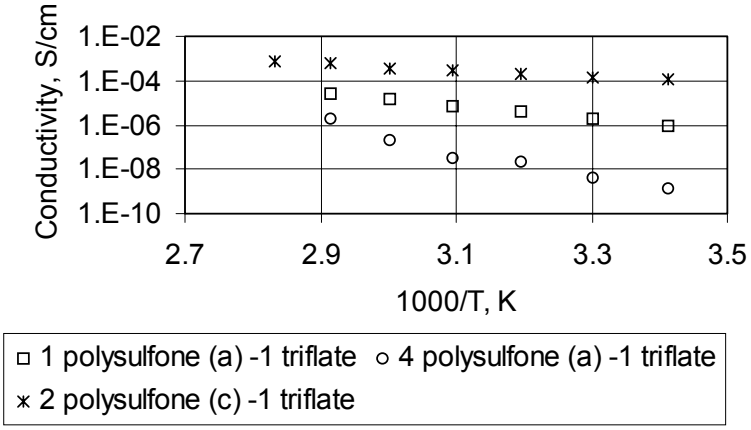

Figure 16. Conductivity of polysulfone (a) and (c) – lithium triflate salt complexes.

Electrolyte Additives

Kim Kinoshita and John B. Kerr
Lawrence Berkeley National Laboratory, MS 62R0203, Berkeley CA 94720-8253
(510)-486-6279, fax (510)-486-4995, email: jbkerr@lbl.gov

Objective

- Identify chemical additives that improve the safety of nonaqueous electrolytes for Li-ion batteries by stabilizing the SEI layer on carbon.

Approach

- Identify species that are incorporated in the SEI layer to improve its stability.
- Conduct electrochemical evaluation of additives to determine the reversible and irreversible capacity loss using the baseline liquid or gel electrolytes.

Accomplishment

- Pyridine stabilizes the thermal reactions of this electrolyte in the bulk of the solutions by intercepting the PF_5 formed from the salt.
- Addition of vinylene carbonate (VC) to the ATD Gen 2 electrolyte in an increase of interfacial impedance on Gen 2 carbon anodes and alters the SEI layer.
- Redox catalysis experiments with VC and similar additives such as methyl benzoate and dicyanobenzene, show that reduction of CO_2 is easier than reduction of EC which in turn is easier than reduction of EMC.

Future Directions

- Use additives such as VC, methylbenzoate and dicyanobenzene to investigate the mechanisms of electrochemical reduction of CO_2, EC and EMC. In particular the effect of ion-pairing due to the presence of Li ions needs to be elucidated.
- Investigate the effect of additives on the build up of impedance in the anode and cathode.
- Investigate the effect of additives on reversible and irreversible capacity loss plus power fade in Li ion cells.

The effect of pyridine as an additive to Gen 2 electrolyte

Thermal treatment of $LiPF_6$-containing electrolytes at > 40°C gives chemical reactions that remove EC, increase transesterification products, and yield polyether carbonate polymers and CO_2 gas. Solutions that do not contain $LiPF_6$ do not react in this manner. Addition of pyridine to the solution suppresses the thermal reactions. It is thought that thus occurs by formation of an adduct between the pyridine, a strong Lewis base, and PF_5, a strong Lewis acid. This adduct does not react with the EC to initiate polymerization. Cyclic voltammetry (CV) and impedance spectroscopy shows that the pyridine reduces on the carbon anode to form a film that interferes with Li intercalation

The effect of addition of additives such as VC into LP40 electrolyte, 1M $LiPF_6$-EC-DEC(1:1 w/w)

The addition of additives such as VC have been found to greatly improve calendar and cycle life in Li-ion batteries according to SAFT. It is generally thought that the reduction of the VC improves the behavior of the anode by forming a film on the electrode that reduces side reactions. We have found evidence in CV and impedance spectroscopy to support this hypothesis. However, we have pursued an alternative scenario regarding the action of such additives. It is known that CO_2 is formed in Li-ion cells and this is reducible at the anode. The products of reduction of CO_2 in PC/R_4NClO_4 on carbon and copper are CO, carbonates and oxalate whereas on Cu in the presence of water the formation of methane, ethane, and ethylene has been reported.

Reduction of CO_2 in the presence of tetra-alkylammonium cations by means of a redox catalyst yields solely oxalate. A redox catalyst is an additive such as VC, methyl benzoate or dicyanobenzene that is able to pass electrons to the compound of interest in solution. Thus the redox catalyst is designated O and its reduced form R:

$$O + e^- \leftrightarrow R$$

$$R + CO_2 \leftrightarrow O + CO_2^{\cdot-}$$

$$2\ CO_2^{\cdot-} \rightarrow {}^-O_2C\text{-}CO_2^- \text{ (oxalate)}$$

The additive is recycled to the electrode and facilitates the reduction of the CO_2. This also occurs with EC and EMC but these compounds are reduced more slowly that CO_2. The oxalate is sufficiently soluble to reach the cathode where it can be re-oxidized to CO_2 resulting in a reversible self-discharge shuttle mechanism. The presence of additives such as VC can increase the reversible self-discharge mechanism at the expense of the irreversible self-discharge mechanism, which results when CO_2 is reduced directly at the anode to CO and carbonate. Experiments are planned with the Cell Development task to measure reversible self-discharge and the effect, if any, of the addition of additives such as VC on this variable. Since reversible self-discharge is not thought to be involved in power fading and impedance rise, this mechanism represents a possible mode of action of VC in Li-ion cells.

Development of Nonflammable Electrolytes for Li-Ion Batteries

Jai Prakash
Illinois Institute of Technology, Department of Chemical and Environmental Engineering,
10 W 33rd Street, Chicago, IL 60616
(312) 567-3639, fax: (312) 567-8874; e-mail: prakash@iit.edu

Objective

- Develop non-flammable electrolytes (NFEs) with high flash point (>100°C), ionic conductivity (10^{-3} S/cm), and wider voltage window (0-5 V *vs*. Li) in an effort to provide better thermal stability and fire safety.

Approach

- Modify existing electrolytes by using novel flame-retardant (FR) additives that are compatible with active electrode materials and the environment.
- Use chemical, electrochemical, and thermal techniques to investigate the stability and performance of electrolytes modified with FR additives.

Accomplishments

- Completed an extensive study on the thermal and electrochemical characterization of the FR additive, hexa-methoxy-tri-aza-phosphazene $N_3P_3[OCH_3]_6$ (HMTAP $N_3P_3[OCH_3]_6$, in Li-ion cells.
- Completed the scale-up synthesis of the flame retardant HMTAP.
- Supplied the HMTAP material to ANL, Electrovaya Company (Canada), and Mitsubishi Chemical Company (Japan).
- Demonstrated the feasibility of using this material as a FR additive in PNGV Li-ion cells.

Future Directions

- This project is complete.

The main focus of this project is to develop electrolytes that meet the criteria for NFEs for Li-ion batteries. Our research in FY 2002 was focused on completing the scale-up synthesis of the FR material hexa-methoxy-tri-aza-phosphazene ($N_3P_3[OCH_3]_6$) and establishing the mechanism of its FR action.

We completed the scale-up synthesis (25 g batch) of the FR hexa-ethoxy-tri-aza-phosphazene (HETAP) and characterized this additive for its structure and purity. The synthesis was carried out by dissolving hexa-chloro-cyclo-triphosphazatriene in pyridine followed by the addition of ethanol. The temperature was maintained at 0-5°C during the addition and the reaction mixture was stored overnight. Diethyl ether was then added in this mixture with stirring, and the pyridinium chloride was removed by filtration. Subsequent distillations produced hexa-ethoxy-cyclotri-phosphazatriene (yield =52%). The FTIR spectra confirmed the molecular structure of the HETAP synthesized. The FTIR spectra of the synthesized HETP compound exhibited two strong absorptions at 2980 and 2934 cm^{-1} (asymmetric stretching of the $-CH_2$ and $-CH_3$ groups), absorption at 2877 and 2819 cm^{-1} (symmetric stretching of the $-CH_2$ and $-CH_3$ groups), and absorption at 1388 and 1364 cm^{-1} (symmetric and asymmetric bending frequency of the ethyl groups). The stretching of P-N and P=N group was also observed at 1213, and 750cm^{-1}. Strong absorption bands at 1262, 1097 cm^{-1} indicated the presence of symmetric and asymmetric stretching of P-O-C group.

The material was then supplied to various organizations including ANL, Electrovaya Co., and Mitsubishi Chemical Co. for its characterization in Li-ion cells. Electrovaya informed us that the HMTP FR additive showed excellent fire safety (70% success rate) in their high capacity Li-ion cells under nail penetration tests.

The thermal properties of the HMTAP in Li-ion cells were investigated in collaboration with ANL using DSC and accelerating rate calorimeter (ARC) methods. It was found that the addition of 5-10 wt% FR additive in the electrolyte shifts the onset of the exothermic peaks to higher temperatures (Fig. 17).

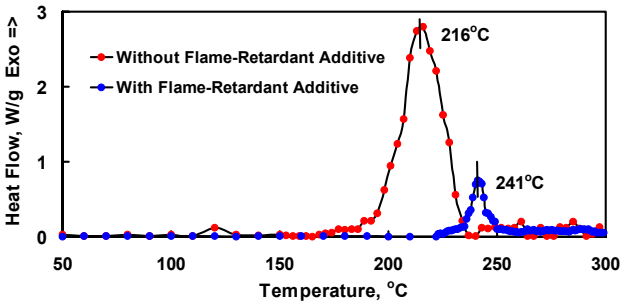

Figure 17. Effect of HMTP additive on fully charged $LiNi_{0.8}Co_{0.2}O_2$ cathode.

The shift of the exothermic peak with 5-10 wt% FR additive in comparison with those for the electrolyte without the FR additive was attributed to the passivation layer formed on the surface of the electrode. In addition, the investigations of the pressure development within the ARC bomb also showed that 5-10 wt% FR additives significantly reduce the pressure buildup in the ARC bomb compared with those for the electrolyte without the FR under similar conditions.

We have completed the spectral characterization of the carbon electrode subjected to the potential of 10 mV (cathodic) and 4.2 V (anodic) *vs.* Li/Li^+ for 3 hr in 1M $LiPF_6$ in EC-DMC (50:50 wt%) containing 10 wt% of HMTP. After each experiment, the electrode surface was washed and studied using FTIR (PARAGON 1000, Perkin Elmer), EDS, ^1H NMR, and ^{31}P NMR ((300 MHz FT-NMR spectrometer, Varian Gemini). ^1H NMR studies confirmed the presence of the $-OCH_3$ group of the HMTP on the electrode surface. In addition, a single peak in the ^{31}P NMR measurement (Fig. 18) suggested that the HMTP is the source of the phosphorous signal. We also observed that the peak position shifts to the lower region compared to the pure HMTP suggesting that Li is coordinated to P in the adsorbed film on the carbon electrode surface. These results indicate the presence of $Li\text{-}P(OCH_3)_2$ species on the electrode surface, which is probably responsible for the thermal safety and flame retardancy. With this new structural information, one can further reduce the self-heat rate of the Li-ion cells by synthesizing new FR additives containing $-P(OCH_3)_2$ groups.

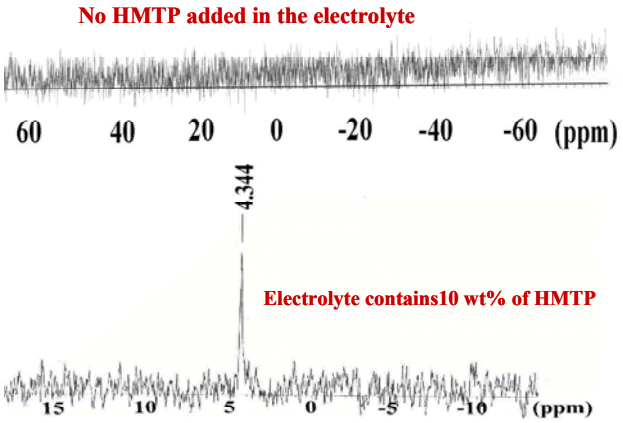

Figure 18 ^{31}P NMR spectrum of a carbon electrode subjected to 10 mV *vs*. Li for 3 hrs.

Publication

J. Prakash, C. Lee, and K. Amine, "A Novel Flame-Retardant Additive for Li-ion Batteries," *U.S. Patent No. 6455200* (2002).

CATHODES

Novel Cathode Materials

Michael M. Thackeray
Argonne National Laboratory, Chemical Technology Division, Argonne IL 60439
(630)-252-9183, fax: (630)-252-4176, email: thacheray@cmt.anl.gov

Objective

- Develop low-cost manganese oxide cathodes to replace cobalt/nickel oxide electrodes in Li-ion cells and vanadium oxide electrodes in Li-polymer cells.

Approach

- Develop and characterize manganese oxides for Li-ion and Li-polymer cells.
- Focus on composite layered $xLi_2M'O_3 \bullet (1-x)LiMO_2$ electrodes (M′=Mn, Ti, Zr, Ru; M = Mn, Ni, Co) for Li-ion cells, and stabilized alpha-MnO_2 for Li-polymer cells.
- Reinstate research to stabilize $LiMn_2O_4$ spinel electrodes.

Accomplishments

- Prepared and evaluated several $xLi_2M'O_3 \bullet (1-x)LiMO_2$ electrode compositions in Li cells; the performance target of 160 mAh/g for 100 cycles at 50°C was achieved.
- Restarted effort to stabilize $LiMn_2O_4$ spinel electrodes.
- Determined significance of the tetrahedral A-site of the spinel in stabilizing electrochemical performance at 50°C.

Future Directions

- Seek improved performance from $xLi_2M'O_3 \bullet (1-x)LiMO_2$ composite electrodes. A performance target of 190 mAh/g for 100 cycles at 50°C in $Li/xLi_2M'O_3 \bullet (1-x)LiMO_2$ cells has been set.
- Attempt to minimize the irreversibility capacity loss of $xLi_2M'O_3 \bullet (1-x)LiMO_2$ electrodes.
- Continue efforts to stabilize $LiMn_2O_4$ spinel electrodes at 50°C.
- Evaluate metal-oxide electrodes in Li/polymer cells in collaboration with J. Kerr at LBNL.

During 2002, the prime focus of the research effort was to continue to exploit the concept of using a layered $Li_2M'O_3$ (rock salt) component (M′=Mn, Ti, Zr, Ru) to stabilize a layered electrode $LiMO_2$ structure (M = Mn, Ni, Co) during the electrochemical cycling of $Li/LiMO_2$ cells. It was discovered during this contract period that when M = Ni and Mn, for example, in $LiMn_{0.5}Ni_{0.5}O_2$, or in a composite $0.31LiTi_2O_3 \bullet 0.69LiMn_{0.5}Ni_{0.5}O_2$ system, electrochemical capacity could be obtained not only by Li extraction from the parent electrode above 3 V *vs*. Li, but also by Li insertion below 2 V without destroying the layered framework of the host electrode. During the electrochemical process above 3 V, the Li ions occupy octahedral sites in a $Li_{1-x}MO_2$-type structure, whereas below 2 V a Li_2MO_2-type structure is formed in which the Li ions occupy tetrahedral sites. When discharged between 4.6 and 1 V, these electrodes can yield extremely high capacities that can exceed 250 mAh/g. The electrochemical reaction path and change in electrode composition during Li insertion into and extraction from $xLi_2M'O_3 \bullet (1-x)LiMO_2$ composite electrodes is shown in a compositional MO_2-Li_2MO_2-$Li_2M'O_3$ phase diagram in Fig. 19. Changes in the oxidation states of these $xLi_2M'O_3 \bullet (1-x)LiMO_2$ composite electrodes were tracked by *in situ* x-ray absorption studies at the Advanced Photon Source at ANL. These studies showed that charge transfer occurred predominantly in a two-electron process both during Li extraction ($Ni^{2+} \rightarrow Ni^{4+}$) and during Li insertion $Mn^{4+} \rightarrow$

Mn^{2+}). The absence of Jahn-Teller ions, Mn^{3+} and Ni^{3+}, during charge and discharge is believed to contribute to the remarkable reversibility of the overall reaction.

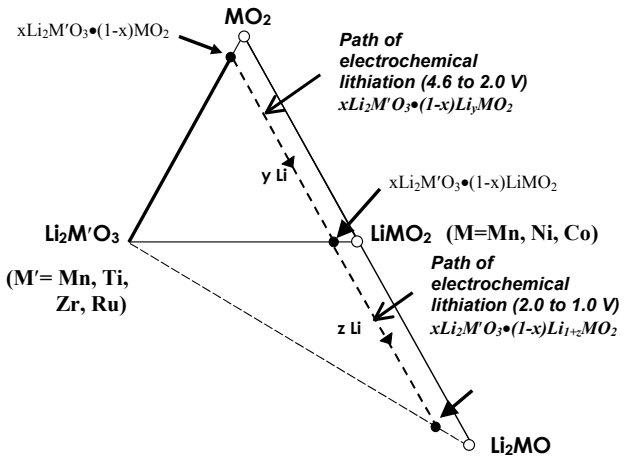

Figure 19. A compositional MO_2-Li_2MO_2-$Li_2M'O_3$ phase diagram.

The discovery of Li_2MO_2 electrode compositions that are stable to electrochemical cycling raises the possibility of using these compounds to combat the irreversible capacity loss effects that occur at graphite or intermetallic negative electrodes.

During 2002, a task to stabilize $LiMn_2O_4$ electrodes at 50°C was reinstated into the project. Electrochemical evaluations and structural analyses by neutron diffraction of substituted $LiMn_{2-x}M_xO_4$ electrodes (M = Li^+, Mg^{2+}, Zn^{2+} and Al^{3+}) have demonstrated that the occupation of the tetrahedral sites of the spinel by the substituted ions may play a significant role in stabilizing the spinel electrode.

No further progress was made on improving the electrochemistry of stabilized alpha-MnO_2 electrodes in Li/polymer cells. However, further work on cathode materials for Li/polymer cells is planned for 2003 in collaboration with J. Kerr at LBNL.

Publications and Presentations

J-S. Kim, C.S. Johnson and M.M. Thackeray, "Layered $xLiMO_2•(1-x)Li_2MO_3$ Electrodes for Lithium Batteries: A Study of $0.95LiMn_{0.5}Ni_{0.5}O_2•0.05Li_2TiO_3$," *Electrochem. Comm.*, **4**, 205 (2002).

C.S. Johnson, J-S. Kim, A.J. Kropf, A.J. Kahaian, J.T. Vaughey and M.M. Thackeray, "The Role of Li_2MO_2 Structures (M= Metal Ion) in the Electrochemistry of $xLiMn_{0.5}Ni_{0.5}O_2•(1-x)Li_2TiO_3$ Electrodes for Lithium Batteries," *Electrochem. Comm*., **4**, 492 (2002).

C.S. Johnson, J.-S. Kim, J.T. Vaughey, A.J. Kropf and M.M. Thackeray, "Structural and Electrochemical Evaluation of $(1-x)Li_2TiO_3$ • $xLiMn_{0.5}Ni_{0.5}O_2$ as an Electrode Material for Lithium Batteries," *11th International Meeting on Lithium Batteries, Monterey, CA,* June 2002.

G.J. Moore, C.S. Johnson and M.M. Thackeray, "The Electrochemical Behavior of Composite $xLiMO_2•(1-x)Li_2RuO_3$ Electrodes in Lithium Cells (M=Co, Ni, Zr, Li)," *11th International Meeting on Lithium Batteries, Monterey, CA,* June 2002.

Y. Paik, C.S. Johnson, J.-S. Kim, M.M. Thackeray, C.P. Grey, "Lithium and Deuterium NMR Studies of Acid-Leached Layered Lithium Manganese Oxides," *11th International Meeting on Lithium Batteries, Monterey, CA,* June 2002.

J.-S. Kim, J.T. Vaughey, C.S. Johnson and M.M. Thackeray, "Elevated Temperature Performance of $LiMn_{2-x}Mn_xO_4$ Electrodes (M=Li, Mg, Al, Zn) as a Function of Tetrahedral Site Occupancy," *202nd Meeting of the Electrochemical Society*, Salt Lake City, UT, October 2002.

J.-S. Kim, J.T. Vaughey, C.S. Johnson, A.J. Kropf and M.M. Thackeray, "Electrochemical Evaluation of $xLi_2TiO_3•(1-x)LiMn_{0.5}Ni_{0.5}O_2$ ($0 \le x \le 0.31$) Electrodes for Lithium-Ion Batteries," *202nd Meeting of the Electrochemical Society*, Salt Lake City, UT, October 2002.

New Cathode Materials Based on Layered Structures

M. Stanley Whittingham
State University of New York at Binghamton, Chemistry and Materials Research Center, Binghamton, NY 13902-6000
(607) 777-4623, fax: (607) 777-4623, e-mail: stanwhit@binghamton.edu

Objective

- Find lower-cost and higher-capacity cathodes, exceeding 200 Ah/kg, that are based on benign materials.

Approach

- Place emphasis on manganese dioxides, both pure and modified with other transition metals, using predominantly low-temperature synthesis approaches.
- Synthesize these materials and characterize them structurally for thermal and chemical stability.
- Evaluate above electrochemically in a variety of cell configurations; then compare with lithium iron phosphates.

Accomplishments

- Determined that layered manganese dioxides can be stabilized, that their electronic conductivity and cell cycling can be significantly enhanced by the addition of other transition metals, and that nickel-based compounds such as $LiNi_{0.4}Mn_{0.4}Co_{0.2}O_2$ exhibit very good properties.
- Completed a study of the $LiFePO_4$ cathode as a base-case system. We have shown that the conductive coating method is not critical, and that the as-synthesized $LiFePO_4$ material has a resistivity of 10^5 – 10^6 ohm-cm.
- Showed that in the charged state, the $FePO_4$ (FeO_6 octahedra) is kinetically stable relative to conversion to the thermodynamically stable quartz form (FeO_4 tetrahedra). However, over-discharge must be avoided as rechargeability is impeded by the formation of Li_3PO_4. The rate capability is reasonable, 1 mA/cm^2 at 20°C, even at high loadings approaching 100 mg/cm^2. This will be the base case against which all our future cathode studies will be compared.
- Showed that vanadium oxides can also be stabilized by the addition of Mn ions, and can achieve capacities over 220 Ah/kg.

Future Directions

- Identify changes in $LiMnO_2$ structure as a function of current density during cell cycling.
- Determine the structure and composition of the nickel-stabilized $LiNi_{1-y}Mn_yO_2$.
- Determine the role of cobalt in these layered compounds $LiNi_{1-y-z}Mn_yCo_zO_2$, and determine how to increase their rate capability.
- Complete, for Li-polymer cells, the evaluation of the Mn-stabilized δ-vanadium oxides and compare them to the iron phosphates. Emphasis in all cases will be placed on understanding the reasons for capacity fade.

The goal of this project is to identify transition metal oxides with superior properties to $LiCoO_2$, including higher capacity, lower cost, and being benign to the environment. Our emphasis remains on low-cost materials with capacities approaching 200Ah/kg, in particular layered manganese oxides. In addition, $LiFePO_4$ was studied as a low cost intermediate capacity system (that might meet the power capabilities for HEV) and δ-vanadium oxides as a very high capacity system.

(a) Stabilized Manganese Oxide Cathodes – low cost, high capacity, safe systems

Layered $LiMnO_2$ has the potential of cycling 1 Li per Mn ion but is unstable relative to the spinel $LiMn_2O_4$ on cycling. Two approaches were

used to stabilize the layer structure of manganese dioxide: (1) the incorporation of pinning ions to disrupt the oxygen cubic close packing thus minimizing the diffusion of Mn which is required for spinel formation, and (2) the partial substitution of some of the Mn ions by later transition metals such as Fe, Co or Ni. In the former we found that vanadium oxide pillars prevented the formation of spinel-like phases; however, the rate capability requires improvement, and we are using Co to achieve this.

In the electronic approach, we make $LiMnO_2$ behave more like $LiCoO_2$ by substituting an element to the right of Co in the periodic table, such as Ni. Earlier we showed that this doping by Ni, Fe or Co enhances the electronic conductivity and cyclability of the manganese oxide. However, 10% substitution did not prevent spinel formation. Higher levels, ≥50%, as in $LiMn_{0.4}Ni_{0.4}Co_{0.2}O_2$, were found to maintain the layered structure. This compound cycled well with capacities approaching 200 Ah/kg at low rates. The rate capability was improved by an aqueous carbon gel coating. The Ni rather than the Mn is the electrochemically active ion, the Mn remaining in the +4 Oxidation state. The cycling behavior is shown for one sample (Fig. 20).

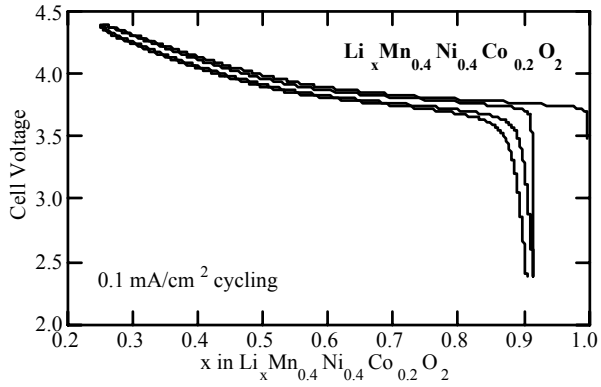

Figure 20. Electrochemical cycling of $Li_yMn_{0.9}Ni_{0.4}Co_{0.2}O_2$ at room temperature.

A range of compositions has been studied, and the first discharge capacity was proportional to the Ni content suggesting that the redox active specie is Ni, which cycles between Ni^{2+} and Ni^{4+}. The charging regime for the Co is mostly above the 4.3 to 4.4 volt cut-off used here. The Co appears to enhance the cyclability maybe through enhanced electronic conductivity, and we are working with G. Ceder at MIT to better understand the role of Co. To better understand the redox processes occurring, XPS and magnetic studies have been initiated. The susceptibility data is consistent with either Ni(III) + Mn(III) or Ni(II) + Mn(IV). The available literature data (from the Nesper group on $LiMn_{0.5}Ni_{0.5}O_2$) is inconsistent with the present ideas on the redox couple; initial interpretation of our XPS data (L. Matienzo of IBM) is underway. We see changes in the oxygen spectrum between different samples, but not between the Ni, Mn or Co spectra.

We have prepared carbon-coated samples of the stabilized layer phase, $Li_{1+x}Ni_{1-y-z-x}Co_zMn_yO_2$. These samples show good rate capability even at room temperature; 1st cycle capacity is 150, 140, and 95 mAh/g at 0.5, 0.83 and 3 mA/cm^2, respectively.

(b) Iron Phosphate Cathodes – low-cost, base-case 150 Ah/kg system

We are nearing completion of our study on the $LiFePO_4$ base-case cathode, which we will use for comparison against other cathodes such as the layered manganese nickel compounds discussed above. Hydrothermal synthesis was not found to be a viable preparative procedure due to lattice iron disorder. We found that the $FePO_4$ fully charged material was kinetically stable, although not thermodynamically stable. However, on over-discharge Li_3PO_4 is formed which is not readily reversible. 100% capacity is readily attained at 0.1 mA/cm^2, dropping to 80% at 1 mA/cm^2 with loadings of 20 to 80 mg/cm^2. The method of carbon coating was not found to be important, and carbon levels of 6 to 12 wt% were found to be effective. The capacity at 50°C increased to 100% at 1 mA/cm^2. The capacity/rate relationship is shown in Fig. 21. Capacity retention on cycling is very good.

Studies are continuing on other iron phosphate phases, both crystalline and amorphous. The Giniite phase is undergoing characterization at Binghamton and at Stony Brook (Clare Grey), and offers the opportunity for extensive exchange of the Fe for other metals such as Mn. However, $LiFe_{1-y}Mn_yPO_4$ was not particularly attractive, cycling only ≈ 0.5 Li at steady state.

(c) Stabilized Vanadium Oxide Cathodes – high-capacity system

We have continued the evaluation of layered vanadium oxides stabilized by Mn and Zn. These have the double-sheet δ structure, and

exhibit initial capacities exceeding 300 Ah/kg double those of lithium iron phosphate. We have optimized the intercalated cations, and are evaluating the dramatic effect morphology and electrolyte cation has on the initial capacity and cycling.

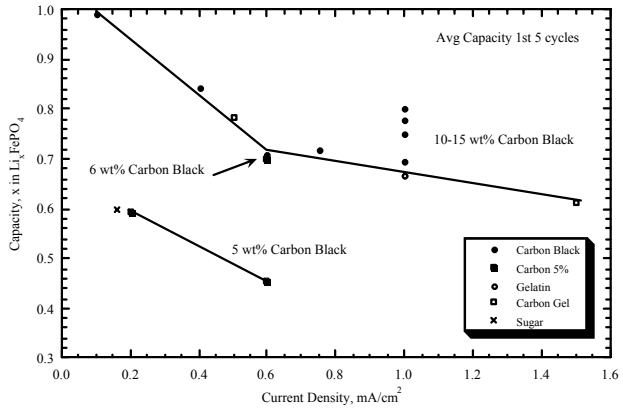

Figure 21. Capacity-rate relationship for $LiFePO_4$ cathodes with various carbon coatings. The capacities are the mean of the first 5 cycles.

Conclusions

$LiFePO_4$ provides a low-cost highly reversible cathode but has a lower volumetric capacity than $LiCoO_2$. It is a good base-case system. The stabilized manganese oxides (aka manganese-stabilized nickel oxides) show promise as the next-generation cathode. The vanadium oxides offer the greatest capacity, but at a lower voltage.

Publications

S. Yang, P.Y. Zavalij and M.S. Whittingham, "Hydrothermal Synthesis of Lithium Iron Phosphate Cathodes," *Electrochem. Commun.*, **3**, 505-508 (2001).

S. Yang, Y. Song, P.Y. Zavalij and M.S. Whittingham, "Reactivity, Stability and Electrochemical Behavior of Lithium Iron Phosphates," *Electrochem. Commun.*, **4**, 234-239 (2002).

Y. Song, S. Yang, P.Y. Zavalij and M.S. Whittingham "Temperature-dependent Properties of $FePO_4$ Cathode Materials," *Mater. Res. Bull.*, **37**, 1249-1257 (2002).

P.Y. Zavalij, F. Zhang and M.S. Whittingham, "The Zinc-Vanadium-Oxygen-Water System: Hydrothermal Synthesis and Characterization," *Solid State Sciences*, **4**, 591-597 (2002).

S. Yang, Y. Song, P.Y. Zavalij and M.S. Whittingham, "Nanocomposite Electrodes for Advanced Lithium Batteries: The $LiFePO_4$ Cathode," *Mater. Res. Soc. Proc.,* **V7.9**,703 (2002) .

Synthesis and Characterization of Cathode Materials

Marca M. Doeff
Lawrence Berkeley National Laboratory, 62R0203, Berkeley CA 94720-8253
(510) 486-5821, fax: (510) 486-4881, e-mail: mmdoeff@lbl.gov

Objective

- Develop low-cost, benign cathodes (*e.g.*, manganese oxides, metal phosphates) having electrochemical characteristics (cycle life, energy, and power densities) consistent with the goals of the USABC and/or FreedomCar.

Approach

- Synthesize candidate materials with optimum purity, particle size, and morphology by various methods.
- Determine physical and structural properties relevant to battery operation.
- Evaluate electrochemical performance in relevant cell configurations.

Accomplishments

- Provided baseline cathode material ($Li_{1.02}Al_{0.25}Mn_{1.75}O_{3.98}S_{0.02}$) to BATT for testing (11/01), completed electrochemical characterization, and made a "no go" recommendation based on the results.
- Demonstrated effect of particle size and nature of residual carbon on electrochemical properties of $LiFePO_4$.
- Synthesized and characterized a series of substituted layered manganese oxides, which discharge up to 200 mAh/g in a Li/liquid electrolyte cell configuration.

Future Directions

- Investigate high-capacity layered substituted manganese oxides with intergrowth structures and compounds with tunnel structures.
- Finish evaluation of sol-gel method to produce $LiFePO_4$ with small particles and make "go-no go" decision.

The spinel $LiAl_{0.25}Mn_{1.75}O_{3.98}S_{0.02}$ has been reported to cycle well when discharged on the 3 V plateau *vs*. Li. We synthesized this compound and $Li_{1.02}Al_{0.25}Mn_{1.75}O_4$ by solid-state and sol-gel methods using Li_2S (optionally) as the sulfur source. We also received a sample from the Korean group who originally reported on this compound, made by sol-gel. XRD, EDS, and ^7Li MAS-NMR (Cairns' group) indicate that sulfur is not present in the bulk of any of the samples. All materials showed low capacity (~ 90 mAh/g) and poor rate capability at 4 V *vs*. Li compared to undoped Merck SP30 spinel. All lost capacity rapidly when cycled below 3 V *vs*. Li, although the donated sample showed a marked resistance to tetragonal phase conversion (cells gave almost no extra capacity, but polarized instead). Because of this, the fade rate was slower and overall capacities lower than for other samples. The difference in behavior is attributed to the unusual particle morphology; a consequence of firing in the presence of sulfur-containing compounds. This is difficult to reproduce due to the reactivity of Li_2S with water and air. Because of poor electrochemical properties and irreproducibility of the synthesis process, we recommended dropping this material from the BATT program.

$LiFePO_4$ suffers from poor utilization in electrochemical cells because of low electronic conductivity and ionic diffusivity. Reduction of the particle size of $LiFePO_4$ by planetary milling greatly improves utilization. Carbon coating $LiFePO_4$ also improves rate capability markedly. We have synthesized $LiFePO_4$ by a sol-gel method, which allows use of iron-nitrate precursors and results in high-purity products with well-controlled particle sizes. The amount, structure, and distribution of residual carbon in sol-gel $LiFePO_4$, as determined by Raman microprobe spectroscopy (R. Kostecki) differ considerably depending on processing details. As a result, products vary greatly in their electrochemical properties. Uncoated materials made from iron acetate or oxalate perform better than sol-gel compounds due to the larger amount of residual carbon in the former. Superior performance, however, is expected for coated sol-gel samples, because coating thicknesses and distribution are more easily controlled.

Tunnel-Li_xMnO_2 with the $Na_{0.44}MnO_2$ structure cycles stably and has excellent rate capability, but limited capacity. O2 layered compounds made from sodium manganese oxides with the P2 structure potentially have higher energy densities but may be less stable than tunnel compounds. CV, galvanostatic cycling, and XRD experiments show no evidence of phase conversion for at least 30 cycles. Spinel formation, which occurs fairly rapidly during cycling of O3 layered manganese oxides is not observed. O2 compounds do not have a cubic close-packed oxygen array, in contrast to O3 and spinel compounds. Because more bond breaking and rearrangement is required to form spinel from the O2 structure during cell cycling, they are inherently more stable.

Capacities vary from ~80-180 mAh/g for the O2 layered compounds depending upon substituents. Best results are obtained for 11% Ni, Co, or Al-substituted manganese oxides. Some of the variation is due to kinetic effects, but Li in an O3 environment (observed by NMR and XRD) was observed in all of the high-capacity electrodes, suggesting a correlation. The sodium-

containing precursors of these compounds are actually intergrowths of P2 and P3 (Fig. 22), which convert to stacking faulted O2/O3 compounds upon ion exchange. The ratios of these components can be controlled by varying Na content of the precursors.

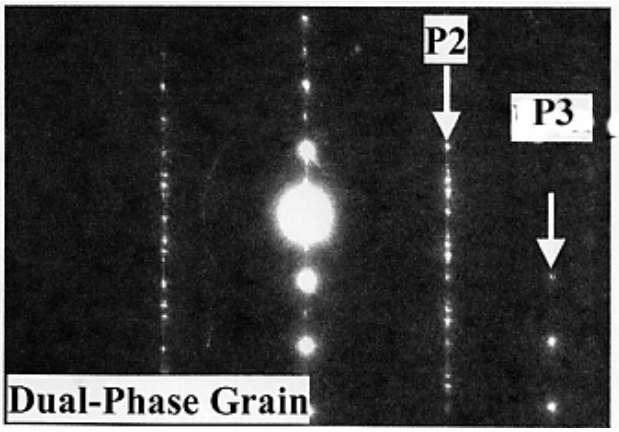

Figure 22. Electron diffraction pattern of $Na_{0.7}Al_{0.11}Mn_{0.89}O_2$, showing that it is a P2/P3 intergrowth. Photograph courtesy of Dr. X. Feng of the Materials Sciences Division, LBNL.

A 100% O3 $Li_xNi_{0.2}Mn_{0.8}O_2$ compound discharges 200 mAh/g in a Li cell (Fig. 23) proving that O3 is the higher capacity/rate component. It is very interesting that the stacking-faulted O2/O3 compounds do not undergo the expected transition to spinel. We speculate that O3 layers are "pinned" by the surrounding O2 layers, impeding phase conversion. It is, however, important to demonstrate stability under conditions that batteries are likely to encounter in vehicular applications (high rates, prolonged cycling, overcharge, etc.), so this requires more extensive investigation. Ideally, the perfect compromise between the high rate/high capacity of O3 and the stability of O2 compounds can be obtained by manipulating the relative amounts and distributions of these components in the intergrowths. Some work in FY2003 will be devoted to this task. We will continue to investigate tunnel compounds with the $Na_{0.44}MnO_2$ and psilomelane structures. (Preliminary results indicate higher initial capacities but more sensitivity to over-discharge for the latter compared to the former.)

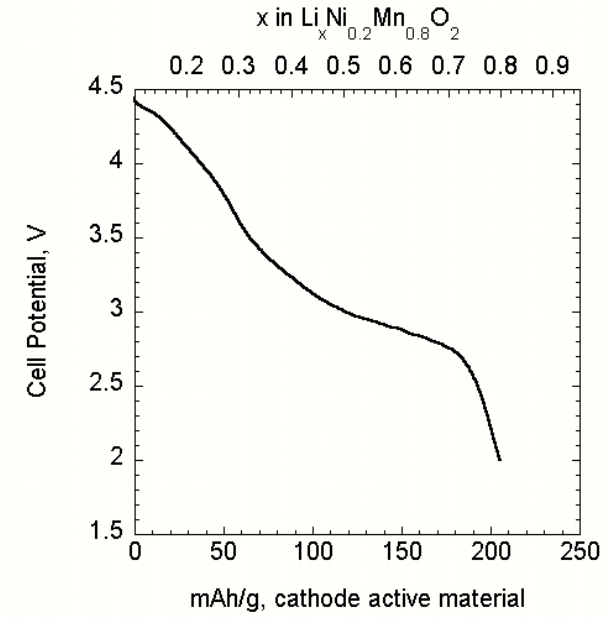

Figure 23. Discharge profile of a Li/1M $LiPF_6$, EC-DMC/100% O3-$Li_xNi_{0.2}Mn_{0.8}O_2$ cell at 0.055 mA/cm^2. The cell was initially charged to 4.5 V.

Publications and Presentations

M.M. Doeff, T.J. Richardson, K.-T. Hwang and A. Anapolsky, "Improved Discharge Characteristics of Tunnel-Containing Manganese Oxide Electrodes for Rechargeable Lithium Battery Applications," *ITE Battery Lett.*, **2(3),** B-63 (2001).

M.C. Tucker, M.M. Doeff, T.J. Richardson, R. Fiñones, J.A. Reimer and E.J. Cairns, "^{7}Li and ^{31}P MAS NMR of $LiFePO_4$-Type Materials", *Electrochem. and Solid State Letters*, **5**, A95 (2002).

M.C. Tucker, M.M. Doeff, T.J. Richardson, R. Fiñones, E.J. Cairns and J.A. Reimer, "Hyperfine Fields at the Li Site in $LiFePO_4$-Type Olivine Materials for Lithium Rechargeable Batteries: A ^{7}Li MAS NMR and SQUID Study," *J. Am. Chem. Soc.*, **124**, 3833 (2002).

M.M Doeff, R. Fiñones and Y. Hu, "Electrochemical Performance of Sol-Gel Synthesized $LiFePO_4$ in Lithium Batteries" *202nd Electrochem. Soc. Meeting*, Salt Lake City, UT, October 2002.

T.A. Eriksson and M.M. Doeff, "A Study of Layered $Li_xM_yMn_{1-y}O_{2+z}$ (M=Fe, Co, Ni, Zn, Al) Cathode Materials," *11th International*

Meeting on Lithium Batteries, Monterey, CA, June 2002.

M.M. Doeff, J. Hollingsworth and J.-P. Shim, "Factors Influencing the Electrochemical Behavior of Sulfur-doped Aluminum-substituted Lithium Manganese Oxide Spinels in Lithium Cells," *201st Electrochem. Soc. Meeting*, Philadelphia, PA, May 2002.

M.M. Doeff, T.J. Richardson, M. Gonzales and K.-T. Hwang, "Effect of Ion Substitution on the Electrochemical Characteristics of Tunnel-containing Manganese Oxide Electrodes," *200th Meeting of the Electrochemical Society,* San Francisco, CA, September 2001.

Novel Cathode Materials

John B. Goodenough
University of Texas at Austin, 1 University Station, C2200, Austin, TX 78712
(512)-471-1646, fax: (512)-471-7681, email: jgoodenough@mail.utexas.edu

Objective

- Evaluate alternative layered oxides as cathode materials for a Li-ion battery that operates between Ni(II) and Ni(IV).

Approach

- Prepare $LiNi_{0.5}Mn_{0.5}O_2$ nanoparticles and coat them with carbon.
- Construct button cells for investigation of charge and discharge characteristics of the cathode material with and without carbon coating.
- Examine, using SEM, the morphology of the particles and the carbon coat.

Accomplishments

- Prepared $LiNi_{0.5}Mn_{0.5}O_2$ nanoparticles and coated agglomerates of particles with carbon.
- Conducted tests with button cells, which demonstrated that carbon coating improves capacity and stability under repeated cycling.

Future Directions

- Investigate ball milling to achieve coating of individual particles.
- Investigate influence of other cations than Mn(IV) on the performance of operation on Ni(III)/Ni(II) and NI(IV)/Ni(III) redox couples.
- Compare performances of spinel *vs.* layered oxides.

$LiMn_{0.5}Ni_{0.5}O_2$ has a face-centered-cubic oxygen array with Li^+ occupying alternate (111) planes of octahedral sites and $Mn_{0.5}(IV)Ni(II)_{0.5}$ occupying the other planes of edge-shared octahedral sites. The Li^+ ions can be reversibly extracted electrochemically (or chemically); extraction of the first 0.5 Li/formula unit oxidizes the Ni(II) to Ni(III); further extraction of Li would oxidize Ni(IV) to Ni(III) as occurs in $Li_{1-x}Co_{0.3}Ni_{0.7}O_2$. However, the 90° M-O-M interactions and the tortuous Ni-O-Ni percolation result in a poor electronic conductivity, which limits the power capability of the material as a cathode in a rechargeable Li^+-ion battery. We have therefore investigated the use of a Li^+-permeable carbon coating on the electrode particles to supply electrons to the interior of the cathode particles.

$LiMn_{0.5}Ni_{0.5}O_2$ (LMNO) was prepared by direct reaction between LiOH, Ni metal, and Mn_2O_3; the ground reactants were heated overnight at 800°C and then reground, compacted into 2.5-cm-diameter pellets and heated to 900°C for 20 h in air.

The carbon source for coating the oxide particles was a carbon xerogel formed from a resorcinal-formaldehyde (R-F) polymer. The $LiMn_{0.5}Ni_{0.5}O_2$ particles were carbon coated by compacting into a pellet a mixture of the oxide and R-F in an 85:15 weight ratio. Li was extracted from the pellet with excess I_2 in an acetonitrile solution. The products were characterized structurally by powder XRD and then combined with acetylene black and teflon in a 70:25:5 weight ratio and rolled into sheets from which cathodes were cut.

Button-type electrochemical test cells used a Li anode and 1 M $LiPF_6$ in 1:1 ethylene carbonate:diethyl carbonate as the electrolyte. Comparison was made between the performances of cells with coated (LMNO-C) and with uncoated (LMNO) oxide particles. The carbon content of the coated particles was 2.5% (w/w) determined by thermogravimetric analysis. SEM showed that both the coated and uncoated oxides contain 10-100 nm particles bound into 10-150 μm agglomerates. A carbon map obtained with an energy-dispersive x-ray spectrometer showed the carbon coating was evenly distributed across the agglomerate surfaces.

Charging was limited to 4.3 V *vs*. Li, and the discharge curves ranging from 4.1 to 3.5 V *vs*. Li gave the discharge capacities as a function of cycle number shown in Fig. 24 for various current densities. Fig. 25 summarizes the average discharge capacities of LMNO and LMNO-C over the first 50 cycles at various current densities. These data show that carbon coating enhances the capacity and reduces the capacity fade. However, better performance can be expected if the carbon coats the individual particles, not just the surface of the agglomerates.

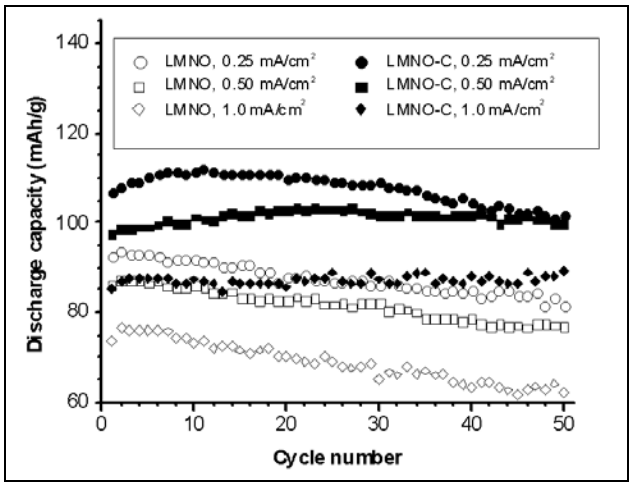

Figure 24.

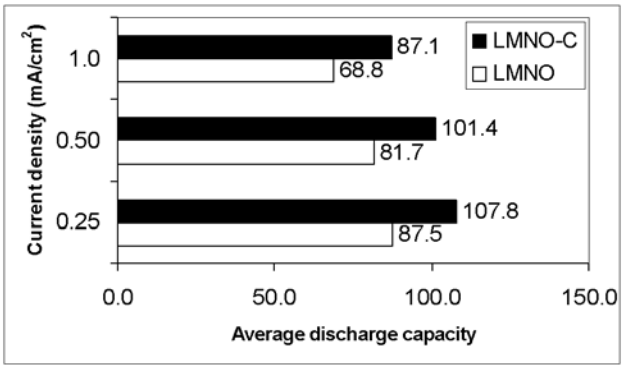

Figure 25.

Publication

B.L. Cushing and J.B. Goodenough, "Influence of Carbon Coating on the Performance of a $LiMn_{0.5}Ni_{0.5}O_2$ Caathode," *Solid State Sciences* **4**, 1487-1493 (2002).

DIAGNOSTICS

Electrode Surface Layers

Frank R. McLarnon and Robert Kostecki
Lawrence Berkeley National Laboratory, 70R0108B, Berkeley CA 94720-8168
(510) 486-4636, fax: (510) 486-426, e-mail: frmclarnon@lbl.gov

Objective

- Establish direct correlations between electrode surface changes, interfacial phenomena, and cell capacity decline.

Approach

- Use ellipsometry, Raman spectroscopy, and advanced microscopic techniques to characterize electrodes taken from baseline BATT Program cells, as well as thin-film electrodes in model cells.
- Measure changes in electrode surface morphology and structure, electrode surface chemistry, and SEI thickness and composition that accompany cell cycle-life tests.

Accomplishments

- Defined relationships between electrode history, electrode surface properties, and temperature for baseline $LiAl_{0.05}Ni_{0.8}Co_{0.15}O_2$ cathodes.
- Characterized structural disordering of graphite anodes during cycling at elevated temperatures and correlated the mechanism of SEI reformation upon cycling with graphite structural degradation.

Future Directions

- Correlate changes of cathode surface morphology and chemistry to the mechanism of $LiFePO_4$ cathode degradation in BATT Program cells.
- Determine the impact of anode carbon disordering on long-term Li-ion cell performance.
- Provide full diagnostic results for model thin-film $LiMn_2O_4$ cathodes.

We used Raman microscopy and AFM to monitor and understand the effect of structural changes that occur in graphitic materials upon extensive cycling at elevated temperatures. By combining these two methods of surface analysis we could evaluate the surface and near-surface changes resulting from exposure of BATT Program anodes to stresses that arise from numerous Li intercalation-deintercalation cycles and elevated temperatures. BATT Program task 1.1 (K. Striebel) provided cycled cells with synthetic graphite anodes (Hitachi Chemical MAG-10), $LiNi_{0.8}Co_{0.15}Al_{0.05}O_2$ cathodes, and either $LiPF_6$-EC-DEC electrolyte for cells Q0120V and PG04, or LP40 electrolyte for cell PG13. The cells were charged and discharged ~400 times at the C/2 rate and 100% DOD between 3.0 and 4.1 V at ambient temperature (Q0120V, PG04) and at 60°C (PG13). All cells exhibited significant capacity loss: 13%, 33%, and 65%, respectively, for cells Q0120V, PG04, and PG13.

The integrated intensity ratio of carbon D/G bands, which is inversely proportional to the size of microparticles and increases with carbon disorder, was used to evaluate carbon structure. The G-band, which is located at 1580 cm^{-1}, arises from the first-order scattering associated with the in-plane E2g mode, whereas the D-band is associated with the break of symmetry occurring at the edges of graphite sheets. Figure 26 shows Raman images of the integrated intensity ratio of D/G carbon Raman bands, represented by different shades of gray, collected from a 40 x 60 mm area with 0.7 μm resolution. The lighter is the shade of gray on the image, the more graphitic is the electrode structure. The Raman images reveal that the graphite undergoes gradual structural degradation upon

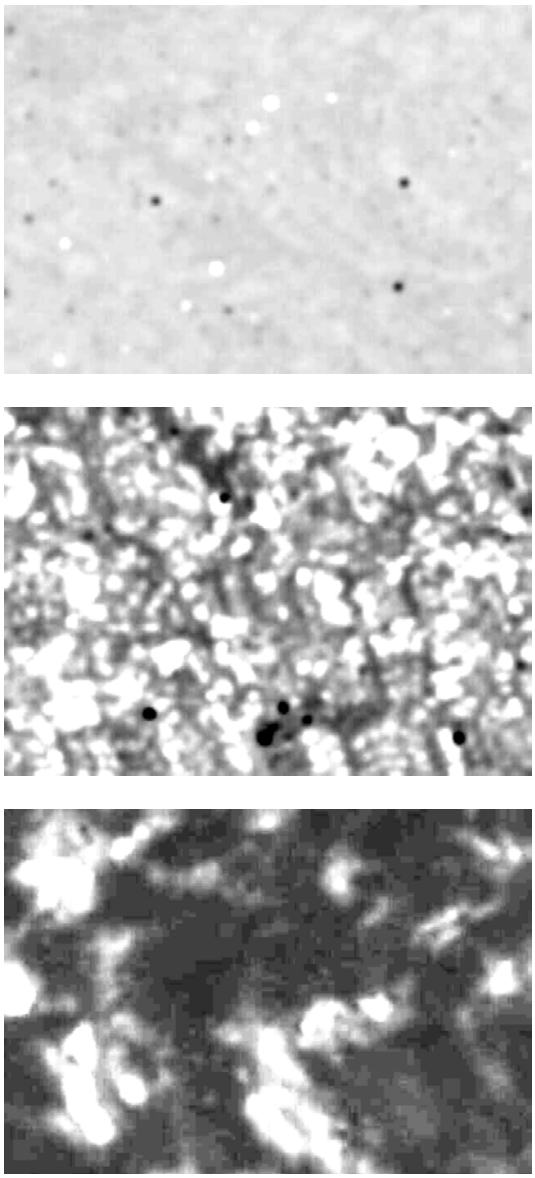

Figure 26. Raman maps of D/G band ratio of graphite BATT Program anodes. A) fresh anode, B) anode from a cell cycled at room temperature, C) anode from a cell cycled at 60°C. The lighter is the shade of gray on the image, the more graphitic is the electrode structure.

cycling. Severe structural disorder was observed in the anode from the cell cycled at 60°C. Interestingly, the structural degradation of graphite did not occur uniformly over the anode surfaces. Even for the anode, which shows substantial damage on its surface (cell PG13), one can still identify regions which consist of undisturbed graphite. Distortions in the graphite structure can create a barrier for Li ion diffusion during the intercalation-deintercalation process, contributing to electrode impedance rise and cell capacity loss. Also, structural degradation of the graphite led to increased anode surface reactivity *vs*. the electrolyte, and the formation of SEI layers. A thick layer of inorganic products from side reactions, signaled by Raman bands at 1000-1100 cm^{-1} that are characteristic for lithium carbonates and phosphates, was observed on the disordered part of the carbon anode. The presence of these products suggests that structural changes in the anode surface greatly affected the composition of the SEI layer and caused a permanent shift in Li inventory in the tested cells, contributing to the observed capacity loss.

We continued *in situ* spectroscopic ellipsometry studies of thin-film $LiMn_2O_4$ spinel electrodes. Our objective was to determine how the electrode composition profile and structure change as the electrode is cycled in EC-DMC (1:1 by vol.) + 1 M $LiPF_6$ electrolyte. We were able to accurately simulate the ellipsometric data in the initial stages of Li^+ intercalation into with a simple model, the one-dimensional growth of a linear Li-ion concentration gradient in the thin-film $LiMn_2O_4$ electrode. From our analysis we derived a Li^+-ion diffusion coefficient of $6.3 \bullet 10^{-12}$ cm^2/s, a value which agrees well with published data, see *J. Electrochem. Soc*., **145**, 3024 (1998). The change in slope of the Ψ-t curve indicates that a phase transition took place. We were able to accurately simulate the ellipsometric data in subsequent stages of Li^+ intercalation with a complex double-gradient model, in which the electrode was assumed to contain two manganese oxide phases. From our analysis, we derived an apparent average Li^+-ion diffusion coefficient of $5.1 \bullet 10^{-12}$ cm^2/s in this region. The positive Ψ-t curve slope implied that an additional phase transition took place as the cathode was charged further.

We also used *in situ* spectroscopic ellipsometry to investigate the formation and growth of SEI layers on thin-film $LiMn_2O_4$ cathodes. We confirmed that a SEI layer formed as soon as the cathode came into contact with the electrolyte (1.0 M $LiPF_6$ in EC/DMC), as signaled by a sharp change of ellipsometric values when electrolyte was injected into the electrochemical cell. To account for the observed change, it was necessary to include in our model a SEI layer between the cathode and electrolyte. Our physical model, in which a SEI layer is included, fit the ellipsometric data very well. By analyzing the ellipsometric data and calculating the

resulting SEI optical constants, we found that SEI layer developed slowly during the first few cycles. We concluded that the SEI layer composition had reached at a stable state after the third charge/discharge cycle

We carried out a series of Raman microscopy and current-sensing atomic force microscopy (CSAFM) diagnostic tests on $LiNi_{0.8}Co_{0.15}Al_{0.05}O_2$ cathodes from ATD and BATT Program cells, and $LiFePO_4$ cathodes from BATT Program baseline cells. We confirmed that Al has a stabilizing effect on the structure of mixed Ni and Co oxides and prevents their decomposition upon cycling or storage at elevated temperatures. Our diagnostic studies of composite cathodes revealed a gradual loss of carbon additive from the cathodes, especially at elevated temperatures. Interestingly, the two carbon components disappear from the cathode surface at different rates, depending on their particle size and structure; *i.e.*, the surface concentration of acetylene black decreases at a higher rate than does graphite. Among possible causes of this phenomenon are carbon migration or peeling, oxide particle dissolution-deposition, and anion intercalation into carbon. CSAFM measurements revealed that the cathode surface electronic conductance decreases dramatically with increasing cell test temperature, which is in concert with the observed carbon loss. Moreover, we determined that the cathode surface consists of partially (and sometimes almost fully) charged $Li_{1-x}Ni_{0.8}Co_{0.15}Al_{0.05}O_2$ particles, despite deep discharges at the end of cell testing. Degradation of electronic contact between grains of active material may be responsible for this effect. We found no clear evidence of nano-crystalline deposits or non-conductive SEI's on the $LiNi_{0.8}Co_{0.15}Al_{0.05}O_2$ cathode surfaces; however, we observed poly-phosphorous compounds that may contribute to SEI layer formation on $LiNi_{0.8}Co_{0.15}Al_{0.05}O_2$ and $LiFePO_4$ cathodes.

Battery Materials: Structure and Characterization

James McBreen
Brookhaven National Laboratory, MSD-Bldg. 555, P.O. Box 5000, Upton, NY 11973-5000
(631) 344-4513, fax. (631) 344-5815, email jmcbreen@bnl.gov

Objective

- Establish direct correlations between electrode material changes, interfacial phenomena, and cell capacity decline.

Approach

- Apply a combination of *in situ* and *ex situ* synchrotron techniques to characterize electrode materials and electrodes taken from baseline BATT Program cells.
- Develop and apply X-ray absorption spectroscopy (XAS) techniques that are sensitive to both surface and bulk processes in electrodes.

Accomplishments

- Completed studies of $LiMn_2O_4$ spinel.
- Completed development of techniques for XAS studies of phosphorous decomposition products in cycled cells and applied it to ATD Program.
- Completed most of the *in situ* XAS and XRD work on $LiFePO_4$ and $LiNi_xMn_{1-x}O_2$.

Future Directions

- Carry out soft x-ray XAS studies of new cathode materials.
- Characterize Mn- and Fe-based cathode materials with improved stability.
- Pursue studies of non-carbon anodes.

Our objectives are to develop and apply advanced diagnostic techniques, with sensitivity to bulk and surface processes, to monitor degradation processes in Li-ion batteries. These techniques are also being used to elucidate properties of starting materials that determine performance and stability of $LiMn_2O_4$ and other low-cost cathode materials with higher capacity ($LiFePO_4$ and $LiNi_xMn_{1-x}O_2$). We use a combination of *in situ* and *ex situ* XAS and XRD to study bulk processes in electrodes. We also use *ex situ* soft x-ray XAS in both the electron yield and fluorescence mode to distinguish between surface and bulk processes on electrodes. In the soft x-ray regime from 500-1000 eV, the escape depth for the Auger electrons is about 50 Å and the sampling depth for the fluorescent signals is about 3000 Å. Thus the former probes close to the surface whereas the latter probes the bulk.

XRD Studies of $LiMn_2O_4$

In FY 2002, we completed an extensive study of $LiMn_2O_4$. *In situ* XRD on $LiMn_2O_4$ that in the 4.1 V region indicates that there are two first-order phase transitions with three cubic phases. The studies of $LiMn_2O_4$ indicate that the cycle life and stability of $LiMn_2O_4$ can be greatly improved by use of excess Li stoichiometry, elimination of oxygen deficiency and by using stable electrolytes that do not generate acidic species in the cell. Excess Li stoichiometry increases the range of lattice constants for all three phases and yields pseudo-single-phase behavior. Increasing oxygen deficiency promotes the conversion of the cubic spinel to a tetragonal phase at low temperature. The transition temperature, the transition kinetics, and the amount of the spinel converted to the tetragonal phase increases with increasing oxygen deficiency.

XRD and XAS Studies of $LiFePO_4$ and $LiNi_{0.5}Mn_{0.5}O_2$

Both *in situ* XRD and XAS reveal the presence of a first-order phase transition during charge ($LiFePO_4 \rightarrow FePO_4$). Principal component analysis of the Fe near edge XAS clearly show that a maximum of two components (indicating the presence of only two distinct phases) can account for the XAS data at all states of charge. *In situ* XRD of $LiNi_{0.5}Mn_{0.5}O_2$ indicates that it has the $R\bar{3}m$ structure. During charge the H1 phase is converted to the H2 phase, accompanied by an elongation of the c-axis and a contraction of the a-axis. Unlike other materials with the $R\bar{3}m$ structure ($LiNiO_2$ and $LiNi_{0.8}Co_{0.2}O_2$) there is no conversion to the H3 phase, even at 4.6 V. However, $LiNi_{0.3}Mn_{0.7}O_2$ did show formation of the H3 phase, indicating that stable operation requires the $LiNi_{0.5}Mn_{0.5}O_2$ composition.

XRD Studies of Carbon Coated Si Anodes

In situ XRD indicate that, during charge, intercalation first takes place in the graphite coating and then in the Si. The graphite coating promotes uniform lithiation of the Si to produce an amorphous material. Without the coating, there is only localized incomplete lithiation of the Si. The coating either acts as a buffer that promotes uniform lithiation or it protects the Si surface from the electrolyte. A combination of both mechanisms is also possible.

Publications

X. Sun, H.S. Lee, X.-Q. Yang and J. McBreen, "Improved Elevated Temperature Cycling of $LiMn_2O_4$ Spinel Through the Use of a Composite LiF Based Electrolyte," *Electrochem. Solid-State Lett.,* **4**, A184 (2001).

M. Balasubramanian, J. McBreen, I.J. Davidson, P.S. Whitfield and I. Kargina, "*In Situ* X-ray Absorption Study of a Layered Manganese-Chromium Oxide Based Cathode Material," *J. Electrochem. Soc.,* **149**, A176 (2002)

X. Sun, X.-Q. Yang, M. Balasubramanian, J. McBreen, Y. Xia and T. Sakai, "*In Situ* Investigation of Phase Transitions of $Li_{1+y}Mn_2O_4$ Spinel During Li-ion Extraction and Insertion," *J. Electrochem. Soc*. **149**, A842 (2002).

J. McBreen and M. Balasubramanian, "Rechargeable Lithium-Ion Battery Cathodes," *JOM* **54**(3), 25 (2002).

W.-S. Yoon, Y. Paik, X.-Q. Yang, M. Balasubramanian, J. McBreen, and C.P. Grey, "Investigation of the Local Structure of the $LiNi_{0.5}Mn_{0.5}O_2$ Cathode Material during Electrochemical Cycling by X-ray Absorption and NMR Spectroscopy," *Electrochem. Solid-State Lett*. **5**, A263 (2002).

X.-Q. Yang, J. McBreen, W.-S. Yoon, and C. Grey, "Crystal Structure Changes of $LiMn_{0.5}Ni_{0.5}O_2$ Cathode Materials During Charge and Discharge Studied by Synchrotron Based *In Situ* XRD," *Electrochem Commun.* **4**, 649 (2002).

X.-Q. Yang, J. McBreen, W.-S. Yoon , M. Yoshio, H. Wang, K. Fukuda and T. Umeno, "Structural Studies of New Carbon Coated Silicon Anode Materials Using Synchrotron Based *In Situ* XRD," *Electrochem. Commun.* **4***,* 893 (2002).

M. Balasubramanian, J. McBreen, K. Pandya and K. Amine**,** "Local Structure of Dilute Gallium Ions in $LiNi_{0.908}Co_{0.085}Ga_{0.003}O_2$ Cathode Material: *InSitu* X-Ray Absorption Study," *J. Electrochem. Soc.* **149**, A1246 (2002).

Interfacial and Reactivity Studies

Philip N. Ross, Jr.
Lawrence Berkeley National Laboratory, MS 2R0100, Berkeley CA 94720-8196
(510) 486-6226, fax: (510) 486-5530, e-mail: pnross@lbl.gov

Objective

- Establish direct correlations between electrode surface changes, interfacial phenomena, and cell failure.

Approach

- Use FTIR spectroscopy and X-ray photoelectron spectroscopy (XPS) to study model electrode/electrolyte combinations, *e.g.*, using glassy carbon electrodes and BATT Program electrolytes, to provide the basis to interpret more-complex spectra recorded for ATD Program cell materials.

Accomplishments

- Completed experimental measurements of the electrochemical potentials of all carbonate solvents of interest in Li-ion batteries.
- Completed experimental measurements of the electrochemical reduction and oxidation potentials of selected electrolyte additives of interest in Li batteries.

Future Directions

- Establish thermal stability of the SEI layer on graphite anodes in ATD Program Gen 2 electrolyte.
- Identify some routes to improved stability *via* electrolyte additives and/or graphite pre-treatment.

The oxidation potentials of a commonly used Li-ion battery electrolyte, EC:DMC (1:1) – 1 M $LiPF_6$ (LP 30 Selectipur from Merck), was measured using a combination of CV with a rotating disk electrode (RDE) and *in situ* infrared reflection absorption spectroscopy (IRAS). The use of the RDE enabled us to distinguish small currents from the oxidation of impurities from the onset of oxidation of the electrolyte. The oxidation potential at a Pt or glassy carbon electrode is at or just above 5.2 V, depending on the criterion used. The IRAS spectra clearly show the appearance of CO_2 in solution from solvent oxidation above 5 V using a glassy carbon electrode. The oxidation potential of an important Li-ion battery additive, VC, was determined from IRAS experiments to be near 4 V. The experimental values of the oxidation potentials determined here are consistent with the predicted values from Density Functional Theory (DFT) for one-electron oxidation (ionization) of the carbonate molecule to the radical cation (molecular ion). Neither the salt nor the electrode material affected the oxidation potential determination in these experiments.

An IR spectroelectrochemical cell with a flat CaF_2 window was used for the *in situ* IRAS experiments. A glassy carbon disk served as the working electrode and Li metal as both counter and reference electrodes. The cell was assembled in the dry box and transferred to the Nicolet Model 670 FTIR spectrometer. FTIR spectra were obtained as a function of potential with the electrode pushed against the CaF_2 window. For each potential step, the working electrode was retracted from the window and the reaction was allowed to progress for 5 min. before returning the electrode to the window. A strain gauge was used to monitor the force applied on the window to assist in returning the electrode to the same position at each potential and to prevent

excessive pressure that could cause window to crack. Spectra were measured with a resolution of 4 cm^{-1} by accumulating 20–30 scans using a high-sensitivity LN cooled MCT detector.

Figure 27 shows the disk and ring current profile when the potential was scanned from 3.5 to 5.5 V using a Pt disk and a Pt ring in a RDE experiment. Oxidation of the EC:DMC(1:1) –1 M $LiPF_6$ electrolyte was observed to start only at potentials above 5.1 V on the Pt disk. The disk currents at potentials above 5 V were independent of rotation rate, indicative of oxidation of a species present in relatively high concentrations, such as the solvent or the solute. There was no evidence of passivation of the disk electrode from the oxidation process.

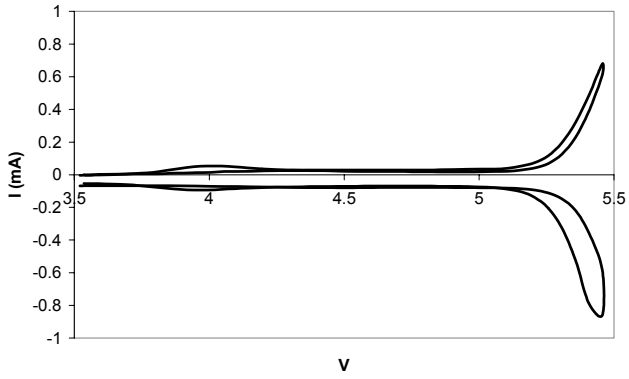

Figure 27. Cyclic voltammetry on a Pt RDE in EC:DMC – 1 M $LiPF_6$ sweeping between 3.5 and 5.4 V (*vs*. Li/Li^+) at 5 mV/s and 1600 rpm.

The disk currents at potentials below 5 V were less than 50 μA, and were *dependent on rotation rate*, *i.e.*, proportional to $\omega^{1/2}$. Since the diffusion-limiting current for oxidation of either the solvent or the salt would be orders of magnitude higher than this value, the small currents below 5 V are attributed to oxidation of the impurities in the electrolyte. We note that the current at 4.5 V in our voltammetry experiment (40 μA) is more than an order of magnitude lower than that reported by Aurbach and coworkers[1] for a similar but not identical electrolyte (1:1 EC:DEC – 1 M $LiClO_4$ on Pt or 1:1 EC:DEC – 1 M $LiAsF_6$ on Au). Using our criterion for the onset of electrolyte oxidation, the oxidation potential derived from the data of Aurbach and co-workers would be around 4–4.1 V for the EC-based solvents used in that study. This is about 1 V lower than in ours, and cannot be attributed to the *criterion* used for determining the onset of oxidation. Our conclusion is that the low oxidation potential reported by Aurbach and co-workers is due to impurities in their electrolyte, most probably water.

In situ IRAS was used to provide more detail about the electrolyte oxidation process using a glassy carbon electrode. IR spectra at potentials from open circuit (ca. 3.8 V) up to 5.6 V are shown in Fig. 28.

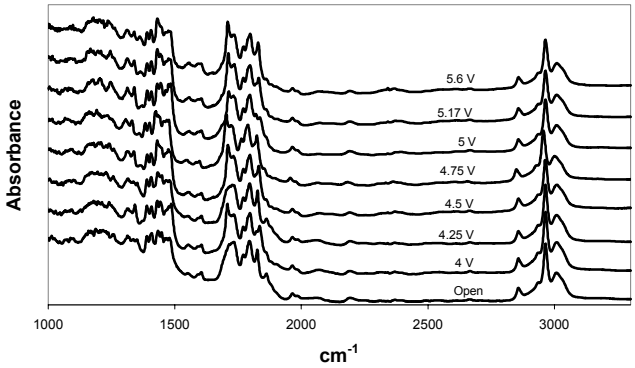

Figure 28. IRAS spectra from a glassy carbon electrode in EC:DMC – 1 M $LiPF_6$ as a function of potential.

All the spectra are dominated by electrolyte features, as expected, and it is necessary to use subtractive normalization (SNFTIR) to isolate the interfacial species. The spectrum at 4 V was taken as the reference spectrum and at each higher potential subtractively normalized spectra were obtained as $\Delta R/R$,

$$\Delta R/R = (R_E - R_{ref})/R_{ref}$$

The result for EC:DMC electrolyte is shown in Fig. 29. It was clear from the SNFTIR spectra in the 2300–2400 cm^{-1} spectral region shown in Fig. 29 that a CO_2 peak begins to appear at about 5 V and above. This result is in good agreement with the CV data, indicating that the electrolyte was oxidized to CO_2 at potentials above 5 V. The intensity of the CO_2 signal obtained at 5.6 V was comparable to that from the electrolyte after it was saturated with CO_2 in a glove bag filled with CO_2, indicating that the electrolyte was saturated with the CO_2 produced by solvent oxidation at that potential. Our SNFTIR results were very similar to those reported by Joho and Novak[2] for the same electrolyte (LP 30) with a Ni working electrode. Joho and Novak[2] also reported that the oxidation potential of alkyl carbonate electrolytes was lowered by the addition of water to nominally dry electrolyte.

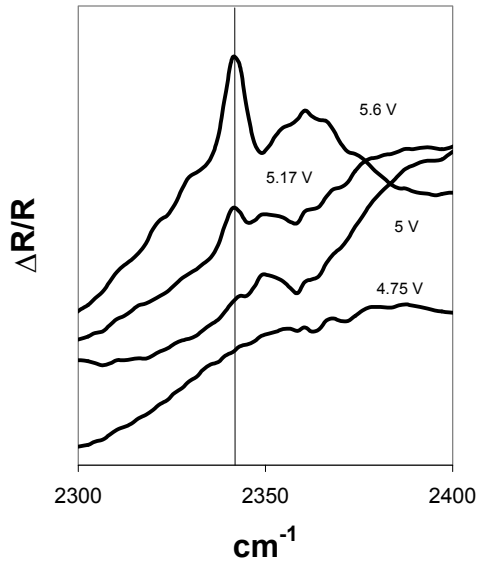

Figure 29. SNFTIR spectra from a glassy carbon electrode in EC:DMC – 1 M $LiPF_6$ as a function of potential derived from the IRAS spectra shown in Fig. 28.

As shown by the reaction Scheme 3 used in our density functional theory (DFT) calculations[3], CO_2 is an expected product in the oxidation mechanisms of both EC and DMC, and both solvents were predicted to have nearly identical (within 0.1 V) oxidation potentials, 5.6 V *vs.* Li/Li^+. The experimental oxidation potential of 5.2 V found here for the EC:DMC (1:1) electrolyte, assuming that the co-solvents have a single oxidation potential, are in reasonable agreement with the calculated potentials, and agree well with the results of Joho and Novak[2], but not that of Aurbach and co-workers[1].

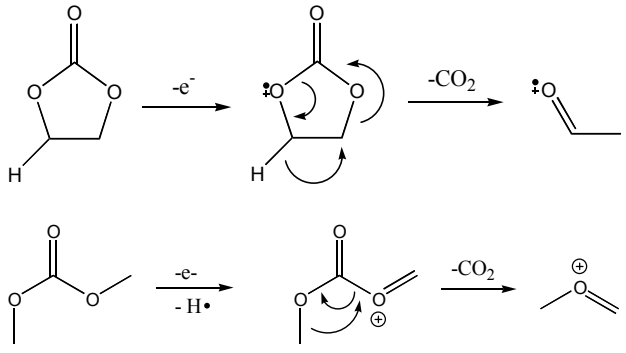

Scheme 3

Because of the relatively impure sample of VC available, we did not use CV to measure the oxidation potential. We were, however, able to observe a distinct oxidation potential using *in situ* IRAS that was not effected by the impurities present. Figure 30 shows a series of SNFTIR spectra for VC – 0.1 M $LiPF_6$ at potentials from 3.25 V up to 4.6 V.

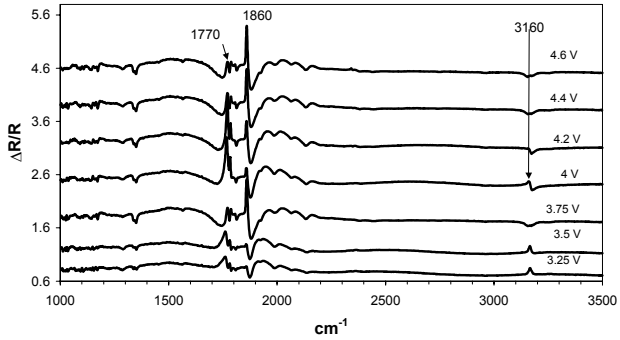

Figure 30. SNFTIR spectra for a glassy carbon electrode in VC – 0.1 M $LiPF_6$ as a function of potential (IRAS spectrum at 2.75 V used as reference).

The reference spectrum was that at open circuit (in this case about 2.7 V). In SNFTIR spectra, positive-going intensity is an increase in concentration of a species and negative going intensity is a decrease in concentration. The electrochemical Stark shift, the effect of the electric field in the inner Helmholtz layer on the vibrational frequency of molecules in the inner layer, is a complication that makes interpretation of any vibrational feature near those of the solvent molecules very difficult. In general, the Stark shift produces bipolar bands in SNFTIR spectra, the most well known being the bipolar bands for the C=O stretching of CO adsorbed on Pt surfaces, and the ΔR/R spectra in Fig. 30 have similar bipolar bands in the C=O stretching region (near 1800 cm^{-1}) and in the vinyl C-H stretching region (at 3160 cm^{-1}) which in our opinion are characteristic of Stark tuning shifts of VC molecules in the inner Helmholtz layer. However, a sharp peak at about 1860 cm^{-1} starts to appear at potentials above 4 V with a concurrent decrease in the intensity the vinyl C-H stretching at 3160 cm^{-1}. These spectral changes are indicative of VC oxidation above 4 V, perhaps initiating at about 4.2 V. There are many C=O containing compounds that have vibrational bands in the region near 1800 cm^{-1}, so that one has to be cautious about assigning the features to a specific compound. We note that the symmetric C=O stretching from a cyclic acid anhydride could produce such an IR feature. The asymmetric stretch for cyclic anhydrides is usually at 1800–1775 cm^{-1} whereas the symmetric stretch is at 1870–1845 cm^{-1}.

The asymmetric stretch usually provides a peak with stronger intensity than the symmetric one. The oxidation of VC produces a relatively strong new band at 1860 cm^{-1}, and possibly a weaker new band at 1770 cm^{-1} uniquely characteristic of a cyclic acid anhydride. There is a reasonable reaction path to produce a cyclic acid anhydride from electrochemical oxidation of VC, as shown in Scheme 4. According to our quantum chemical calculation[3], the VC molecular ion would be expected to decompose into CO and a vinyl radical cation, as shown in Scheme 4a. However, the VC used in our experiment has a purity of only 97%, with water being one of the impurities. One-election oxidation of VC to the molecular cation is followed by reaction with water, loss of a $H^{\cdot}$ radical, yielding hydroxy vinylene carbonate. This is followed by keto-enol tautomerization to give the cyclic carbonate of glycollic acid, $C_3H_2O_4$, as shown in Scheme 4b. Because the reaction with water occurs after ionization of the VC molecule to the molecular ion, the oxidation potential is not affected by the presence of water, *i.e.*, the water only affects the subsequent reactions of the cation with the electrolyte. The observed VC oxidation potential near 4 V is in very good agreement with the value of 4.06 V given by the DFT calculations.

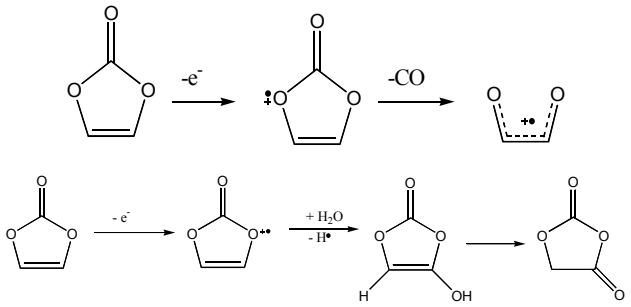

Scheme 4

References

[1] M. Moshkovic, M. Cojocaru, H.E. Gottlieb, and D. Aurbach, *J. Electroanal. Chem.* **2001**, *497*, 84.
[2] F. Joho and P. Novak, *Electrochim. Acta* **2000**, *45*, 3589
[3] X.R. Zhang, J.K. Pugh and P.N. Ross, *J.Electrochem. Soc.*, **148**, E183 (2001).

Corrosion of Aluminum in Lithium Cell Electrolytes

James W. Evans and Thomas M. Devine (Lawrence Berkeley National Laboratory)
University of California, 316 Hearst Mining Building, MC 1760, Berkeley CA 94720
(510) 642-3807, fax: (510) 642-9164; e-mail: evans@socrates.berkeley.edu

Objectives

- Determine the role of $LiBF_4$ and $Li(CF_3SO_2)_2N$ (LiTFSI), in EC and DMC electrolytes, in the corrosion of aluminum, as well as the corrosion rate and corrosion mechanism of Al in these electrolytes.
- Characterize and quantify corrosion of Al when used in present or candidate Li cell electrolytes by using the electrochemical quartz crystal microbalance (EQCM) and some microscopy techniques. This is in order to predict the 15-year performance of Al collectors with extreme-value statistical analyses.

Approach

- Use *in situ* EQCM combined with electrochemical techniques to understand the corrosion mechanism of Al in $LiBF_4$ and $Li(CF_3SO_2)_2N$ / EC + DMC electrolyte.
- Characterize the surface morphology, the corrosion product, and passivation layer by microscopy and other surface analysis techniques, *e.g.,* SEM, infrared spectroscopy.

Accomplishments

- Determined the role of $LiBF_4$ and LiTFSI in EC and DMC electrolyte in the corrosion of Al.
- Analyzed the corrosion product and mass change (corrosion rate) of Al in $LiBF_4$ and LiTFSI/EC+DMC.
- Reached conclusions concerning the corrosion mechanism of Al in $LiBF_4$ and LiTFSI /EC+DMC.

Future Directions

- Study the effect of other new battery electrolytes, cathode composites, and environmental factors on the corrosion of Al.
- Characterize and quantify corrosion of Al when used in present or candidate Li cell electrolytes from commercial and lab-made batteries.
- Develop a model to describe the role of corrosion in the capacity loss of Li-ion battery.

This program focuses on characterizing and quantifying corrosion of Al current collector in battery electrolyte. LiTFSI, $LiPF_6$ and $LiBF_4$ are widely used as the electrolyte in Li-ion batteries. LiTFSI is one of the most reactive salts causing corrosion of Al. Hence, use of this salt in Li batteries has been limited, despite of its superior properties over other salts in terms of less moisture sensitivity and relatively high thermal stability. In fact it is difficult to find one single electrolyte that fulfills all the requirements for an electrolyte, and mixed electrolytes combining the best characteristics of single electrolytes are therefore interesting.

We have used EQCM to monitor, *in situ,* the mass change occurring on the electrode surface during CV. The equivalent weight (mass change per mole of electron, mpe) obtained from the EQCM may help to give some information of corrosion reaction on the surfaces. In case of uniform corrosion, both current and mass change by EQCM helps to identify the corrosion and passivation products and to understand the corrosion mechanism.

In the present work, corrosion of Al in $LiBF_4$, LiTFSI and in these two mixed salts in EC/DMC solvent was studied by EQCM. Information on surface chemistry was obtained from FTIR spectroscopy. Figure 31 clearly shows that the presence of $LiBF_4$ in LiTFSI electrolyte significantly suppressed the corrosion current, and corrosion was not observed when 0.5 M $LiBF_4$ was added. The complicated mass change of increase-decrease-increase in LiTFSI solution indicates deposition (or adsorption) of precipitates occurring at the first anodic scan, but some dissolution (desorption) of the precipitates at the beginning of cathodic scan followed by accumulation of precipitates. Mass accumulation is pronounced when $LiBF_4$ is present. Although mpe change during cycling does not match with mpe values of any expected deposited species, the calculated mpe of -227 on anodic scan when adding of 0.5 M $LiBF_4$ reflects the high molecular weight precipitates deposited on the surface of Al to form a protective layer.

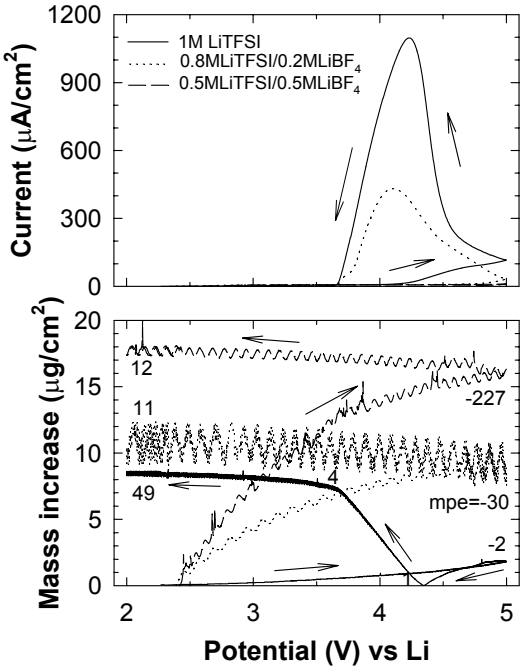

Figure 31. Comparative plots of CVs and the corresponding mass increase for the Al at the first cycle in 1 M LiTFSI/EC+DMC, 0.8M LiTFSI + 0.2 M $LiBF_4$/EC+DMC and 0.5 M LiTFSI + 0.5 M $LiBF_4$/EC+DMC; sweep rate = 5 mV/s .

Examination of the surface chemistry of Al has been carried out by FTIR spectroscopy. In Fig. 32(a) and (b), peaks at 1371, 1157 and 1209 cm^{-1} assigned to $\nu_a(SO_2)$, $\nu_s(SO_2)$ and $\nu_a(CF_3)$, respectively, must be of $TFSI^-$, indicating that corrosion products include this functional group. The broad peak around 3370 cm^{-1} reveals the presence of OH^-. Figure 32(c) shows peaks at 2925, 2854, 1727, 1000-1200 cm^{-1} of $\nu_s(CH)$, $\nu_a(CH)$and $\nu(C=O)$ respectively, together with other peaks from organic species. In particular, peaks of 1675 and 1354 cm^{-1} assigned to $\nu(CO_2)$, a coordination type C-O bond, are from lithium oxalate ($Li_2(CO_2)$). Apparently, the passivation layer consists of much organic species. The peak at 1065 cm^{-1} is attributed to some B-F bonding, and the very sharp peak at 3676 cm^{-1}

corresponds to ν(OH) indicating the presence of free LiOH. Based on both the FTIR spectral findings and EQCM results, as well as consideration of the steric hindrance raised by large size of $N(SO_2CF_3)_2^-$ anion and the presence of OH^-, we suppose that the corrosion products present on Al after the experiment with LiTFSI/EC+DMC would be $Al[N(SO_2CF_3)_2]_{2-x}(OH)_x$ and some organic species. On the other hand, these passivation products are expected to contain organic species such as $ROCO_2Li$ and lithium oxalate.

Use of a mixed electrolyte of LiTFSI and $LiBF_4$ might be an effective way to increase the corrosion resistance of Al current collector and to improve the performance of Li-ion batteries. Severe pitting corrosion of aluminum in LiTFSI/EC+DMC electrolyte has been certainly suppressed in the presence of ≥ 20% $LiBF_4$ in the electrolyte. EQCM-CV response and SEM images showed that $LiBF_4$ plays an efficient role in building up a stable passive surface layer, protecting Al from the pitting corrosion. Surface chemistry studied by employing FTIR spectroscopy suggests that $Al[N(SO_2CF_3)_2]_{3-x}(OH)_x$ is the major corrosion products. However, the passive layer also includes organic precipitates which are solvent decomposition products such as $ROCO_2Li$, lithium oxalate and also insoluble inorganic salts such as $Al(BF_4)_3$. It is anticipated that mixing of these two salts helps to increase the corrosion resistance of Al current collector and to improve thermal stability and moisture sensitivity of the electrolyte in Li-ion batteries.

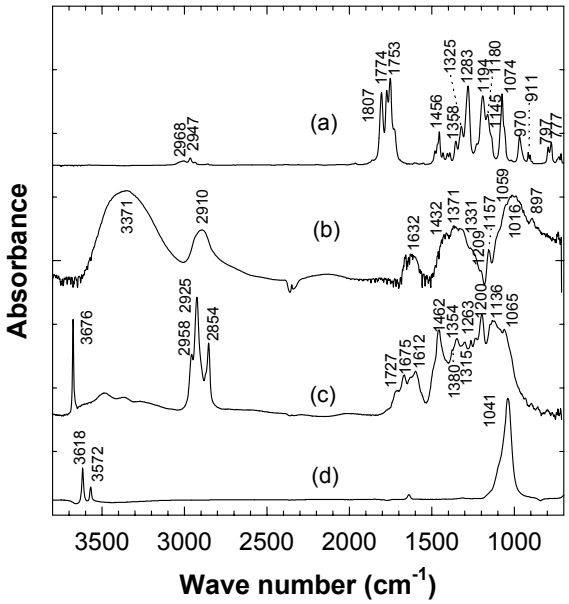

Figure 32. FTIR spectra of (a) 1 M LiTFSI/EC+DMC electrolyte solution, and of Al after CV-EQCM (b) in 1 M LiTFSI/EC+DMC, (c) in 0.8 M LiTFSI + 0.2M $LiBF_4$/EC+DMC and of (d) $LiBF_4$ salt alone.

Synthesis and Characterization of Electrodes

Elton J. Cairns
Lawrence Berkeley National Laboratory, 70R0108B, Berkeley CA 94720-8168
(510) 486-5028, fax (510) 486-730, e-mail ejcairns@lbl.gov

Objective

- Make direct observation of Li in BATT Program cathode materials, characterize the local atomic and electronic environment, and determine changes in this environment with cycling.

Approach

- Use ^{7}Li MAS-NMR to characterize BATT Program electrodes before and after cycling.
- Determine the NMR isotropic chemical shift, linewidth, lineshape, and relaxation times for each Li species. Extend this to other important nuclei.
- Use NMR data on model failure mechanisms to interpret the spectra.

Accomplishments

- Obtained ^{7}Li MAS NMR spectra for several $LiMPO_4$ (M=Fe, Ni, Mn, Co) and $Li[Mn_xFe_{1-x}]$ PO_4 olivine compounds and established the hyperfine shift mechanism. Showed that no structural changes occur with cycling.
- Obtained ^{7}Li MAS NMR spectra for layered $Li_y[M_{0.11}Mn_{0.89}]O_2$ (M=Al, Ni, Co, Zn, Cu, Fe) and determined various local environments in each composition. Identified the phases present in the most stable compositions, and clarified the structure of these materials.
- Obtained ^{7}Li MAS NMR spectra for Gen 2 electrodes after electrochemical cycling and at various states of charge. Identified Li loss from the NiO_x sites as a significant mechanism of capacity loss.

Future Directions

- Continue NMR work using 65 MHz magnet and spinning speeds of 20-25 kHz to improve resolution of spectra, giving more detailed information.
- Determine relaxation time for layered $Li_y[M_{0.11}Mn_{0.89}]O_2$ compounds to give additional information on the Li sites.
- Obtain ^{7}Li spectra for electrochemically cycled layered $Li_y[M_{0.11}Mn_{0.89}]O_2$ compounds for use in identifying capacity loss and stability information.
- Obtain the NMR spectra of layered compounds at various temperatures to aid in interpretation of spectra.
- Obtain 2-dimensional exchange spectra of layered compounds to determine the proximity of the Li cations in different local environments to aid in structure determination.
- Obtain ^{7}Li and ^{31}P NMR spectra of $LiFePO_4$ and $Li[Fe,Mn]PO_4$ at different states of charge and after repeated cycles to provide information on structural stability.
- Examine Gen 2 and Gen 3 electrodes to identify capacity loss mechanisms, as appropriate.

Olivine $LiMPO_4$ (M=Fe, Mn, Ni, Co)

Various olivine compounds, provided by M. Doeff, were studied using ^{7}Li MAS NMR. These studies revealed information about the nature of the hyperfine interaction. A single ^{7}Li isotropic resonance with a large spinning sideband envelope was seen for all the $LiMPO_4$ compounds, suggesting the presence of a single local environment for the Li cation (Fig. 33). Depending on the transition metal (TM) ion, various isotropic resonances are observed. Resonances at 68, -8, -49, and -86 ppm were observed for Mn, Fe, Ni, and Co- olivine, respectively. We found that each unpaired electron in the A' orbital contributes -28 ppm to the total Li NMR shift, whereas each unpaired electron in the A'' orbital contributes +80 ppm to the total shift. This work was extended to $Li[Mn_xFe_{1-x}]PO_4$ with various values of x. NMR spectra of these compositions suggest that Mn and Fe are homogeneously mixed. The Li NMR shift is a linear combination of those expected for pure Mn and pure Fe materials. These results provide a sound basis for the interpretation of spectra for cycled materials, and the interpretation of changes brought about by cycling.

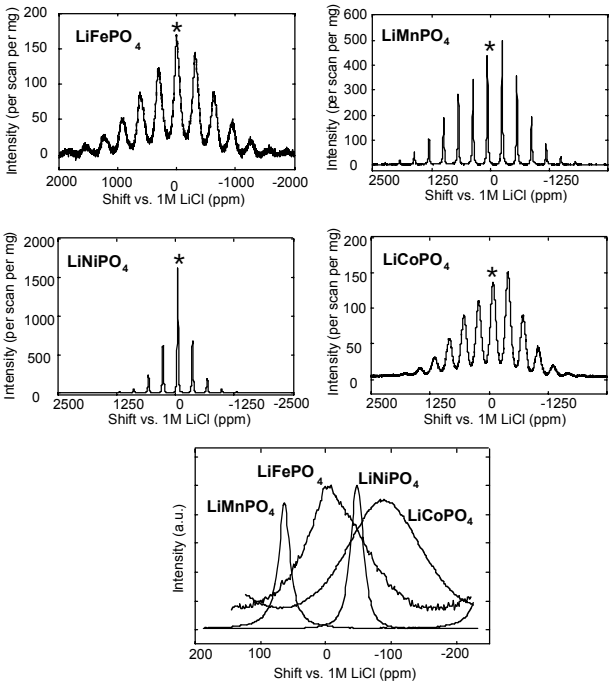

Figure 33. ^{7}Li MAS NMR spectra of olivine $LiMPO_4$ acquired with a 100 MHz magnet and 10 kHz spinning speed. The isotropic resonances are denoted with an asterisk.

Gen 2 Electrodes

NMR spectra of Gen 2 electrodes were obtained after electrochemical cycling using various protocols (Fig. 34). Two dominant resonances were observed for the fresh electrodes, a broad resonance at approximately 580 ppm and a sharp resonance at 0 ppm. The broad resonance at a higher shift is assigned to the Li cations containing Ni in their coordination environment ($LiNiO_2$ type). The sharp resonance at 0 ppm is assigned to Li with Co in the coordination sphere ($LiCoO_2$ type). The electrodes that showed capacity loss after electrochemical cycling exhibit a loss in the Li NMR signal for the resonance at 580 ppm. No noticeable change was observed for the resonance at 0 ppm for all the electrodes. Thus, it appears that the capacity loss is caused by changes in the Ni and/or its coordination sphere, possibly a preferential loss of Li from the vicinity of the Ni. NMR spectra of Gen 2 electrodes were also obtained at different states of charge. In the early stages of charging, the broad resonance at 580 ppm decreased in intensity and a new resonance at 313 ppm appeared, gradually shifting to lower frequencies as the charging proceeded. However, the resonance at 0 ppm appears to remain unchanged. This suggests that the oxidation of Ni^{3+} to Ni^{4+} occurs first, whereas the Co^{3+} is not oxidized until 4.4 V.

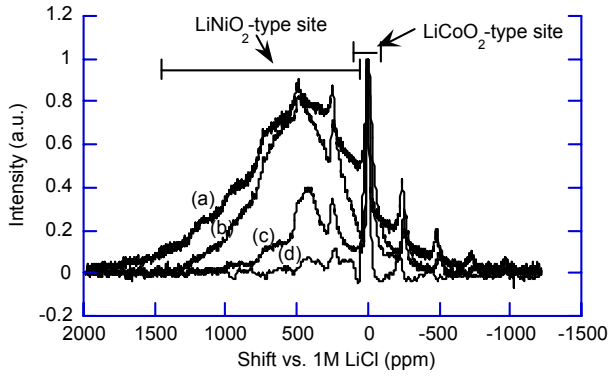

Figure 34. ^{7}Li MAS NMR spectra of Gen 2 electrodes ($LiAl_{0.05}Co_{0.15}Ni_{0.8}O_2$). Successive damage results in the loss in Li NMR signal from the $LiNiO_2$–type site. (a) Fresh electrode, (b) cycled once #I116, (c) stored, lost 24% power #A212, (d) cycled 140 times, lost substantial capacity #PG13.

Layered $Li_y[M_{0.11}Mn_{0.89}]O_2$ (M=Ni, Al, Cu, Fe, Zn, Co)

Lithium manganese oxides, which adopt a layered structure similar to that of $LiCoO_2$, have been studied as a promising cathode material for Li rechargeable cells. Various structural models have been proposed for the layered compounds (*i.e.*, O2, O3, P2, P3, T2) according to the stacking of oxygen and the site occupancy of the cations. Bruce *et al.* first synthesized the layered $LiMnO_2$ phase that is isostructural with $LiCoO_2$. This material is classified as O3-type and shows poor cycling characteristics resulting from the transformation to a spinel structure over repeated charging and discharging cycles. Recently, new layered compounds that adopt a structure related to the O2 structure were prepared by Dahn *et al*. In contrast to O3 $LiMnO_2$, it was reported that O2 $LiMnO_2$ does not convert to a spinel structure during cycling. However, the structure of these materials is not well defined due to the similarity between the structures and their poor crystalinity. Thus, our research has been focused on NMR spectroscopy to study the local Li environments as well as the long range effects in an attempt to better understand the relationship between the structure and the electrochemical properties.

^{7}Li MAS NMR spectra of various O2-type compounds, $Li_y[M_{0.11}Mn_{0.89}]O_2$ with M=Cu, Zn, Ni, Co, Fe, were acquired at 65 MHz magnetic field and at spinning speeds of 22 kHz (Fig. 35). M. Doeff provided these compounds. The low field and high spinning speed of MAS reduces the magnitude of the dipolar interaction between the Li nuclei and the unpaired electron on Mn, yielding spectra with higher resolution. Various combinations of resonances at ~700, 300, ~100 and -5 ppm were observed, depending on the metal substituent. All the compounds show a broad resonance at 650~720 ppm and a sharp resonance at -5 ppm. Additional resonances are observed at 100~124 ppm for Ni-, Co-, Fe- and Al-doped materials and at 300 ppm for Cu-doped material. Previously, it was shown that the predominant factor affecting the Li NMR shift in lithium manganese and lithium nickel oxides is the Fermi-contact interaction (Ref. *Phys. Rev. B*, 1997, 55, 12018). The Li NMR shift is determined by the sum of the individual contributions of the paramagnets in the cation coordination sphere. The size and the direction of the shift depend on the type of the bonds and the orbital overlap. Taking the same postulate, the local coordination environment of the Li cations in the various sites is examined for

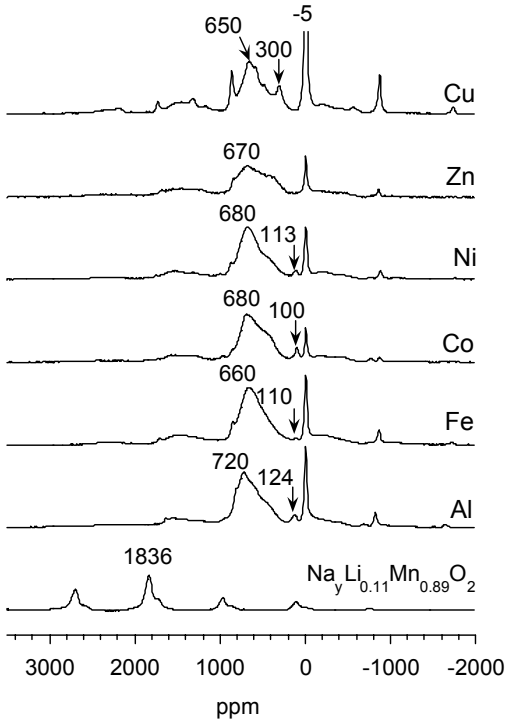

Figure 35. ^{7}Li MAS NMR spectra of O2 layered $Li_y[M_{0.11}Mn_{0.89}]O_2$ acquired with a 65 MHz magnet and 22 kHz spinning speed. The isotropic resonances are denoted in the figure.

our system. For Li in the tetrahedral site of a T2 structure with 10 Mn in the first coordination sphere, a shift of 270~430 ppm is predicted. A total contribution of 940~1160 ppm is predicted for Li in the octahedral site of an O2 structure containing 13 Mn in the coordination sphere. Therefore, the resonance at 300 ppm is assigned to the Li cations in the T2 environment and 650~720 ppm to Li in the O2 environment. The resonance at 100~124 ppm is attributed to Li in the O3 type environment, based on the previous study (Ref. *JACS*, 1998, 120, 12601). It appears that the compounds adopt predominantly an O2 structure with minor O3 or T2 type environments. Whether O3 and T2 type environments result from separate phase or stacking faults is not clear and further study is necessary. To check the presence of Li cations in the transition metal layer, $Na_y[Li_{0.11}Mn_{0.89}]O_2$ was prepared and a Li NMR shift of 1840 ppm is obtained. None of the O2 type $Li_y[M_{0.11}Mn_{0.89}]O_2$ studied shows a resonance at that high a frequency, suggesting that Li is not intercalated into the transition metal layer.

It appears that the O2-type compounds, which contain the O3 environment, exhibit higher specific capacity and the O2-type compound with T2 environment shows better capacity retention. Thus, optimizing the ratio of O2, O3, and T2-type environments would provide electrodes with higher capacity and better capacity retention.

Publications

M.C. Tucker, M.M. Doeff, T.J. Richardson, R. Finones, E.J. Cairns, and J.A. Reimer, *J. Am. Chem. Soc*. **2002**, 124, 3832

M.C. Tucker, M.M. Doeff, T.J. Richardson, R. Finones, J.A. Reimer, and E.J. Cairns, *Electrochem. and Solid State Lett*. **2002**, 5, 95.

NMR and Modeling Studies

Gerbrand Ceder and Clare P. Grey

Massachusetts Institute of Technology, Department of Materials Science and Engineering, 13-5056, Cambridge, MA; (617) 253-1581, fax: (617) 258-6534; email: gceder@mit.edu

State University of New York at Stony Brook, Department of Chemistry, 669 Chemistry Building, Stony Brook, NY 11794-3400; (631) 632-9548; fax: (631) 632-5731; email: cgre@sbchem.sunysb.edu

Objective

- Evaluate alternative layered oxides as cathode materials for a Li-ion battery that operates between Ni(II) and Ni(IV).

Approach

- Use solid-state NMR and XAS to characterize local structure and oxidation states of the nearby cations (in the 1st and 2nd cation coordination spheres) as a function of state of charge and number of charge cycles.
- Use First Principles calculations (DFT) to identify redox-active metals, relative stability of different structures, the effect of structure on cell voltages and to identify promising cathode materials for BATT applications.
- Use calculations and NMR to characterize the stability of these materials and the effect of doping on conductivity by identifying low-activation-energy pathways for cation migration.

Accomplishments

- Used Li NMR results to determine the local environments in the materials $Li[Li_{(1-2x)/3}Mn_{(2-x)/3}Ni_x]O_2$, where x = 0.5, 0.33 and 0.1, and to determine which site are deintercalated as a function of SOC.
- Estimated cell voltages for different local environments and determined energies of different cation ordering schemes.

Future Directions

- Perform detailed investigations of cathode materials following extended cycling.
- Investigate the effect of cation doping on the structure and electrochemical behavior of these materials.

Since the start of this project (June 1, 2002) we have made considerable progress in understanding the local structure of $Li[Li_{(1-2x)/3}Mn_{(2-x)/3}Ni_x]O_2$ and its effect on electrochemical properties. Lithium NMR results for the compositions x = 0.5, 0.33 and 0.1 show the presence of Li in both the Li and TM layers of these layered materials all systems (Table 2). The NMR results for $Li[Ni_{0.5}Mn_{0.5}]O_2$ are consistent with Ni^{2+} substitution into the Li layers as found in $LiNiO_2$. For compositions with $x \leq 1/3$, the fraction of Li in the Li layers is close to that predicted based on the stoichiometry of the materials.

Table 2.

Nickel Content (x)	Theoretical Li content in TM Layers* (% of total Li)	% Li in TM layer** (error)
1/2	0	7(1.5)
1/3	1/9 (8)	10 (2)
1/10	8/30 (20)	19 (2)
0	1/3 (25	22 (3)

**i.e.,* (1/3 – 2x/3)
***% based on total Li content

The Li local environments in the TM layers resemble the Li environments in the Mn layers of Li_2MnO_3 and can be represented by the local environment $Li(OMn)_{6-n}(ONi)_n$, where $n \leq 1$. These NMR are confirmed with Mn and Ni extended x-ray absorption fine structure (EXAFS) studies performed in collaboration with Dr. J. McBreen's group at BNL, which show that the Mn-ion local environments contain a larger number of Li ions than the Ni-ion local environments.

First Principles calculations have been performed on $(1–x)\ Li[Ni_{0.5}Mn_{0.5}]O_2 \bullet x\ Li[Li_{1/3}Mn_{2/3}]O_2$ and show that the environments for Li in the TM layers surrounded by more Mn ions are more stable than those surrounded by more Ni ions, and that Li doping in the TM layers reduces the tendency for Ni incorporation in the Li layers. A more detailed analysis of the Ni-Mn-Li arrangements in these materials is underway. Both the First Principles calculations and XAS experiments show that the redox process involves Ni, with the Mn ions remaining as Mn^{4+} during the 1st charge cycle at 4 V. The multiple electron change on Ni offers the possibility to engineer materials with high capacity.

A more detailed picture of the change in charge distribution with Li content is provided by generating charge density difference plots. Figure 36 shows the difference in charge density on the 100 plane of the spinel structure between the totally lithiated ($LiNi_{0.5}Mn_{0.5}O_2$) and the totally delithiated ($Ni_{0.5}Mn_{0.5}O_2$) states. Figure 36 demonstrates that charge is gained in sigma-type bonds of the Ni as the Li content increases. Conversely the charge on Mn remains roughly constant. The area where the t_{2g} orbitals point between the oxygens show little sign

of change. This is consistent with all the redox activity being concentrated in the Ni e_g orbitals.

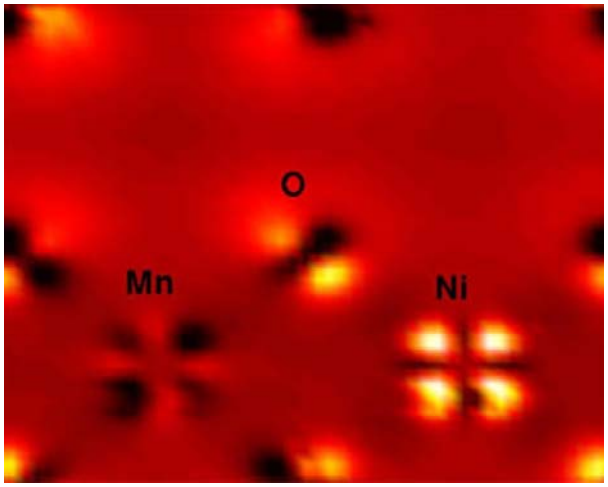

Figure 36. Change in spin density when Li is removed from $Li(Ni_{0.5}Mn_{0.5})O_2$. Bright(dark) regions indicate regions of high(low) change.

Additional evidence about the valence of Mn and Ni is provided by First Principles calculations of metal-oxygen bond lengths. As with spin, the Mn-O bond length is found to vary little with Li composition, confirming that little or no change to its valence state occurs. In contrast, the Ni-O bond length changes dramatically with Li composition. A Jahn-Teller distortion is observed at half lithiation which is consistent with Ni^{+3}.

First Principles calculations have also shed light on the precise sequence of Ni oxidation as Li is removed from the compound. Our calculations indicate that oxidation occurs locally whereby at high Li concentration, removal of each Li is accompanied by a change in valence of one Ni from +2 to +3. Only after all Ni ions have been oxidized to +3 will oxidation to +4 occur with further Li removal. Interestingly, First Principles results predict that Li sites in the Li layer with an immediate environment rich in Ni are more stable than those with a Mn-rich environment. Hence, the Li ions removed first are those closest to the Mn ions, even though Mn does not participate in the redox process.

The NMR results for the compositions x = 0.5, 0.33 and 0.1 clearly demonstrate that the Li is removed from both the Li layers and the TM layers on cycling. Calculations were performed in order to understand this phenomenon in more detail and indicated that Li is removed from the Li and TM layers at similar potentials. The latter process is facilitated by Li vacancies in the TM layers. Li NMR showed that the Li ions return to the TM layers on discharging and that the process is reversible (Fig. 37).

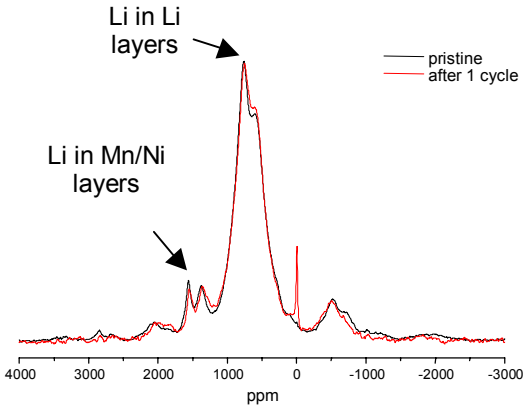

Figure 37. ^6Li MAS NMR $Li[Li_{1/9}Mn_{5/9}Ni_{1/3}]O_2$ shows that Li in both the Li layers and TM layers is removed but then returns following the first charge cycle.

The average voltage calculated by *ab initio* methods for the extraction of Li from the Li plane was found to vary from 2.84 to 2.98 V, whereas the voltage for Li from the TM plane ranged from 3.23 to 3.27 V. These numbers display the usual underestimation of the potential by the computational approach, but can be used to make relative comparisons. It was also found that Li should readily leave the TM plane provided a neighboring tetrahedron is surrounded by three Li vacancies.

Presentations

W.–S. Yoon, Y. Paik, C.P. Grey, X.-Q. Yang and J. McBreen, "^{6}Li MAS NMR and *In Situ* XRD Studies of Lithium Nickel Manganese Oxides," *11th International Meeting on Lithium Batteries*, Monterey, CA, June 2002.

G. Ceder, D. Carlier, J.Reed and A. an der Ven, "Thermodynamics and Kinetics of Layered $Li(Li,Ni,Mn)O_2$," *11th International Meeting on Lithium Batteries*, Monterey CA, June 2002.

G. Ceder, D. Carlier, J.Reed E. Arroyo and A. an der Ven, "First Principles Approaches to Investigate and Predict the Properties of Li Intercalation Oxides," Short Course on Materials for Energy: Batteries and Fuel Cells, Madrid, Spain, November 4-6, 2002.

MODELING

Improved Electrochemical Models

John Newman (Lawrence Berkeley National Laboratory)
University of California, Department of Chemical Engineering, 201 Gilman Hall, MC 1462, Berkeley CA 94720
(510) 642-4063, fax: (510) 642-4778, e-mail: newman@newman.cchem.berkeley.edu

Objectives

- Develop experimental and computational methods for measuring and predicting transport, kinetic, and thermodynamic properties.
- Model the behavior of electrochemical systems to optimize performance, identify limiting factors, and mitigate failure mechanisms.

Approach

- Refine galvanostatic polarization technique to measure transport properties.
- Develop molecular dynamics simulation of diffusion in multicomponent solutions.
- Develop thermal model that accounts for concentration effects in insertion electrodes.
- Develop model of dendrite formation on Li metal.
- Develop model of growth of the SEI layer.
- Model the $LiFePO_4$ electrode to identify limiting factors.
- Simulate the use of conductive polymers for overcharge protection.

Accomplishments

- Analyzed the effect of side reactions on measurements of transference numbers and activity coefficients by the galvanostatic polarization method.
- Demonstrated how ion association with increasing salt concentration causes increased viscosity and decreased conductivity in electrolytes containing $LiPF_6$ in carbonate solvents.
- Derived equations for determining the heat of mixing in electrochemical systems.
- Examined effect of mechanical stresses on dendrite initiation.
- Developed model of electron and ion transport through the SEI layer.
- Developed model of the $LiFePO_4$ electrode and compared to experiments.

Future Directions

- Refine model of effect of mechanical stresses on dendrite initiation.
- Compare SEI model with data to refine kinetic and transport parameters.
- Examine the roles of diffusion, kinetics, and conductivity in the performance of $LiFePO_4$.
- Analyze use of two polymer layers of different stabilities and transport properties.
- Simulate use of conductive polymers for overcharge protection.
- Develop improved method for measuring transference numbers.

We modeled the effect of a side reaction at the Li electrode on measurements of transport properties in polymer electrolytes. Measurements of diffusion coefficients and conductivity are not significantly affected, but measurements of transference numbers and activity coefficients using the galvanostatic-polarization and concentration-cell experiments can be substantially affected by side reactions. The presence of side reactions can be detected by performing transition-time experiments. The occurrence of side reactions can be mitigated by using a difference reference electrode such as $Li_4Ti_5O_{12}$ during the concentration-cell experiments. Future work will examine new experimental

techniques to remove the effect of side reactions from measurements of transference numbers.

The MD model has been successfully used to understand how interatomic interactions affect transport of $LiPF_6$ in carbonate-based electrolytes. Association between the anion and cation causes rigid networks that reduce the conductivity as the salt concentration increases.

Equations have been derived to predict the magnitude of the heat of mixing in electrochemical systems (equal to the amount of heat released while a cell relaxes after the current is turned off). The heat of mixing is small in systems with good transport properties.

Lithium metal has the highest energy density of any electrode. However, it will never be safe to use commercially unless one can prevent the risk of dendrites shorting the cell. We have shown that any dendrite initiated will be a problem, and that separators of sufficiently high elastic modulus could suppress dendrite initiation. Future work will combine the model of mechanical stress into the electrochemical model for dendrite initiation.

The model of the SEI layer indicates that only part of the initial irreversible capacity of graphite electrodes goes into forming a solid interphase layer of the thickness observed experimentally; the rest of the irreversible capacity must form soluble products. Future work will compare the model to data from the literature in order to refine parameters such as the transference number for electrons and rate constants.

The full-cell-sandwich model, dualfoil.f, has been modified to include the two-phase reaction, which occurs in $LiFePO_4$, and results have been compared to experiments performed in Striebel's lab. The model shows that accessible capacity in these cells is limited by mass transport within the iron phosphate, and *not* by electronic conductivity. Future work will focus on improving the match between the model and high-rate experiments.

Publications and Presentations

K.E. Thomas, R.M. Darling and J. Newman, "Mathematical Modeling of Lithium Batteries," W. A. van Schalkwijk and B. Scrosati, eds., in: *Advances in Lithium-Ion Batteries*, New York: Kluwer Academic/Plenum Publishers, p. 345 (2002).

W.C. Wong and J. Newman, "Monte Carlo Simulation of the Open-Circuit Potential and the Entropy of Reaction in Lithium Manganese Oxide" *J. Electrochem. Soc.*,**149,** A493-A498 (2002).

D.R. Wheeler and J. Newman, "A Less Expensive Ewald Lattice Sum," *Chem. Phys. Lett.*, **366**, 537-543 (2002).

J. Newman, K.E. Thomas, H. Hafezi and D.R. Wheeler, "Modeling of Lithium-Ion Batteries," *11th International Meeting on Lithium Batteries*, Monterey, CA, June 2002.

K.E. Thomas and J. Newman, "Heats of Mixing and Entropy in Porous Insertion Electrodes," *11th International Meeting on Lithium Batteries*, Monterey, CA, June 2002.

Failure Mechanisms in Li-Ion Systems: Design of Materials for High Conductivity and Resistance to Delamination

Ann Marie Sastry
The University of Michigan, Department of Mechanical Engineering and Applied Mechanics, Ann Arbor, MI 48109-2125 (313) 764-3061;, fax: (313) 747-3170, e-mail: amsastry@engin.umich.edu

Objectives

- Develop experimental and computation methods for measuring, and predicting electrical conductivity of Li-ion electrodes.
- Identify and optimize network morphologies resistant to electrochemical degradation.

Approach

- Extend of the Schumann-Gardner multilayer theory to measure electrical resistivity and contact resistance in electrodes.

- Develop image analyses to quantify electrode particle morphologies.
- Develop 2D and 3D conduction simulations based on particle morphologies.

Accomplishments

- Provided an experimental technique to determine electrode resistivity and contact resistance between active materials and current collectors.
- Validated of conduction models and simulations for BATT electrodes (collaboration with Striebel) for variety of particle types and manufacturing processes.

Future Directions

- Develop 3D pixilated conduction models.
- Integrate electrochemical, mechanical, and conduction model to benchmark theoretical results of damage analysis.
- Study contact of particles and current collectors.

We are identifying and optimizing network morphologies capable of resisting electrochemical degradation. It is well known that carbonaceous Li-ion anodes are subject to electrolytic decomposition, and exfoliation of graphitic particles. However, phase diffusion limits fast discharge of lithium iron phosphate, which has recently attracted attention as Li-ion cathode. Both failure modes are closely related to the morphology of the electrodes. Thus, we are intensively modeling and measuring conductive properties of both electrodes and potential additives for use in Li-ion systems.

The conduction modeling builds on our previous numerical work, incorporating real material morphology and careful selection of boundary conditions to reduce the numerical difficulties posed by singularities in the field solution, due to phase contrast, sharp corners, etc. This approach can assist to identify the key parameters that optimize network morphology, and it also can predict the materials effective conductivity. In order to verify the accuracy of this approach, we developed an accurate experimental method — the four-point-probe technique (Fig. 38), which allowed independent characterization of contact resistance and layer resistivity.

Validation of the models was made in several types of materials received from LBNL and HQ (Table 3). Tested anodes were comprised of wide variety of particle shapes, including those comprised of fibers, particles and flakes. The modeling results showed significantly better prediction than effective medium theories. Also, we noted an overall trend of slightly increasing resistivity with density, pointing to particle breakup in compression of electrodes. Thus, though increasing conductive additive may initially improve conductivity, excessive compression may in fact increase both contact resistance and top-layer resistivity. We will explore this further with additional image analysis.

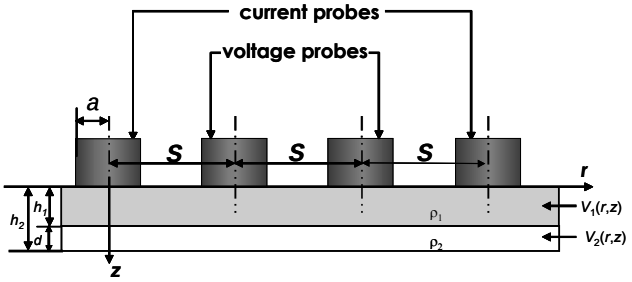

Figure 38. Schematic of test apparatus (four-point-probe) used in the measurement of resistivity.

The variation in conductivity of the various graphitized carbon materials was clearly shown to be related to the morphology of the active materials. Ultimately, the trade-offs among factors in electrochemical performance can be resolved with improved simulations of materials performance. An obvious subject of future work is combined electrochemical, conduction and mechanical modeling of these materials.

The importance of 3D *vs.* 2D modeling was also explored in this project year. We have developed analytical percolation solutions which have direct relevance to the conduction question, and compared 2D and 3D solutions, both analytically and numerically (Fig. 39). This will be the subject of intensive investigation in the coming year. Further work on interaction between particles and the current collector is also warranted.

Table 3. Selected experimental results for anode resistivity and contact resistance.

electrode no.	electrode condition	electrode thickness (μm)	resistivity of active material (μΩcm)	stdev resistivity of active material (μΩcm)	contact resistance (μΩcm²)	stdev contact resistance (μΩ cm²)	uncertainty (%)
028-09-4	unpressed	100	7.99E+05	2.39E+05	3.24E+05	8.60E+04	15.55%
028-09-5	pressed	90	7.50E+05	2.28E+05	3.87E+05	9.38E+04	15.65%
028-09-6	pressed	85	7.71E+05	1.11E+05	4.93E+05	4.45E+04	15.73%
028-12-5	unpressed	91	7.91E+04	1.49E+05	1.86E+04	4.48E+04	15.77%
028-12-6	pressed	83	1.49E+05	9.21E+04	1.69E+04	1.04E+04	15.75%
028-12-7	pressed	80	8.73E+04	4.86E+04	1.45E+04	4.20E+03	16.56%
028-12-1	unpressed	94	1.60E+04	2.40E+03	1.85E+02	9.60E+01	15.07%
028-12-3	pressed	83	1.18E+04	2.11E+04	1.05E+03	1.51E+03	16.23%
028-12-4	pressed	81	1.44E+04	2.35E+04	1.22E+03	1.51E+03	16.30%
028-67-1	unpressed	179	1.51E+06	1.87E+05	3.59E+06	7.36E+05	15.93%
028-67-2	100 (kg/cm²)	129	3.81E+05	4.32E+04	1.54E+06	1.11E+05	16.00%
028-67-3	200 (kg/cm²)	115	1.88E+05	3.41E+04	1.50E+06	9.54E+04	16.03%
028-67-4	300 (kg/cm²)	109	1.91E+05	1.78E+04	1.10E+06	1.95E+05	16.02%
028-68-1	unpressed	150	2.64E+05	3.17E+04	1.18E+04	1.48E+03	15.21%
028-68-2	100 (kg/cm²)	125	1.62E+05	3.30E+04	1.44E+04	7.72E+03	15.33%
028-68-3	200 (kg/cm²)	103	6.39E+04	1.91E+04	2.22E+04	2.16E+02	15.43%
028-68-4	300 (kg/cm²)	105	6.73E+04	3.20E+04	3.29E+04	7.91E+03	15.62%
028-69-1	unpressed	141	3.15E+04	9.88E+03	2.07E+03	5.93E+02	16.47%
028-69-2	100 (kg/cm²)	121	1.74E+04	1.96E+03	4.47E+03	4.89E+02	15.12%
028-69-3	200 (kg/cm²)	117	4.75E+04	4.25E+04	6.32E+03	3.73E+03	15.38%
028-69-4	300 (kg/cm²)	112	1.12E+05	1.28E+05	7.57E+03	4.88E+03	19.43%

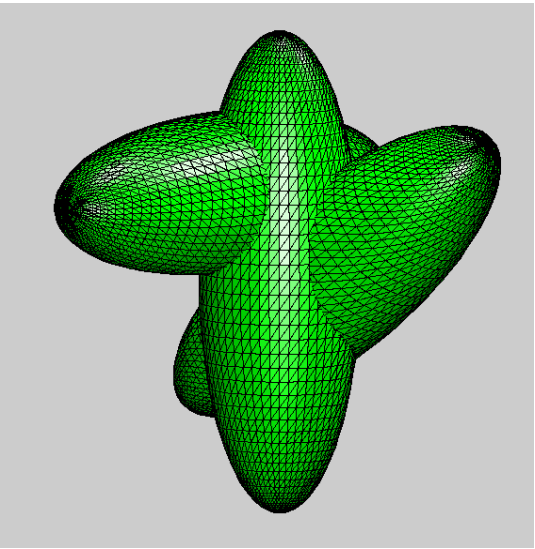

Figure 39. 3D mesh generation for complex particle geometries.

Publications

C.-W. Wang, Y.-B. Yi and A.M. Sastry, "Multiphase Conductive Networks: Simulations and Closed-Form Solutions for Selection of Conductive Anode Additives," *202nd Meeting of the Electrochemical Society*, Salt Lake City, UT, October 2002.

C.-W. Wang, A.M. Sastry, K.A. Striebel and J. Shim, "Exact Solution for Contact and Top-Layer Resistivity in Two-Layer Electrodes: Applications for Li-ion Anodes," *202nd Meeting of the Electrochemical Society*, Salt Lake City, UT, October 2002.

K. Striebel, J. Shim, C.-W. Wang and A.M. Sastry, "Anode Performance and Matrix Conductivity in Lithium Battery Electrolytes," *202nd Meeting of the Electrochemical Society*, Salt Lake City, UT, October 2002.

ACKNOWLEDGMENTS

This work was supported by the Assistant Secretary for Energy Efficiency and Renewable Energy, Office of FreedomCAR and Vehicle Technologies of the U.S. Department of Energy under Contract No. DE-AC03-76SF00098. The support from DOE and the contributions by the participants in the BATT Program are acknowledged. The assistance of Ms. Susan Lauer for coordinating the publication of this report is gratefully acknowledged.

LIST OF ACRONYMS

AFM	Atomic force microscopy
ANL	Argonne National Laboratory
AOP	Annual Operating Plan
ASI	Area specific impedance
ATD	Advanced Technology Development
BATT	Batteries for Advanced Transportation Technologies
BHT	Butylated Hydroxytoluene
BNL	Brookhaven National Laboratory
CPE	Composite polymer electrolyte
CSAFM	Current-sensing atomic force microscopy
CV	Cyclic voltammetry
DEC	Diethyl carbonate
DFT	Density functional theory
DMC	Dimethylcarbonate
DMF	Dimethyl formamide
DOD	depth-of-discharge
DOE	Department of Energy
DSC	Differential scanning calorimetry
EC	Ethylene carbonate
EDS	Electron dispersive spectroscopy
EDX	Energy dispersive x-ray analysis
EIS	Electrochemical impedance spectroscopy
EMC	Ethyl methyl carbonate
EQCM	Electrochemical quartz crystal microbalance
EV	Electric vehicle
EXAFS	Extended X-ray absorption fine structure
FR	Flame retardant
FTIR	Fourier transform infrared
GBL	γ-butyrolactone
HETAP	Hexa-ethoxy-tri-aza-phosphazene
HEV	Hybrid electric vehicle
HMTAP	hexa-methoxy-tri-aza-phosphazene
HQ	Hydro-Québec
ICL	Irreversible capacity loss
IIT	Illinois Institute of Technology
IRAS	Infrared absorption spectroscopy
LBNL	Lawrence Berkeley National Laboratory
LiTFSI	Lithium bis(trifluoromethane-sulfonyl)imide
LN	Liquid nitrogen
MAS	Magic Angle Spinning

MCT	Mercury Cadmium Telluride
MD	Molecular Dynamics
MIT	Massachusetts Institute of Technology
mpe	Mole of electron
MW	Molecular weight
NFE	Nonflammable electrolyte
NG	Natural graphite
NMR	Nuclear magnetic resonance
OAAT	Office of Advanced Automotive Technologies
OCV	Open circuit voltage
PA	Power-Assist
PC	Propylene carbonate
PEG	Polyethylene glycol
PEO	Poly(ethylene oxide)
PMO	Poly(methylene oxide)
PNGV	Partnership for a New Generation of Vehicles
PPO	Poly(propylene oxide)
PTMO	Poly(trimethylene oxide)
PVDF	Poly(vinylidene fluoride)
RDE	Rotating disk electrode
R-F	Resorcinal formaldehyde
SEI	Solid electrolyte interphase
SEM	Scanning electron microscopy
SNFTIR	Subtractive normalization Fourier transform infrared
SOC	State of charge
SPE	Solid polymer electrolyte
SUNY	State University of New York
TEM	Transmission electron microscopy
TESA	Tetra-ethyl-sulfamide
TM	Transition metal
TMO	Trimethylene oxide
UHV	ultra high vacuum
USABC	United States Advanced Battery Consortium
VC	vinylene carbonate
WAXD	Wide-angle x-ray diffraction
XAS	X-ray absorption spectroscopy
XPS	X-ray photoelectron spectroscopy
XRD	X-ray diffraction

ANNUAL REPORTS

1. Exploratory Technology Research Program for Electrochemical Energy Storage – Annual Report for 2000, LBNL-47960 (June 2001).
2. Exploratory Technology Research Program for Electrochemical Energy Storage – Annual Report for 1999, LBNL-45767 (May 2000).
3. Exploratory Technology Research Program for Electrochemical Energy Storage – Annual Report for 1998, LBNL-42694 (June 1999).
4. Exploratory Technology Research Program for Electrochemical Energy Storage – Annual Report for 1997, LBNL-41950 (June 1998).
5. Exploratory Technology Research Program for Electrochemical Energy Storage – Annual Report for 1996, LBNL-40267 (June 1997).
6. Exploratory Technology Research Program for Electrochemical Energy Storage – Annual Report for 1995, LBNL-338842 (June 1996).
7. Exploratory Technology Research Program for Electrochemical Energy Storage – Annual Report for 1994, LBL-37665 (September 1995).
8. Exploratory Technology Research Program for Electrochemical Energy Storage – Annual Report for 1993, LBL-35567 (September 1994).
9. Exploratory Technology Research Program for Electrochemical Energy Storage – Annual Report for 1992, LBL-34081 (October 1993).
10. Exploratory Technology Research Program for Electrochemical Energy Storage – Annual Report for 1991, LBL-32212 (June 1992).
11. Technology Base Research Project for Electrochemical Energy Storage – Annual Report for 1990, LBL-30846 (June 1991).
12. Technology Base Research Project for Electrochemical Energy Storage – Annual Report for 1989, LBL-29155 (May 1990).
13. Technology Base Research Project for Electrochemical Energy Storage – Annual Report for 1988, LBL-27037 (May 1989).
14. Technology Base Research Project for Electrochemical Energy Storage – Annual Report for 1987, LBL-25507 (July 1988).
15. Technology Base Research Project for Electrochemical Energy Storage – Annual Report for 1986, LBL-23495 (July 1987).
16. Technology Base Research Project for Electrochemical Energy Storage – Annual Report for 1985, LBL-21342 (July 1986).
17. Technology Base Research Project for Electrochemical Energy Storage – Annual Report for 1984, LBL-19545 (May 1985).
18. Annual Report for 1983 – Technology Base Research Project for Electrochemical Energy Storage, LBL-17742 (May 1984).
19. Technology Base Research Project for Electrochemical Energy Storage – Annual Report for 1982, LBL-15992 (May 1983).
20. Technology Base Research Project for Electrochemical Energy Storage – Report for 1981, LBL-14305 (June 1982).
21. Applied Battery and Electrochemical Research Program Report for 1981, LBL-14304 (June 1982).
22. Applied Battery and Electrochemical Research Program Report for Fiscal Year 1980, LBL-12514 (April 1981).